Final report on

EUMETSAT study

'Detection and monitoring of instability from hyperspectral sounders, using IASI in view of MTG-IRS'

performed by the Hungarian Meteorological Service

Contract number EUM/CO/18/4600002186/TA
Order No 4500017305

HUNGARIAN METEOROLOGICAL SERVICE
1870-2020

Table of Content

Executive summary

The aim of the study was to provide detailed analyses of possible usage of the IASI L2 IRON data in nowcasting in the view of MTG IRS. Convective environment of the thunderstorms was investigated with use of several environmental parameters (indices). IASI L2 EARS (MWIR data received through EumetCast), IASI L2 IRON, NWP and in-situ observations (radiosonde and Synop) data were used to determine these parameters. Besides looking into how IASI L2 data could add value to the forecasts, one of the main goals was to provide information on the IASI L2 IRON data focusing on the benefits and limitation.

A long-term comparison of GII and IASI L2 IRON parameters was done for a 6-month period over various parts of the world. Good correspondence between IASI L2 IRON, MWIR and GII data were found. Performance degradation was observed for IASI L2 IRON data in cloudy cases, as expected.

During the summer 2019 IASI L2 EARS data have been evaluated by forecasters. One of the aims of the evaluation was to look for value added cases. Unfortunately, only a couple of cases with added value was found which is due to the facts that Hungary is a small country and the morning Metop overpasses are usually happening a longer time before the convection starts (most of the convection is in the afternoon, early evening). With half hour IRS data even for a smaller area we expect to have more interesting and value added cases. In addition with IRS data one will be able to see the temporal tendencies of humidity content and instability.

For the case studies IASI L2 indices were compared with NWP and in-situ measurements. Unfortunately during the Metop overpasses we do not have radiosonde measurements. So in the lack of ground truth we have looked into the storm development itself, whether the storm cloud have developed in the environment defined by the IASI retrieval.

IASI L2 IRON retrievals were studied together with MWIR data in cloud free and different cloudy situations. On cloud-free areas, and areas covered by thin cirrus or small cumulus the structure of the retrieved parameters and the profiles are usually similar, the differences are not high in general. The IRON profiles and parameters calculated from them are considerably different from the MWIR and forecasted ones for opaque mid/high level clouds. In addition the uncertainties in the IRON retrieval for these cloud types are much higher than in the MWIR data. It is worth considering masking the areas covered by opaque clouds and/or non-reliable IASI pixels. Thermal inversion can also be recognised in the profiles.

The quality indicators were found mostly significant to the quality of the retrieved profiles and very useful. However, uncertainty profiles would be needed to locate levels of highest confidence.

In summary we found that stronger instabilities, moisture boundaries are captured in IASI L2. However, a dry bias is observed in the products in the bottom layer in mild to strong pre-convective situations compared to the forecast, yielding to low CAPE values which can be misleading for the forecasters.

Blending IASI profiles with ground based measurements shows potential to better characterise instabilities especially when they are very near-surface based . It may yield more accurate surface based instability indices.

1. Introduction

The present study is a continuity of our previous work (Putsay et al., 2017).

The aims of our previous study were:

- **To perform complex case studies of various types of storms using remote sensing (satellite, radar, lightning), in-situ and NWP data.** To **analyse the convective environment together with the development of the convective clouds/system.** Evaluate temporal evolution of different characteristics, features, observations. To study the possible relationships between lightning characteristics and severe convection development.
- **To give suggestions which environmental parameters might be useful and reasonable to retrieve from the IASI L2 product.** To analyse (in case studies) the usefulness of the retrieved IASI based environmental parameters and their potential added value.
- Perform a comparison between **SEVIRI GII** parameters and the same parameters retrieved from the **IASI L2** product to analyse the **consistency** between them.

In the present study the focus is on the **IASI L2 IRON data** – as **proxy data for MTG/IRS** including the usefulness of synergetic use of IASI data with ground measurements.

The main objectives of the study were:

- to compare the SEVIRI GII parameters with the same parameters calculated from IASI L2 IR-only data to analyze the consistency between them;
- to perform complex case studies with MWIR (based on microwave and infrared measurements) and IRON (based on infrared measurements) IASI L2 data. This includes searching for cases when the IASI L2 parameters considerably differs from the model forecast;
- to create a database of typical IASI and ECMWF profile pairs;
- to merge the IASI profiles with surface measurement.

2. Data and Methodology

Since May of 2018, we receive IASI EARS L2 profiles regularly trough EumetCast. IASI derived environmental indices and profiles are visualized in the Hungarian Advanced Workstation – HAWK (Kertész, 2000; Rajnai et al., 2005). The following parameters are calculated and provided to the forecasters routinely:

- Total Pecipitable Water (TPW),
- mean relative humidity in the lowest 0-3 km width layer (0-3km RH),
- K-index,
- Best lifted index,
- Maximum Buoyancy,
- MLCAPE,
- 400/700 hPa lapse rate,
- 600/925 hPa lapse rate.

IASI data along with the results of our previous study was presented to the forecasters.

During the 2019 convective season (from June to September) five severe weather forecasters checked daily the IASI derived environmental parameters. They compared the IASI information with NWP data and evaluated them taking into account what kind of thunderstorms formed later on. Each day they made notes whether the given day was interesting from IASI point of view. They were looking for added values compared to NWP, while noting if IASI provided the same information, was very poor, or misleading. After summer, selected cases were analysed manually. Cases from our previous study were also reanalysed with IASI IR-only data.

In the **case studies**, the synoptic situation, the convective environment and the types of the convective cloud (system) were analysed.

Radiosonde measurements, NWP data, and parameters retrieved from IASI L2 profiles (both MWIR and IR-only) provided by EUMETSAT were used to study the environment.

- IASI L2 MWIR products contain temperature and humidity profiles retrieved from the combination of IASI, AMSU and MHS data. Taking advantages of the microwave measurements, it also works for cloudy areas.
- The IASI L2 IRON products provide temperature and humidity profiles retrieved from IASI infrared measurements. The dataset contained retrievals for both cloud free and cloudy areas.

Both IASI retrievals are NWP independent and the data is available over Hungary around 8-9 UTC and 18-21 UTC. Its spatial and temporal resolution is lower compared to NWP and GII data.

To estimate the **possible usefulness** of the environmental parameters derived from the profiles of the IASI L2 product **for nowcasting purposes,** we did the followings. For the studied cases we

- calculated several environmental parameters from IASI L2 products and compared them (visually) with ECMWF derived parameters to check their consistency, possible usefulness and possible added values;
- in some locations, we studied the ECMWF and IASI profiles to understand the reasons behind the differences between the IASI derived and ECMWF forecasted parameters;
- the main characteristics of the radiosonde measurements (usually available 3 hours later) and the surface Synop data were also used.

From IASI L2 data, we can derive parameters on instability and moisture, but as it does not contain wind profile we cannot get information on lift or wind shear. (Wind shear controls the severity of storms.) Unfortunately, independent reference is not available for validation, there are only very few soundings in time of the IASI data availability (e.g. at 09 UTC over Hungary).

During the **consistency study,** the GII instability parameters were compared with parameters retrieved from IASI Level 2 profiles. GII products (König et al, 2001) are derived by EUMETSAT using SEVIRI data and ECMWF forecasts. These parameters are calculated only for cloud-free areas and available in 15/5 minutes.

The IASI L2 profiles, used during the comparison (so called IASI L2 IRON), was retrieved without any microwave information from accompany instrument onboard the satellite. Thus, these data were only used for cloud free scenes.

3. Case Studies

3.1. Experiences with IRON data

In the IASI L2 IRON files provided by EUMETSAT, profiles were included for all scenes (clear and cloudy as well). We expected either no data for **area covered with thick clouds**, or profile data only above the cloud tops. (As thick clouds are opaque in the IR spectral region – satellite do not “see” inside/below the thick cloud in IR region.) However, presently the IRON retrieval provides full profile output (down to the surface) for all types of clouds. Note, the vertically averaged error is usually high for these pixels. **We suggest to mask the area covered by thick clouds or to provide profiles only above the cloud tops.**

IRON data were compared with MWIR data and ECMWF forecasts. As microwave information is not used in these retrievals, differences between the IRON and MWIR data were found in both cloud free and cloud covered cases.

In cloud free areas fewer differences can be seen between retrieved profiles and parameters, the structures are very similar (Fig. 3.1 and Fig. 3.3). Examples of the difference between the profiles over cloud free land and sea can be seen in Fig. 3.2. Table 3.1 contains the averaged temperature and dew point error values for the example profiles. On 04 June 2018 ECMWF forecasted a local TPW maximum for Croatia which is missing from both IASI L2 MWIR and IRON data (Fig. 3.3).

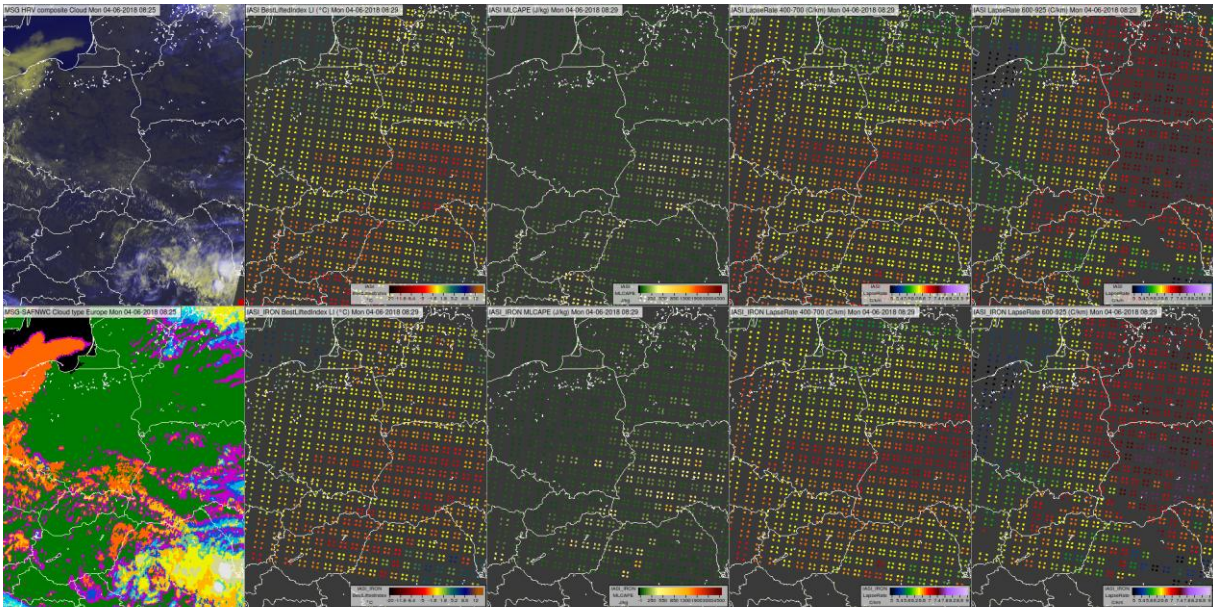

Fig. 3.1: Upper row: HRV Cloud RGB image, IASI MWIR Best Lifted index, MLCAPE, Lapse Rate between 400 and 700 hPa, Lapse Rate between 600-925 hPa; Bottom row: NWCSAF Cloud Type, IASI IRON Best Lifted index, MLCAPE, Lapse Rate between 400 and 700 hPa, Lapse Rate between 600-925 hPa on 4 June 2018 08:29 UTC.

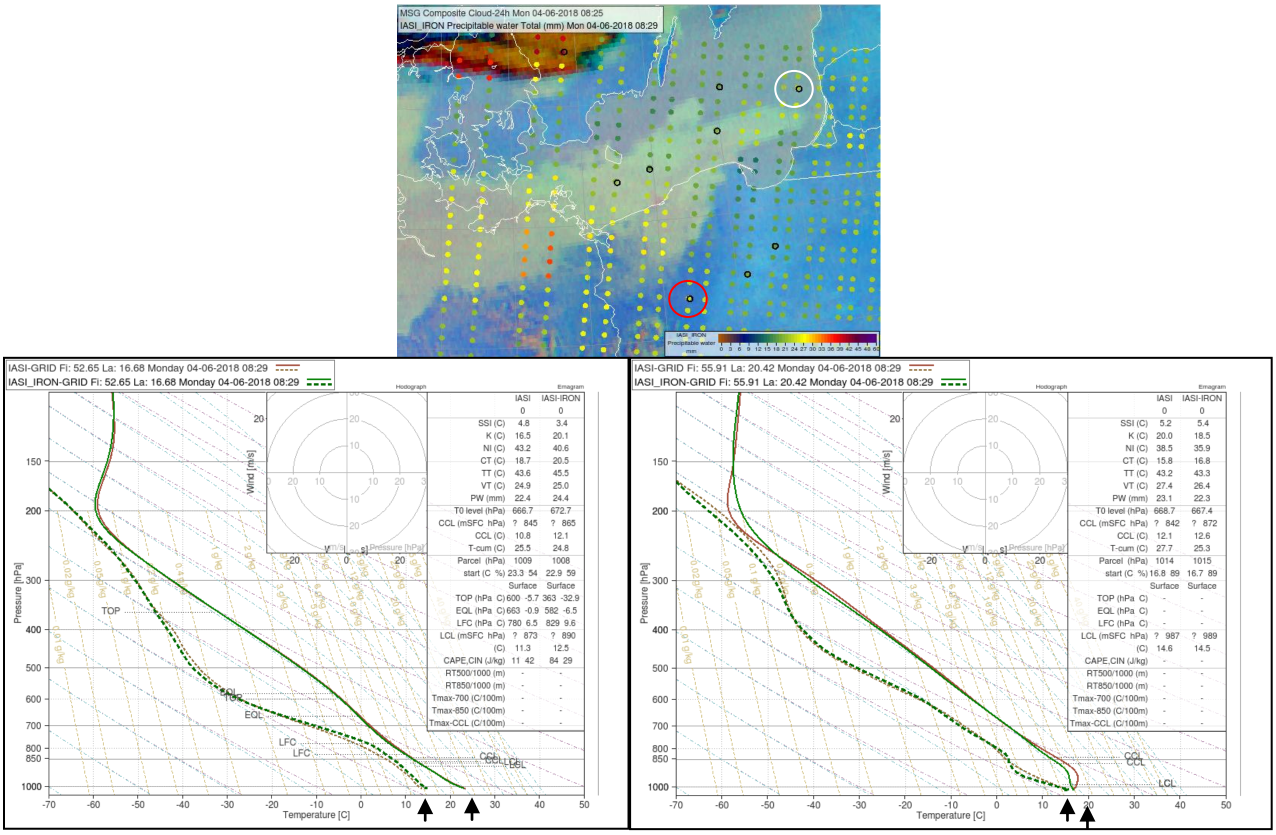

Fig. 3.2: Example profiles for pixels over cloud free land (left) and sea (right). The solid brown and green lines represent the MWIR and IRON temperature profiles, respectively; while the broken brown and green lines represent the MWIR and IRON dew point temperature profiles, respectively. On the top the locations of the IASI pixels over land and sea are marked with red and white circles. The black arrows (in the bottom panels) mark the measured 2m temperature and dew point temperature values.

	LAND		SEA	
	MWIR	**IRON**	**MWIR**	**IRON**
IASI T error [C]	0.97	0.84	0.95	0.83
IASI Td error [C]	1.7	1.98	2.28	2.16
TPW [mm]	22.4	24.5	23.1	22.3

Table 3.1: Vertically averaged error and TPW values for the profiles showed in Fig. 3.2.

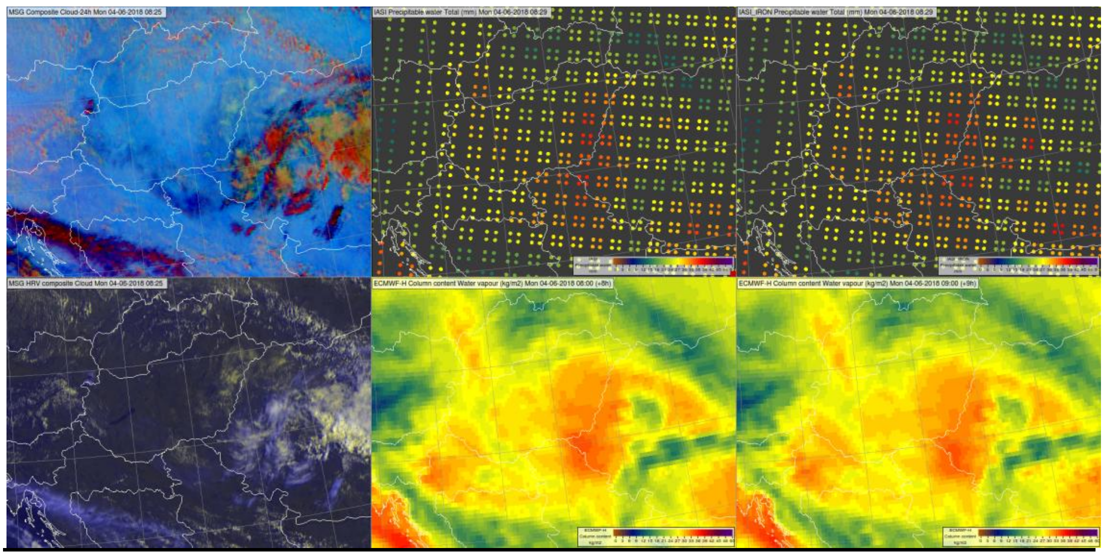

Fig. 3.3: Upper row: SEVIRI 24-hour Microphysics RGB image at 08:25 UTC, IASI MWIR TPW at 08:29 UTC, IASI IRON TPW at 08:29 UTC; Bottom row: SEVIRI HRV Cloud RGB image at 08:25 UTC, ECMWF forecasted TPW valid for 08 UTC, ECMWF forecasted TPW valid for 09 UTC on 4 June 2018.

Over cloud covered areas more differences could be seen between the IRON and MWIR profiles depending on the cloud types. Low level small cumulus clouds didn't have a large effect on the IRON profiles (Fig. 3.4). The bottom right panel of **Fig. 3.3** confirms the presence of small cumulus clouds over the area where the profile is presented in Fig. 3.4.

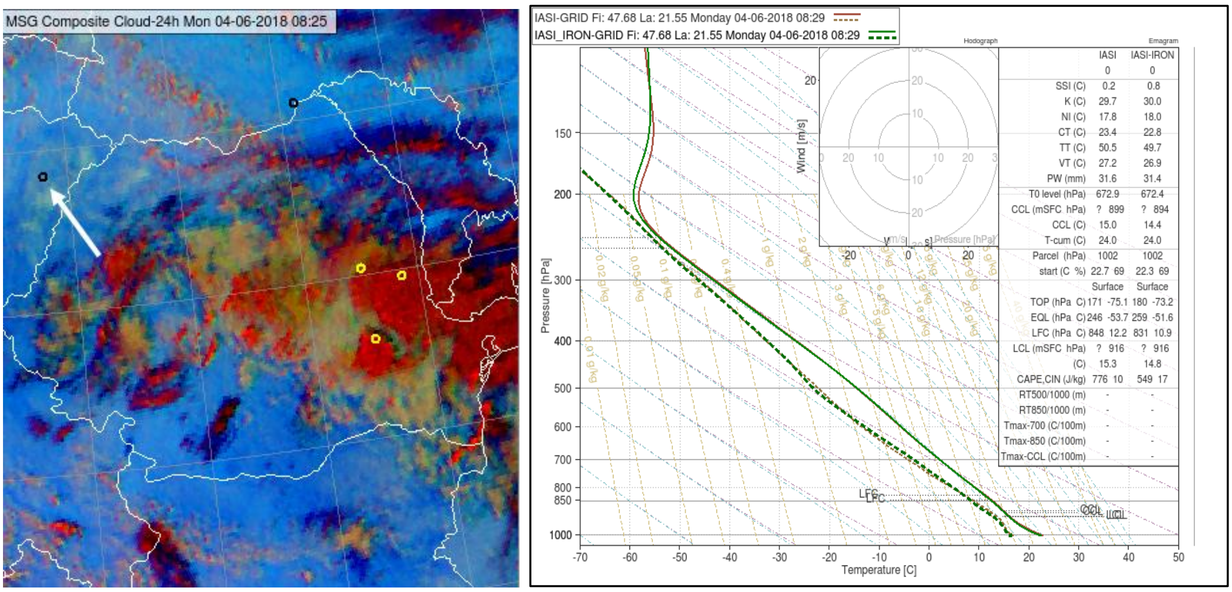

Fig. 3.4: Example profile for pixel covered by small low-level cumulus clouds (right). The solid brown and green lines represent the MWIR and IRON temperature profiles, respectively; while the broken brown and green lines represent the MWIR and IRON dew point temperature profiles, respectively. The location of the IASI profile is marked with white arrow (left).

For thick stratus or fog some differences were present in the IASI MWIR and IRON moisture profiles. The IRON retrieval was still able to produce the inversion like the MWIR retrieval (Fig. 3.5).

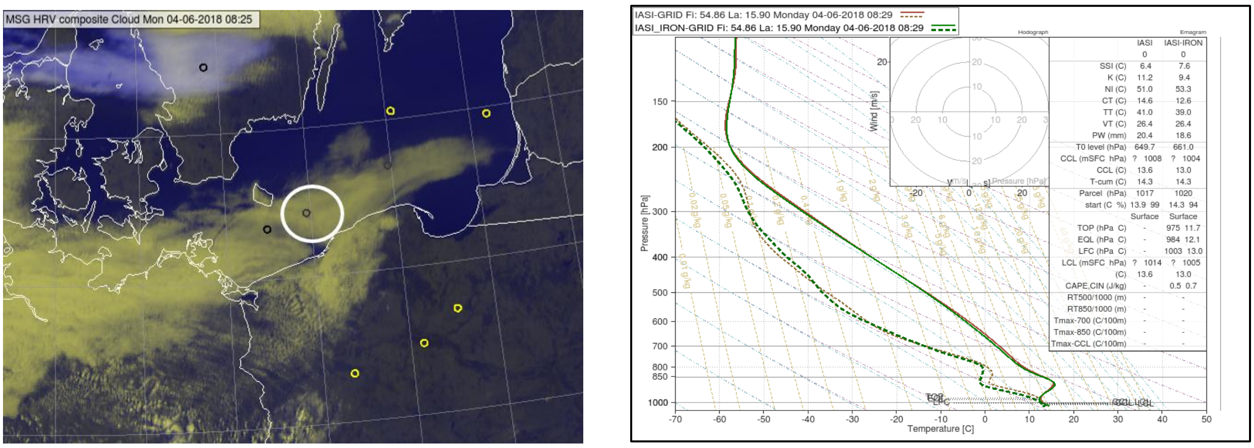

Fig. 3.5: Example profile for pixel covered by thick stratus or fog (right). The solid brown and green lines represent the MWIR and IRON temperature profiles, respectively; while the broken brown and green lines represent the MWIR and IRON dew point temperature profiles. The location of the IASI pixel is marked with white circle (left).

As expected high- and mid-level thick opaque clouds have a very large effect on the IRON profiles below the cloud top. The IRON temperature and dew point profiles are often completely different from the MWIR profiles (Fig. 3.6). Very often the IRON retrieval for these cases indicates lower surface temperature and dew point values which are not supported by the Synop measurements.

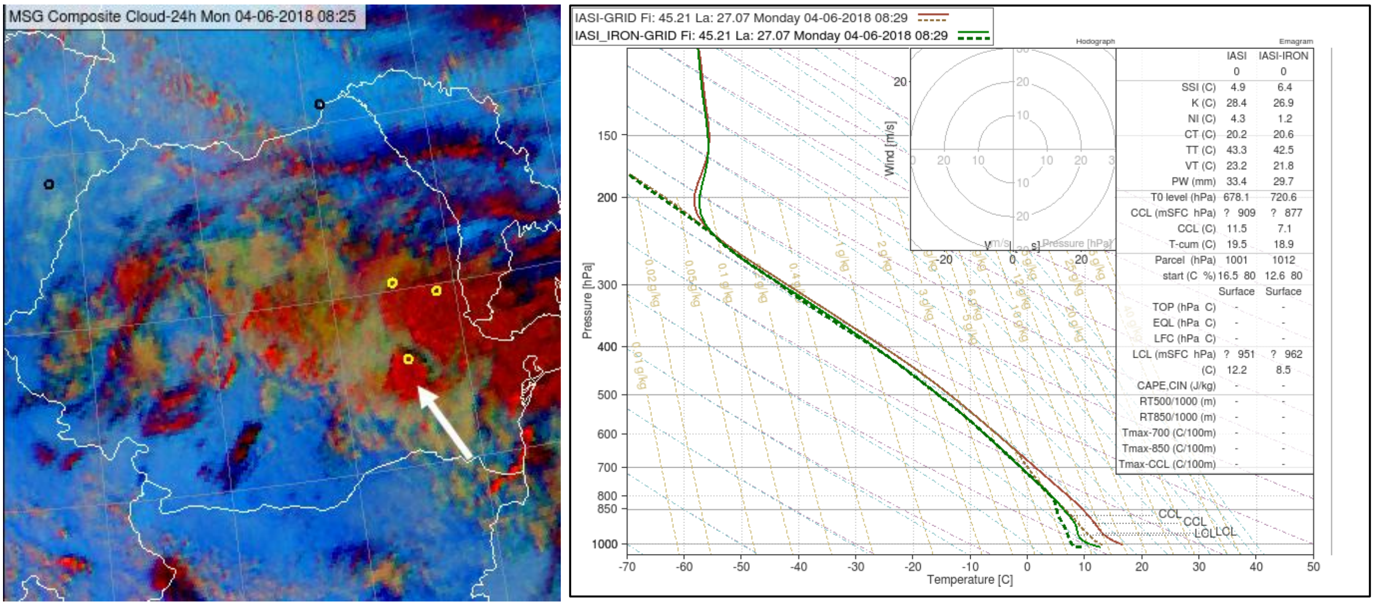

Fig. 3.6: Example profile for an IASI pixel covered by thick high-level opaque clouds (right). The solid brown and green lines represent the MWIR and IRON temperature profiles, respectively; while the broken brown and green lines represent the MWIR and IRON dew point temperature profiles. The location of the IASI pixel is marked with white arrow (left).

The effect of the cirrus cloud can be very different depending on the thickness of the cloud. Thin cirrus clouds have small effect on the IRON retrievals while thick cirrus clouds can make the profiles useless. The two different effect of the cirrus are shown in Fig. 3.7.

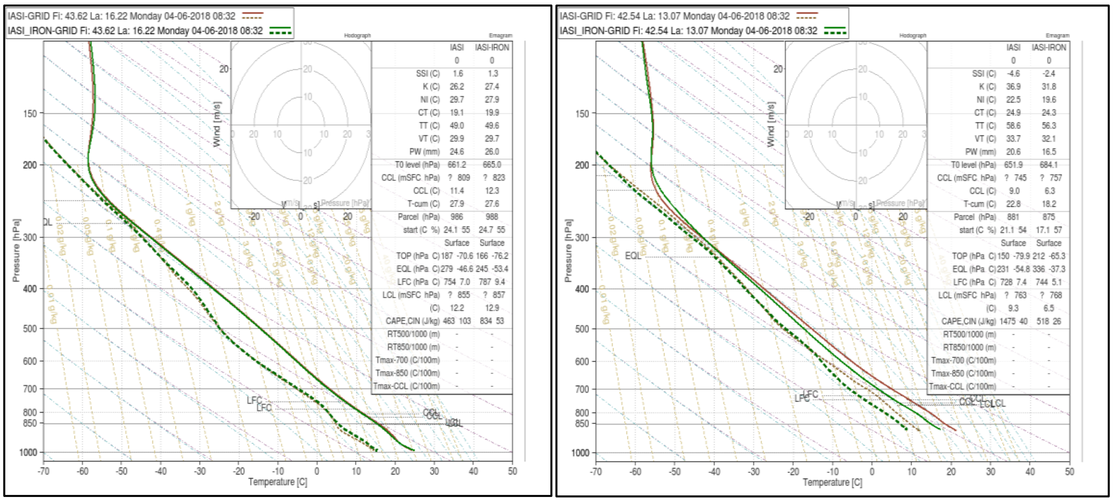

Fig. 3.7: Example profiles for pixel covered by thin (left) and thick (right) Cirrus clouds. The solid brown and green lines represent the MWIR and IRON temperature profiles, respectively; while the broken brown and green lines represent the MWIR and IRON dew point temperature profiles.

3.2. IASI L2 profiles and environmental parameters

In this chapter some main features are discussed what we found working with IASI MWIR and IRON profiles and environmental parameters.

3.2.1. Over-saturation

The IASI profiles (regardless on the retrieval type) show over-saturation (the dew point temperature is larger than the temperature) in some cases. **Fig. 3.8** shows an example. Taking into account the vertically averaged errors of the retrieved profiles, the super-saturation is just within the error bars in this case.

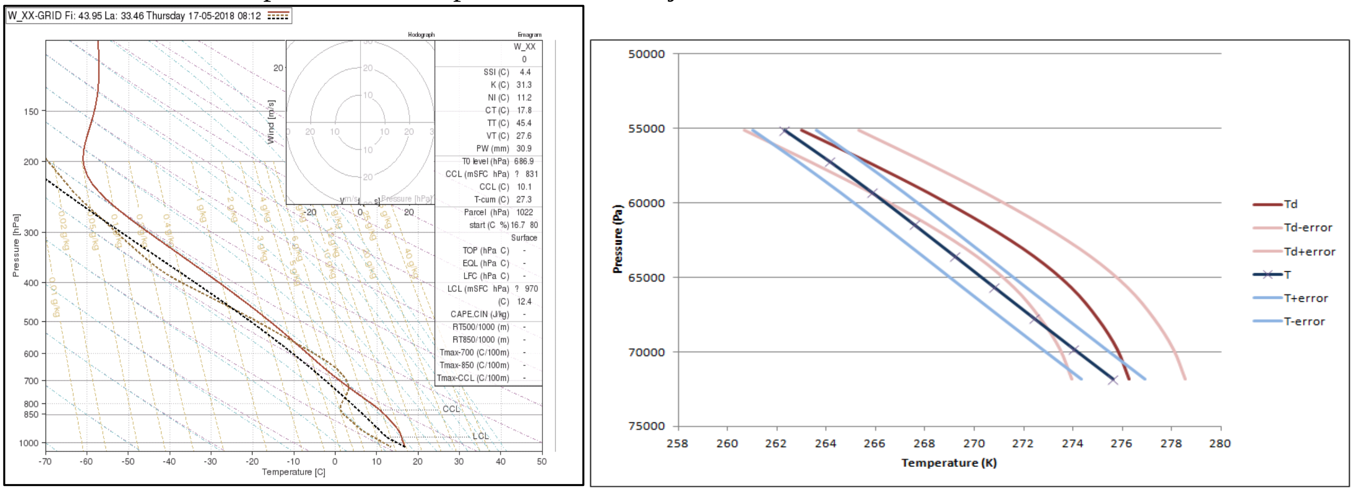

Fig. 3.8: Example of over-saturation in the IASI profile (left), where the solid brown line is temperature and the broken brown line presents the dew point temperature. Enlargement of the profile in the over-saturation region together with the error bands (right).

As the over-saturation here is not a real physical phenomena we maximize the dew point value with the temperature before we present the product to the forecasters.

3.2.2. Smoothness and uncertainties of the profiles

The IASI profiles are usually smoother than the forecasted ones.

The vertically integrated error fields complement the actual profiles and contain very important information. It is useful to be checked before using/trusting the IASI profiles. These values would be even more useful if they were not integrated through the whole profile but for different layers.

The humidity profiles usually have higher uncertainty than the temperature profiles. Comparing the profiles with the ECMWF profiles, we often found the temperature curves very close to each other, while the humidity curves differ more (Fig. 3.9). Additionally, underestimation of the humidity in the lowest layer was very often observed.

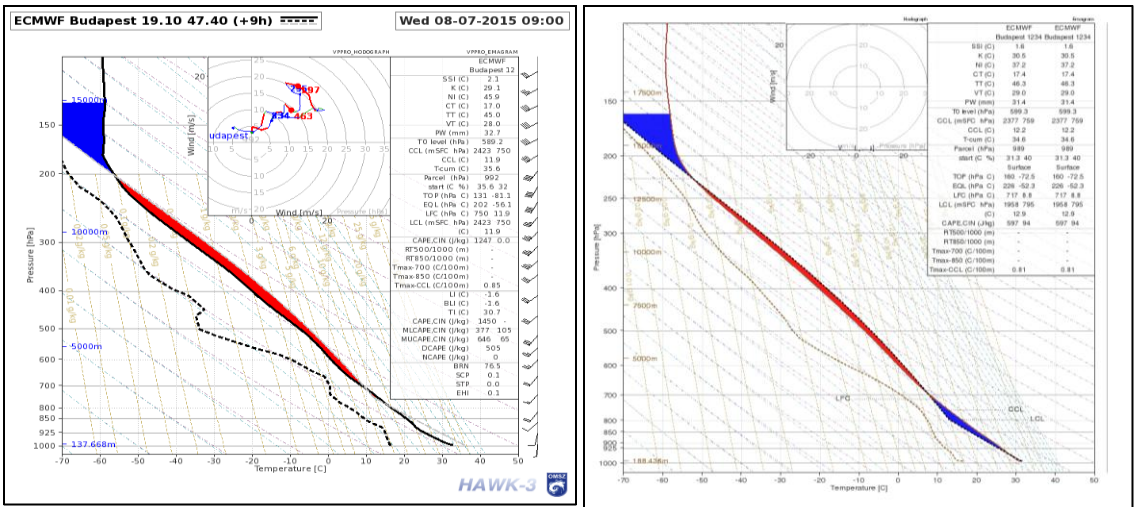

Fig. 3.9: ECMWF forecasted profiles valid for 09 UTC on 08 July 2015 (left) and 08:50 UTC IASI MWIR profiles at the same day (right). The broken lines show the dew point while the solid lines show the temperature profiles.

3.2.3. Moisture boundaries

Moisture boundaries can be often seen in the cloud free areas of SEVIRI 24-hour Microphysics RGB imagery where darker blue colour means more humidity; lighter blue colour means less humidity in the atmosphere. Fig. 3.10 shows such boundary in Poland (dryer area is marked by the left arrow, moister area is marked by the right yellow arrow). Looking at IASI TPW on both side of this boundary we found 7 mm difference (Fig. 3.11). The moisture difference can also been seen in the humidity profiles shown in Fig. 3.12.

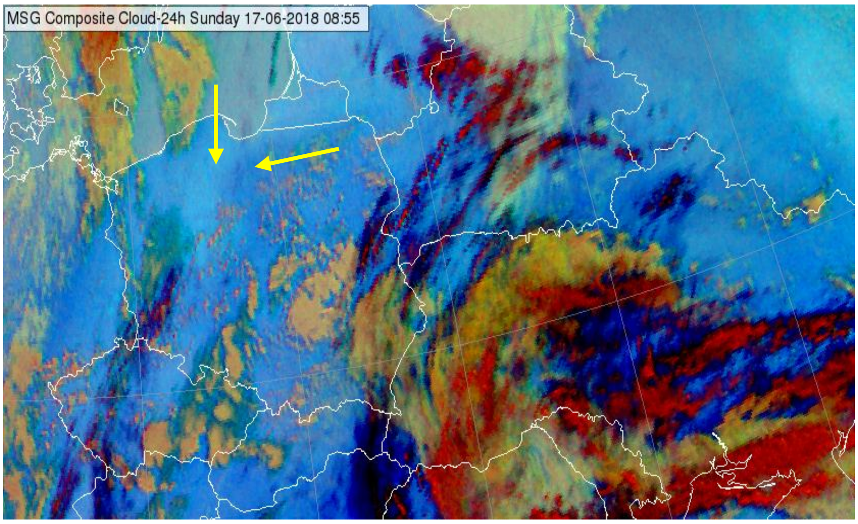

Fig. 3.10: SEVIRI 24-hour Microphysics RGB image at 08:55 UTC on 17 June 2018. Yellow arrows show the dryer and the moister areas on the two sides of the moisture boundary over Poland.

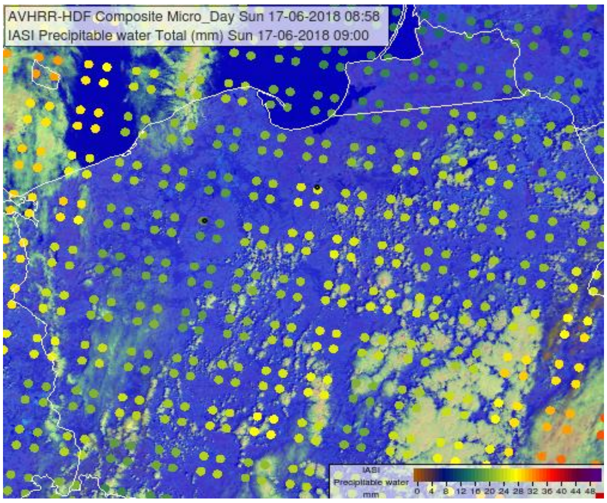

Fig. 3.11: IASI MWIR TPW at 09 UTC on 17 June 2018 overlaid on the AVHRR Day Microphysics RBG. The two black dots mark IASI pixels on the two sides of the moisture boundary.

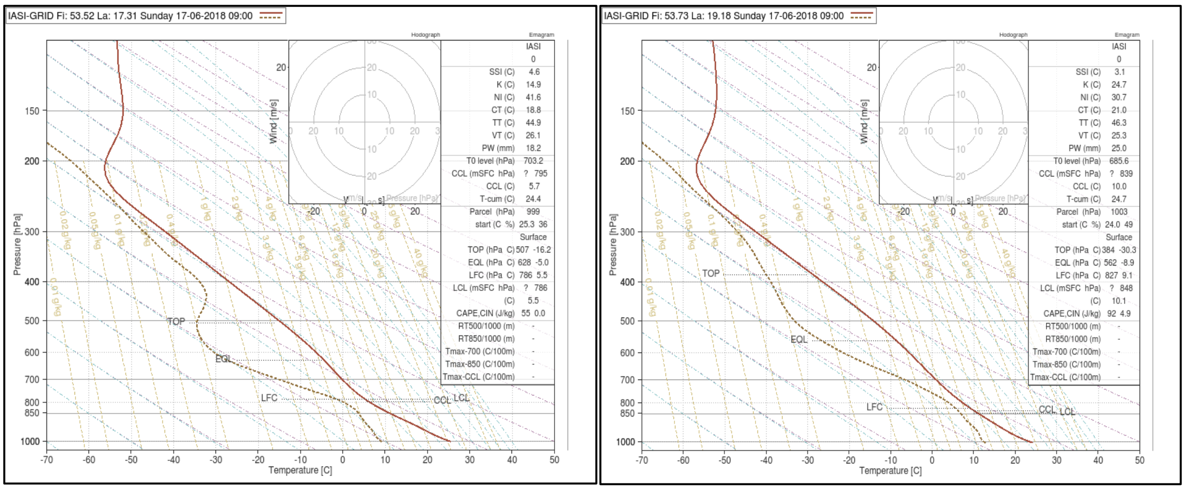

Fig. 3.12: IASI temperature (solid line) and dew point (broken line) profiles for the IASI pixels marked in Fig. 3.11. The left panel shows the IASI profile on the drier side while the right panel present the profile on the moister side.

Another example of moisture boundary can be seen in Fig. 3.13. The IASI TPW values well reflect the difference in the humidity (10 mm). Fig. 3.14 shows the corresponding profiles on both sides.

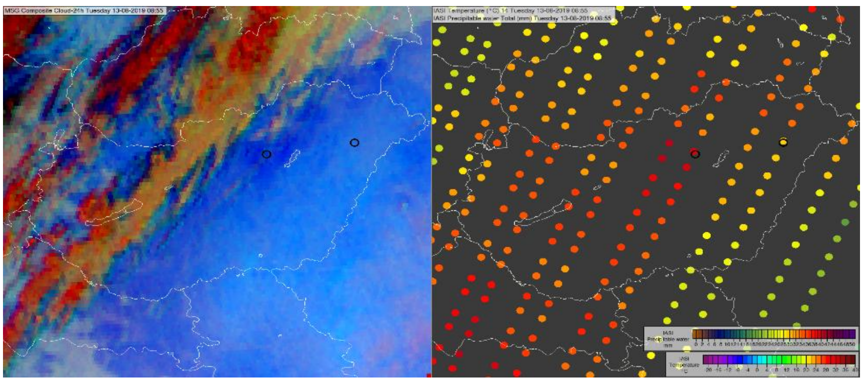
Fig. 3.13: SEVIRI 24-hour Microphysics RGB image (left) and IASI TPW at 08:55 UTC on 13 August 2019.

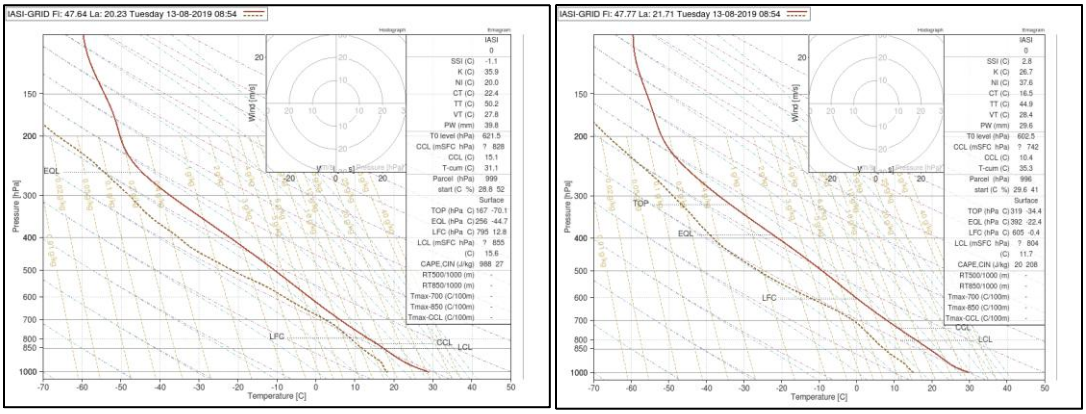

Fig. 3.14: IASI temperature (solid line) and dew point (broken line) profiles for the IASI pixels marked in Fig. 3.13. The left panel shows the IASI profile on the moister side, while the right panel present the profile on the drier side.

3.2.4. Underestimated Mixed Layer CAPE (MLCAPE)

In our previous work (Putsay et al., 2017) we studied the different CAPE parameters and presumed that for the IASI data MLCAPE would be the most suitable. *We chose MLCAPE, because we expected it to be more accurate than other kinds of CAPE values as in this case the virtual air parcel is initiated with the average temperature (T) and dew point (Td) values of a layer, instead of the T and Td values of a single level.*

However, looking at many cases we found that the IASI derived MLCAPE (both MWIR and IRON) is very often underestimated compared to the model forecast. This may cause problem: if an IASI derived parameter differs strongly and often from ECMWF then the forecasters may not trust it. An example is shown in Fig. 3.15. The MLCAPE values were 318 J/kg for the IASI pixel indicated by the blue arrow and 661 J/kg in the ECMWF forecast at the same time. Analysing the profiles one can see that the ECMWF dew point is much higher in the mixing layer (Fig. 3.16). That is why the ECMWF MLCAPE is significantly higher. ECMWF profile seems to be more realistic in the low-layer as SEVIRI HRV Cloud RGB shows small low level cumulus clouds in this area (Fig. 3.15). Note that right panel of Fig. 3.16 shows both the IASI L2 MWIR and IRON profiles (in brown and blue colours). IRON profile is almost the same as the IASI MWIR profile.

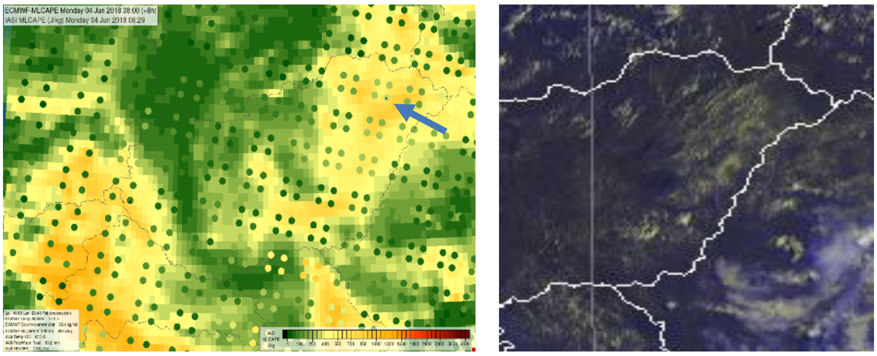

Fig. 3.15: IASI MWIR MLCAPE at 08:29 UTC overlaid on top of the ECMWF forecasted MLCAPE valid at 08 UTC, 4 June 2018 (left). SEVIRI HRV Cloud RGB image at 08:25 UTC (right).

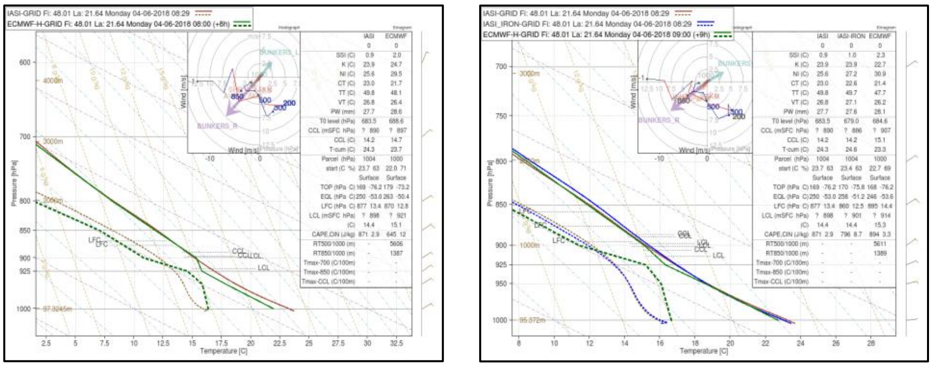

Fig. 3.16: 08 UTC ECMWF and 08:29 UTC IASI MWIR profiles at the pixel marked by the blue arrow in Fig. 3.15 (left). 09 UTC ECMWF, 08:29 UTC IASI MWIR and IRON profiles at the same location (right). The brown, blue and green lines represent the IASI MWIR, IRON and ECMWF profiles, respectively. The solid lines represent the temperature; the broken lines represent the dew point temperature profiles.

<u>Two reasons why IASI MLCAPE is often strongly underestimated:</u>

In the ECMWF model a whole parametrization module is responsible for the mixing of the boundary layer in convective situations. This often results a “typical shape” of the dew point profile in the low layer which is usually not present in the IASI profile (Fig. 3.17). The IASI dew point often decreases faster with altitude in the boundary layer than the ECMWF forecasted dew point. In addition, the surface dew point is often lower than the forecasted one. These conditions together cause the reduction of the IASI average humidity in the lowest 100 hPa where we initiate our MLCAPE calculation, hence the IASI MLCAPE underestimation.

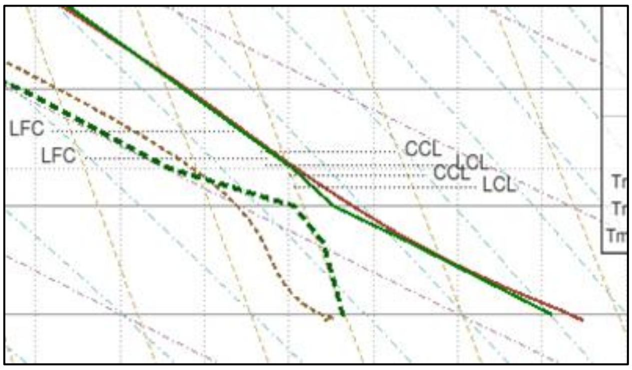

Fig. 3.17: Typical shape of IASI dew point profile (brown broken line) and ECMWF dew point profile (green broken line) in the low layer in convective situation (if the moisture content is enough high).

Although IASI MLCAPE is usually strongly underestimated compared to the forecast - in extreme unstable situation it can reach relatively high values (see Fig. 3.18 showing both MWIR and IRON retrievals). In these cases the IASI derived MLCAPE delineates the most unstable areas. So it is worth paying attention if IASI MLCAPE reaches higher values in a larger area.

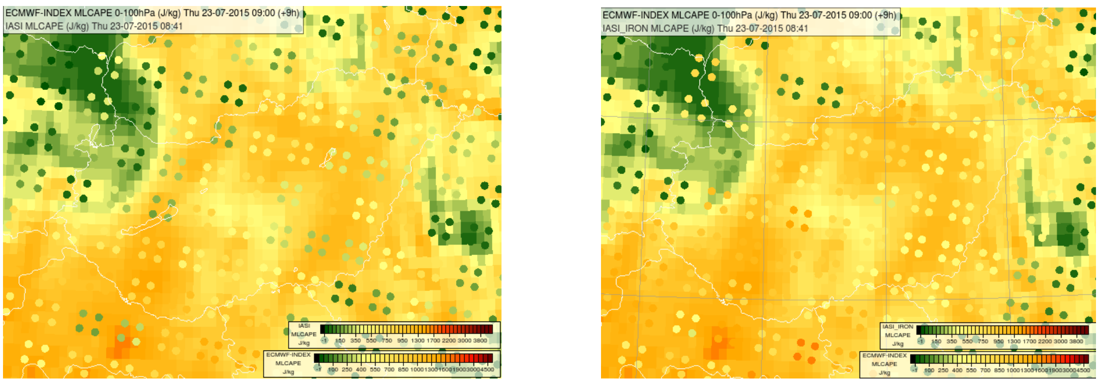

Fig. 3.18: IASI MWIR (left) and IRON (right) MLCAPE at 08:41 UTC overlaid on the ECMWF forecasted MLCAPE valid at 09 UTC, 23 July 2015.

3.2.5. Feature "foot" in the ECMWF profile near the surface

Very often near the surface levels a sudden increase in the ECMWF temperature and humidity profiles are present (Fig. 3.19). In such cases ECMWF 2 meter temperature and dew point values are much warmer than at the lowest model level just above it. The same feature often can be observed in the radiosonde measurements as well (Fig. 3.20). This sudden increase is missing from the IASI profiles most of the times. This is one of the reasons why the "surface based" instability indices (like surface based CAPE, SBCAPE) are often higher in ECMWF data.

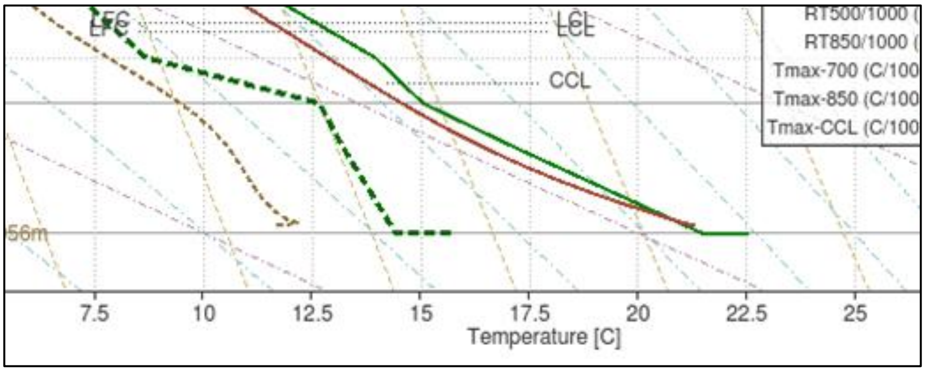

Fig. 3.19: Example of „foot" feature in the forecast on 2 June 2019 at 08:43 UTC close to Budapest. Green lines show the ECMWF temperature (solid) and dew point (broken) profiles while the brown lines represent the IASI profiles.

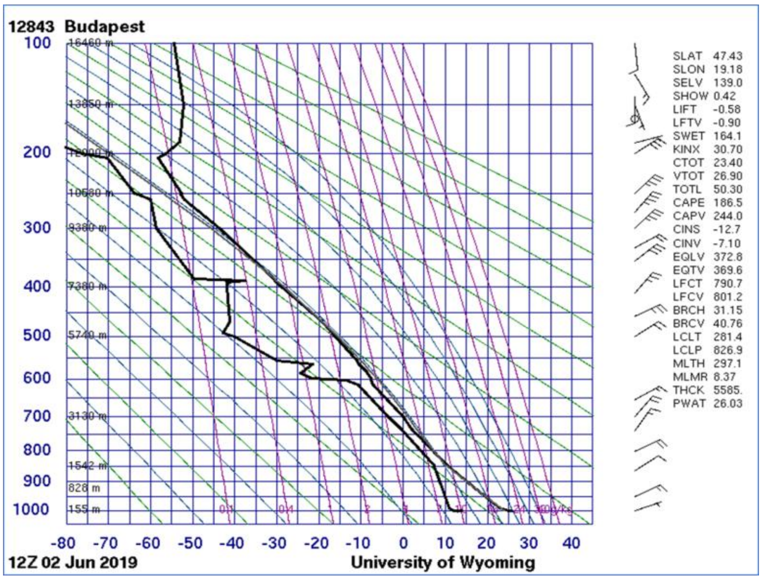

Fig. 3.20: "Foot" feature in the radiosonde profile on 2 June 2019 at 12 UTC.

3.2.6. Sunglint

Sometimes the vertically averaged error of the IASI profiles can be very high (up to 5-6 K). When we experience so high values the profiles cannot be trusted. It might be useful to mask these pixels. In Fig. 3.21 an example of very high uncertainty is shown. Sunglint was present in the shortwave channels of the AVHRR instrument. This resulted in a useless profile with multilayer clouds for a cloud free pixel (Fig. 3.22). The vertically averaged error for the dew point was 5.27 K.

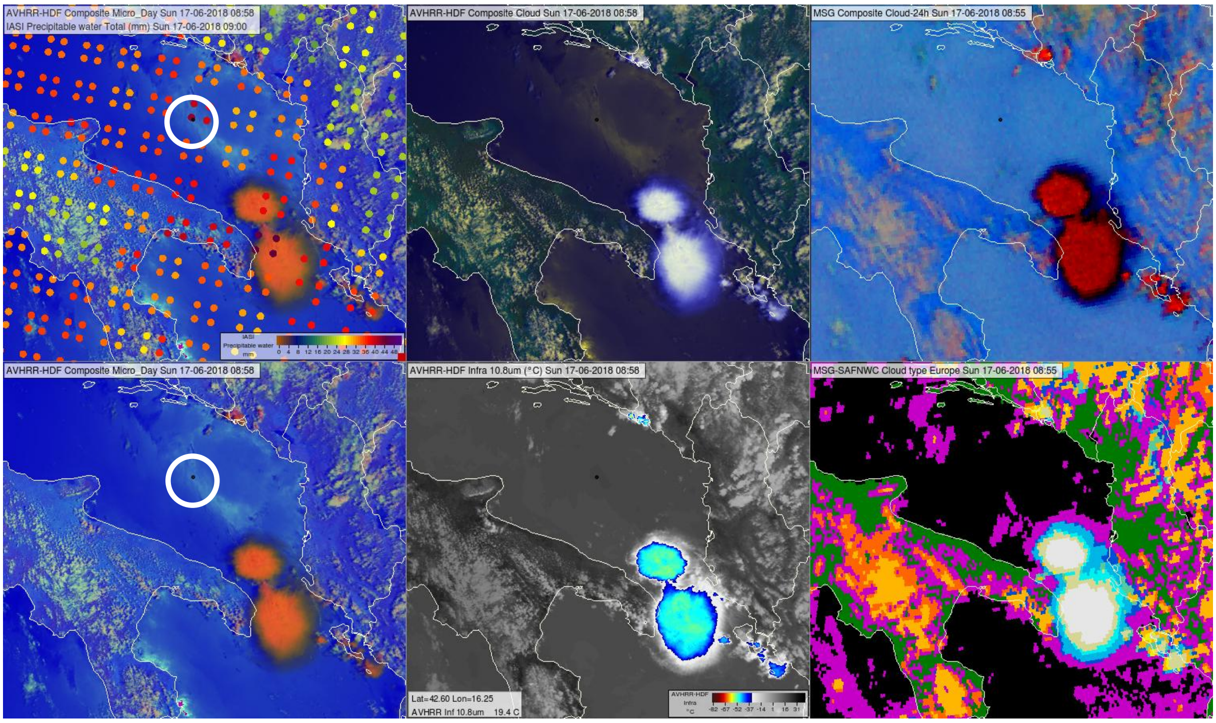

Fig. 3.21: Upper row: 09 UTC IASI MWIR TPW overlaid on AVHRR Day Microphysics RGB image taken at 08:58 UTC, AVHRR Cloud RGB at 08:58 UTC, SEVIRI 24-hour Microphysics RGB at 08:58 UTC; Bottom row: AVHRR Day Microphysics RGB at 08:58 UTC, AVHRR IR10.8 at 08:58 UTC, NWCSAF Cloud Type at 08:55 on 17 June 2018. The white circle indicates the location the IASI profile is presented in Fig. 3.22.

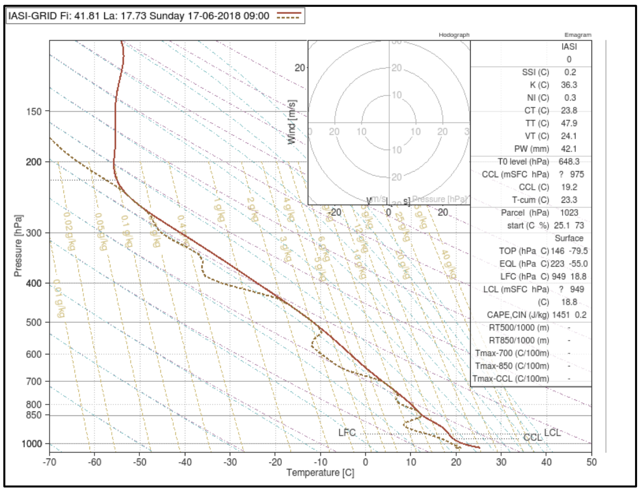

Fig. 3.22: IASI MWIR profile for the pixel marked with white circle in Fig. 3.21 on 17 June 2018 at 09 UTC.

3.2.7. Features related to fronts

ECMWF profiles behind the surface fronts show cooler and dryer airmass in the low layer in many cases. These often cannot be observed in the IASI profiles. An example of such a situation is shown in Fig. 3.23 when a strong front passed over Hungary.

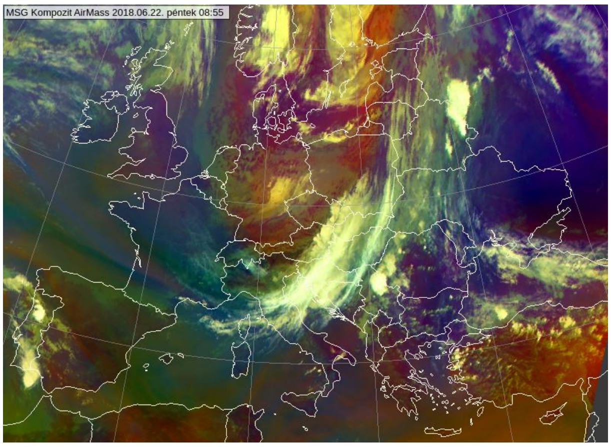

Fig. 3.23: SEVIRI Airmass RGB for 22 June 2018, 08:55 UTC.

Significant differences can be observed between the ECMWF forecasted and IASI L2 derived TPW and K-index, mainly in Slovakia, north Hungary and east Austria (Fig. 3.24). This makes us question which one could be more realistic. Looking at the IASI uncertainties we found rather large values (larger than 2.5 K for dew point and larger than 1.5 K for temperature) along the thick frontal cloudiness, which suggests that those moister profiles yielded by IASI L2 may be erroneous.

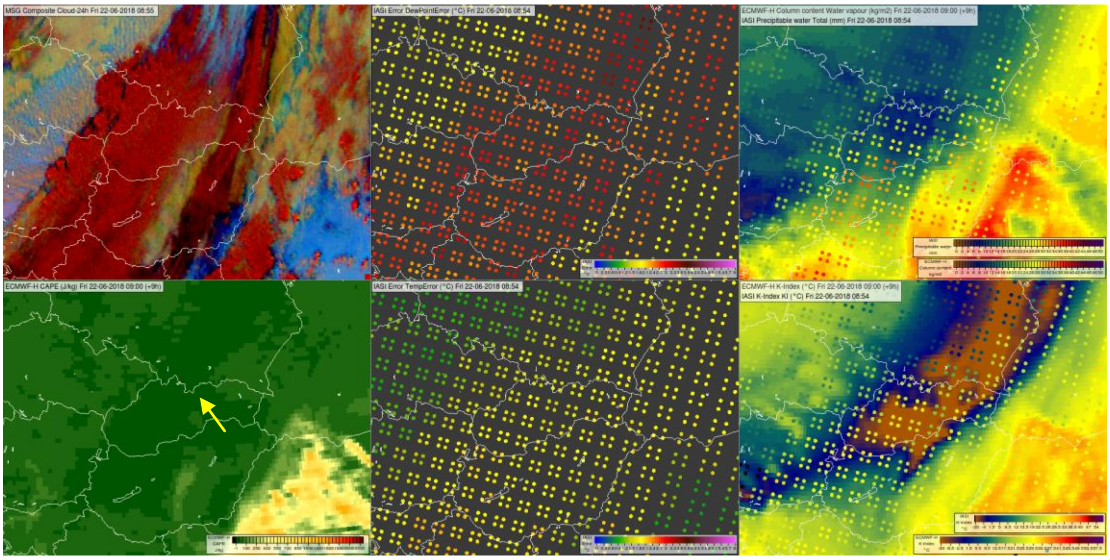
Fig. 3.24: Upper row: SEVIRI 24-hour Microphysics RGB at 08:55 UTC, IASI MWIR dew point error at 08:54, IASI MWIR TPW at 08:54 UTC overlaid on ECMWF TPW valid for 09 UTC; Bottom row: ECMWF CAPE valid for 09 UTC, IASI MWIR temperature error at 08:54 UTC, IASI MWIR K-index at 08:54 UTC overlaid on ECMWF K-index valid for 09 UTC on 22 June 2018. The yellow arrow shows the location of the profiles presented in Fig. 3.25.

Fig. 3.25 shows IASI and ECMWF profiles for a location close to Poprad city (Slovakia) together with the 12 UTC Poprad radiosonde measurement. Below 850 hPa the forecasted profile is drier and colder than the IASI profile. The forecasted dew point profile shows a very dry layer between 850 and 500 hPa. The radiosonde measurements confirm the presence of the very dry airmass in the mid/low layers.

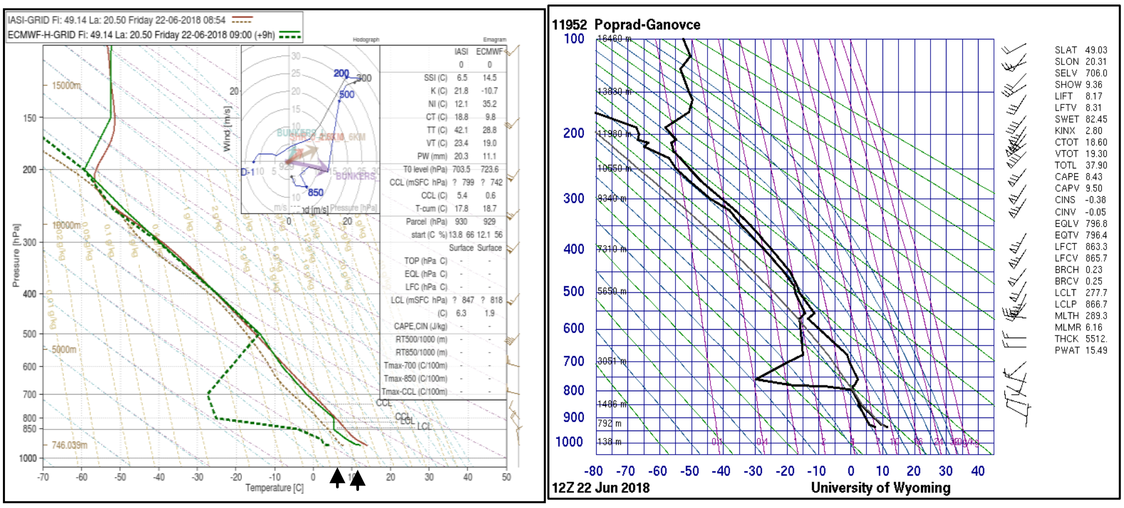

Fig. 3.25: Left: IASI MWIR (brown) and ECMWF (green) temperature (solid line) and dew point (broken line) profiles behind the front on 22 June 2018 at 08:54 and 09 UTC. Right: Radiosonde measurements in Poprad on 22 June 2018 at 12 UTC.

3.2.8. Thermal inversion

IASI profiles can reflect thermal inversion. On 19 December 2018, a so called winter ‚cold pool' situation was in Hungary. This means that most of the country was covered by stratus/fog. In Fig. 3.26 low clouds or fog can be observed in pinkish colours. As one can see the Tisza River through it, stratus/fog has to be thin close to the river. Many of the hill tops are seen as they are higher than the cloud tops. In Fig. 3.26 one can see that the temperature inversion is present in both IASI and ECMWF profiles. Air is saturated close to ground in both profiles.

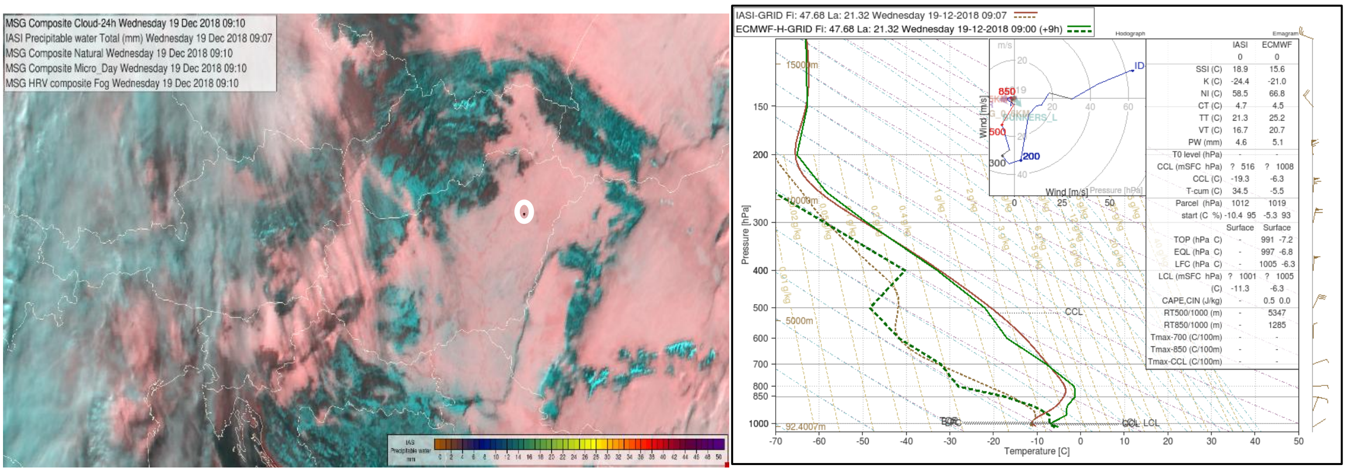

Fig. 3.26: Left: SEVIRI HRV Fog RGB on 22 June 2018 at 09:10 UTC. Right: IASI MWIR (brown) at 09:07 UTC and ECMWF (green) valid for 09 UTC temperature (solid line) and dew point (broken line) profiles. The circle in the left panel show the location of the profiles shown in the right panel.

Another example of a thermal inversion case is shown in Fig. 3.27. Fog/stratus was present in the encircled area. According to the NWCSAF Cloud Type (CT) product it was very low cloud. However, the NWCSAF Cloud Top Temperature and Height (CTTH) product retrieved around 3000 m cloud top height in several pixels. Note that ECMWF didn't forecast this particular cloud for that time, the forecast for the area is cloud free.

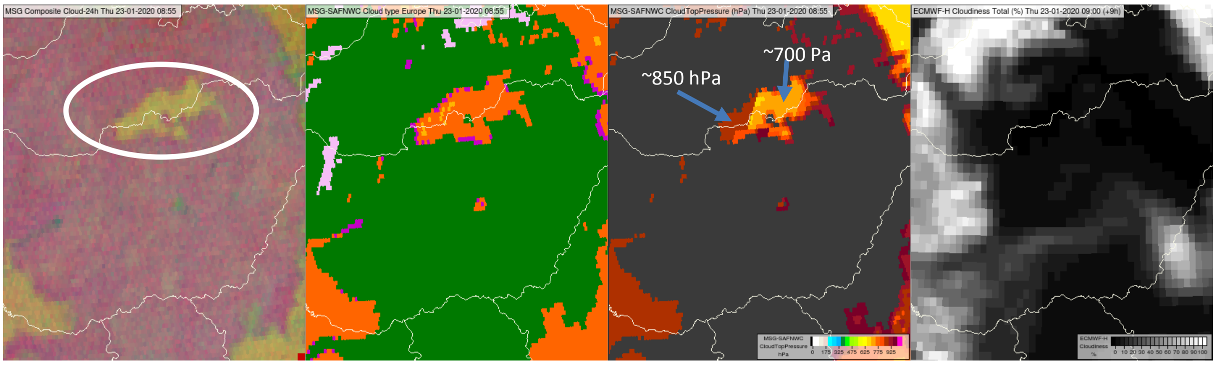

Fig. 3.27: SEVIRI 24-hour Microphysics RGB, NWCSAF Cloud Type, NWCSAF Cloud top pressure at 08:55 UTC, ECMWF forecasted cloudiness valid for 09 UTC on 23 January 2020.

In winter cold-pool situation, when there is fog/stratus, temperature profiles often show thermal inversion. In this case the thermal inversion was missing from the forecasted profiles (likely because it predicted clear sky) while IASI temperature profile shows characteristics of stratus with inversion (Fig. 3.28).

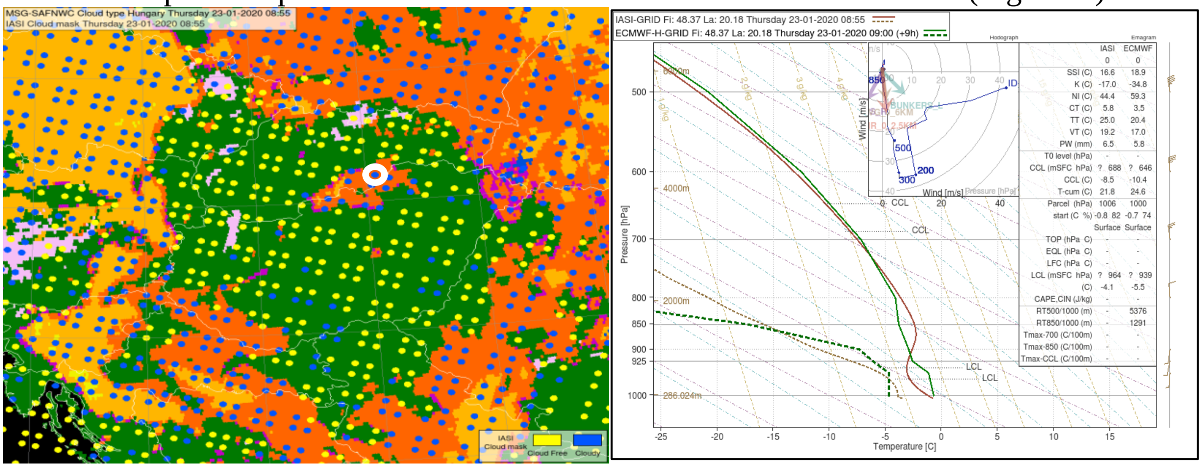

Fig. 3.28: Left: IASI MWIR cloud mask overlaid on SEVIRI NWCSAF CT on 23 January 2020 at 08:55 UTC. Right: IASI MWIR (brown) at 08:55 UTC and ECMWF (green) valid for 09 UTC temperature (solid line) and dew point (broken line) profiles. The location of the profiles is marked with the circle in the CT image.

NWCSAF uses NWP (in our processing chain ECMWF) forecasted profiles for the cloud top pressure/height retrieval. It uses different methods for profiles with and without thermal inversion. In this case using the IASI profile in the cloud top height retrieval might have helped.

3.2.9. Indication of clouds from water-vapour saturation in vertical profiles

We compared IASI profiles with simultaneous AVHRR/SEVIRI images and Cloud Type (CT) product to check whether in the IASI profile the dew point and temperature curves are close to each other in those layers where the imagery and CT indicate clouds.

The IASI profiles have uncertainties. For each profile we know the vertically averaged temperature and dew point errors. This makes more complicated to evaluate whether an IASI profile “indicates” a cloud layer or not. Using these error ranges the same profile might show both cloud free or cloudy environment.

- At the levels where the **dew point depression** is less than the **temperature error plus the dew point error** the relative humidity might be 100%, so cloud is possible. (As we have information only about the vertically averaged temperature and dew point errors, we could evaluate the profile only by supposing that these errors are roughly similar at all levels.)
- At the levels where the dew point depression is much larger than the temperature error plus the dew point error, the relative humidity is much less than 100%, so cloud is not likely.

Note we cut all the Td values higher than the corresponding T value. In such layers the probability of clouds is high.

In Fig. 3.29 location ‘a’ indicates cloud free area, location ‘b’ shows area covered by small cumulus clouds and location ‘c’ is in a cumulonimbus cloud. The profiles in these locations are shown in Fig. 3.30. They are reflecting very well the environment in the chosen locations. At location ‘b’ low level cloud is well seen and possibly also covered by thin Cirrus cloud. At location ‘c’ the profile suggests a deep convective cloud.

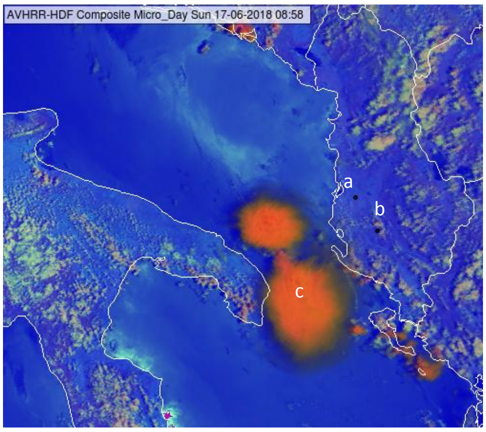

Fig. 3.29: AVHRR Day Microphysics RGB at 08:58 UTC on 17 June 2018.

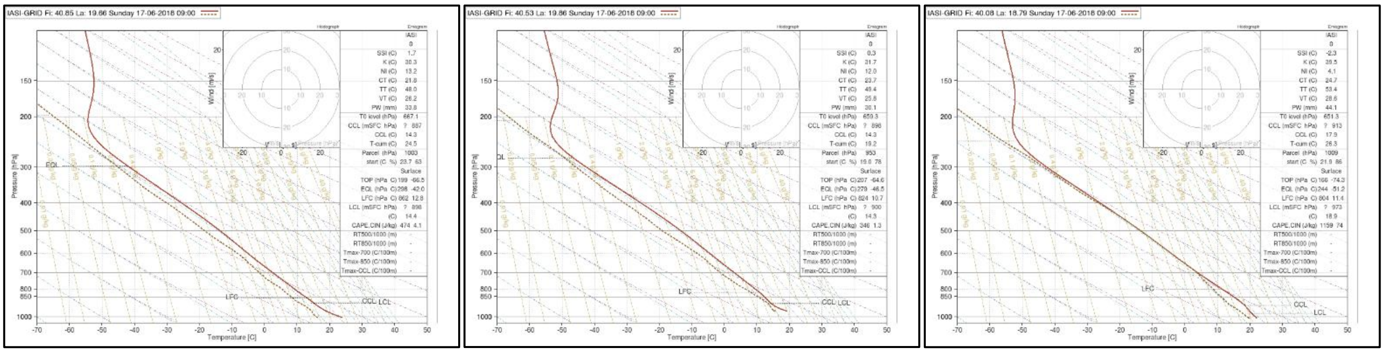

Fig. 3.30: IASI temperature (solid line) and dew point (broken line) profiles at location ‘a’ (left), at location ‘b’ (middle) and at location ‘c’ (right) indicated in Fig. 3.29.

Fig. 3.31 shows a profile at the location indicated by the left panel. According to the RGB image and the NWCSAF Cloud Type product this cloud is a mid-level cloud. IASI profile suggests mid-level cloud and cirrus cloud.

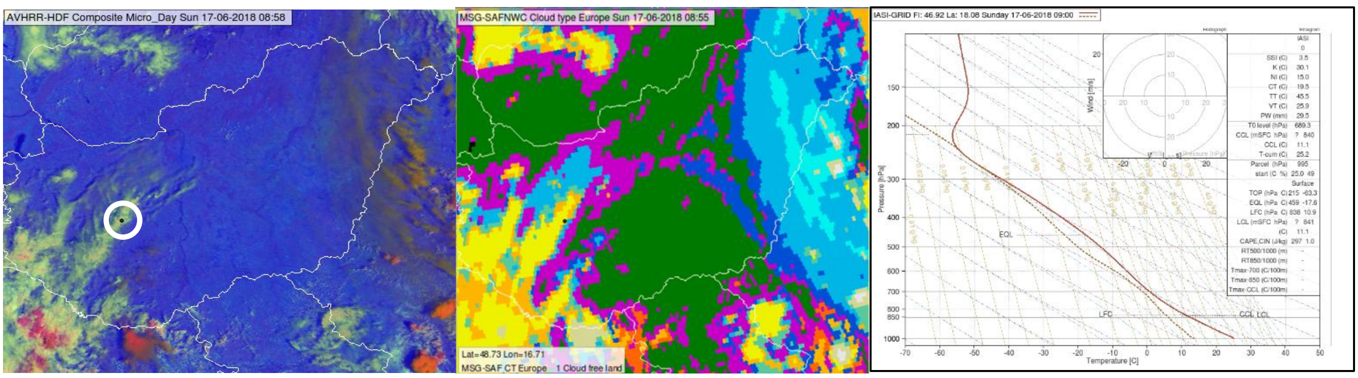

Fig. 3.31: AVHRR Day Microphysics RGB (left), NWCSAF Cloud Type product (middle panel) and IASI temperature (solid line) and dew point (broken line) profiles at the location marked by the circle (right) at 08:58 UTC on 17 June 2018.

3.3. Cases with added value

Over the convective period we found added value to the ECMWF forecast only in few per-cents of the cases. This is due to the fact that the ECMWF forecast is very often reliable and we only regarded Hungary which is a very small country. For a bigger area with half hourly IRS data there might be more ‘added-value’ cases.

3.3.1. Case 4 June 2018

The IASI derived parameters and profiles presented in this case study were derived from **IASI L2 (MWIR)** product, except the Fig.3.38, where **IASI L2 (IRON)** product is also shown. In the MWIR products the retrieved profiles are based both on infrared and microwave measurements, while in the IRON products they are based only on infrared measurement. The vertically averaged uncertainty of the IASI derived T and Td profiles were low to moderate in the studied areas.

On 4 June 2018 there were no fronts close to Hungary (Fig. 3.32). Thunderstorms formed during the day inside a warm and moist airmass. Hungarian weather forecasters expected several thunderstorms to form in the country during this day. However, in south-western Hungary fewer thunderstorms formed than expected.

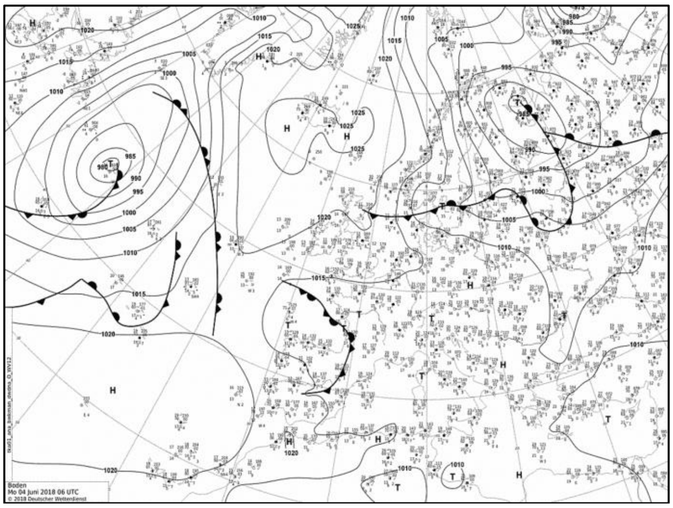

Fig. 3.32: Surface chart for 06 UTC. (Source: wetter3.de)

Fig. 3.33 shows the cloudiness at the time of the METOP overpass before the thunderstorm formed and in the afternoon.

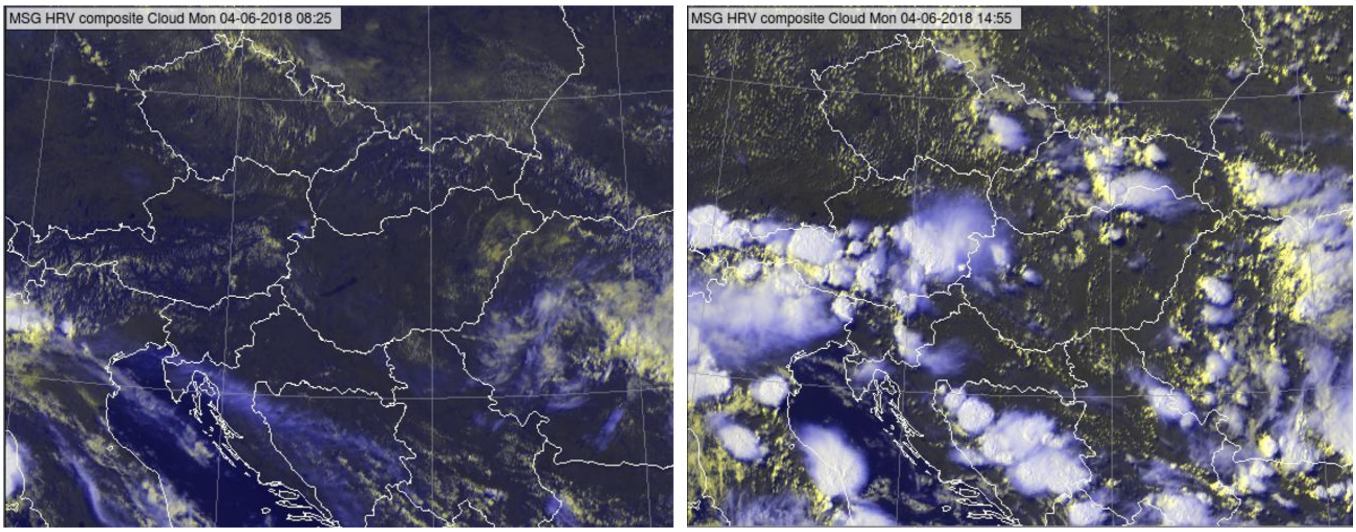

Fig. 3.33: SEVIRI HRV Cloud RGB at 08:25 (left) and 14:55 UTC (right).

In northwest of Croatia (and surrounding area), the IASI derived TPW was much lower than the forecasted one (Fig. 3.34). Here almost no thunderstorm formed and the thunderstorms formed elsewhere and advected above this area dissipated rather fast.

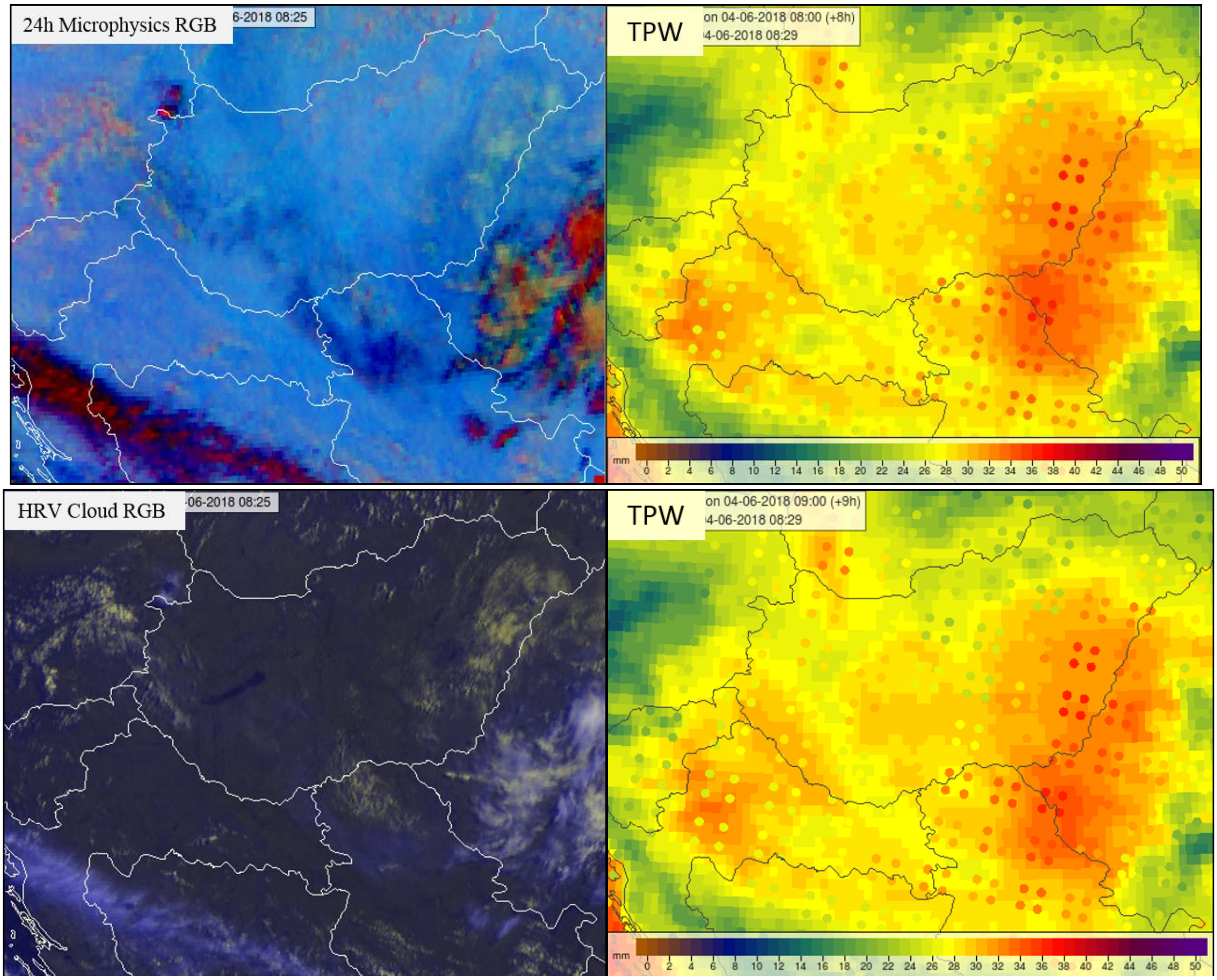

Fig. 3.34: SEVIRI 24-hour Microphysics RGB (upper left), ECMWF forecasted TPW valid for 08 UTC overlaid by IASI derived TPW measured at 08:29 UTC (upper right), SEVIRI HRV Cloud RGB (bottom left), ECMWF forecasted TPW valid for 09 UTC overlaid by IASI derived TPW measured at 08:29 UTC (bottom right). SEVIRI images were taken at 08:25 UTC.

IASI derived TPW shows a maximum around the Hungarian-Romanian border elongated to the south (see Fig. 3.35). Similar shape is seen in the 24-hour Microphysics RGB with darker blue shades on the cloud free regions indicating low-level moisture. HRV Cloud RGB image (bottom left panel of Fig. 3.34) shows here more small cumulus clouds than outside this region confirming the higher moisture content. ECMWF also forecasted a TPW maximum along this region, but the shape of this maximum is broader; see the right panels of Fig. 3.34. Fig. 3.36 shows instability indices. IASI derived lower instability for northwest Croatia than ECMWF forecasted.

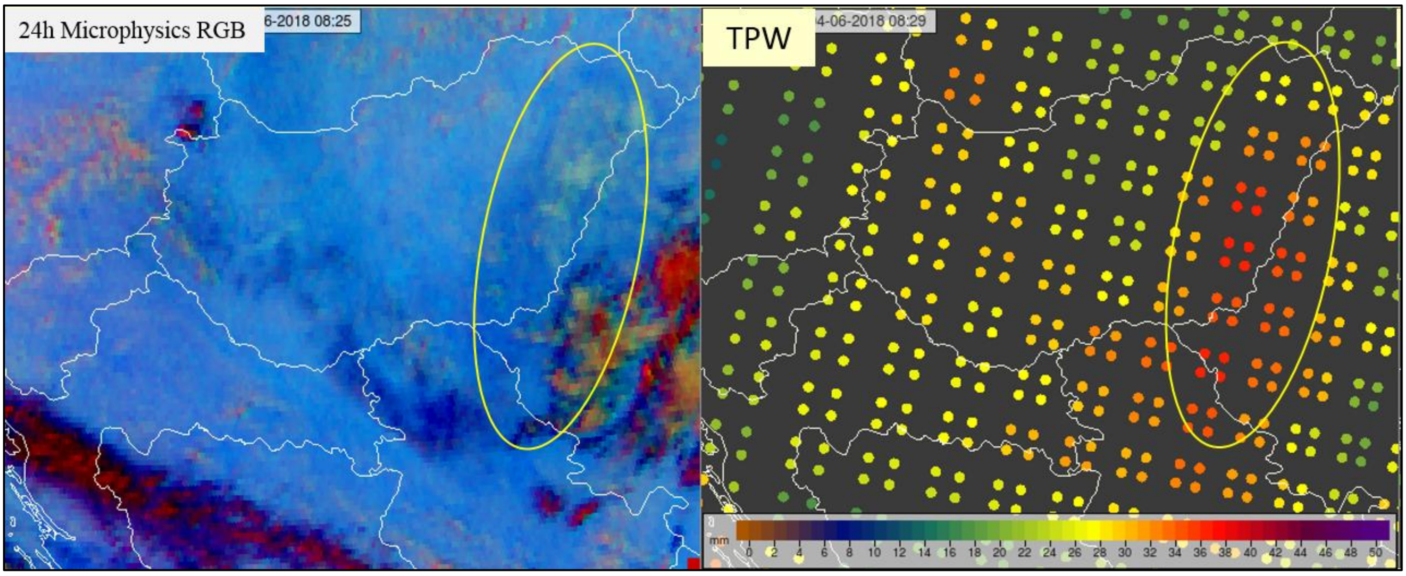

Fig. 3.35: SEVIRI 24-hour Microphysics RGB taken at 08:25 UTC (left), IASI derived TPW measured at 08:29 UTC (right).

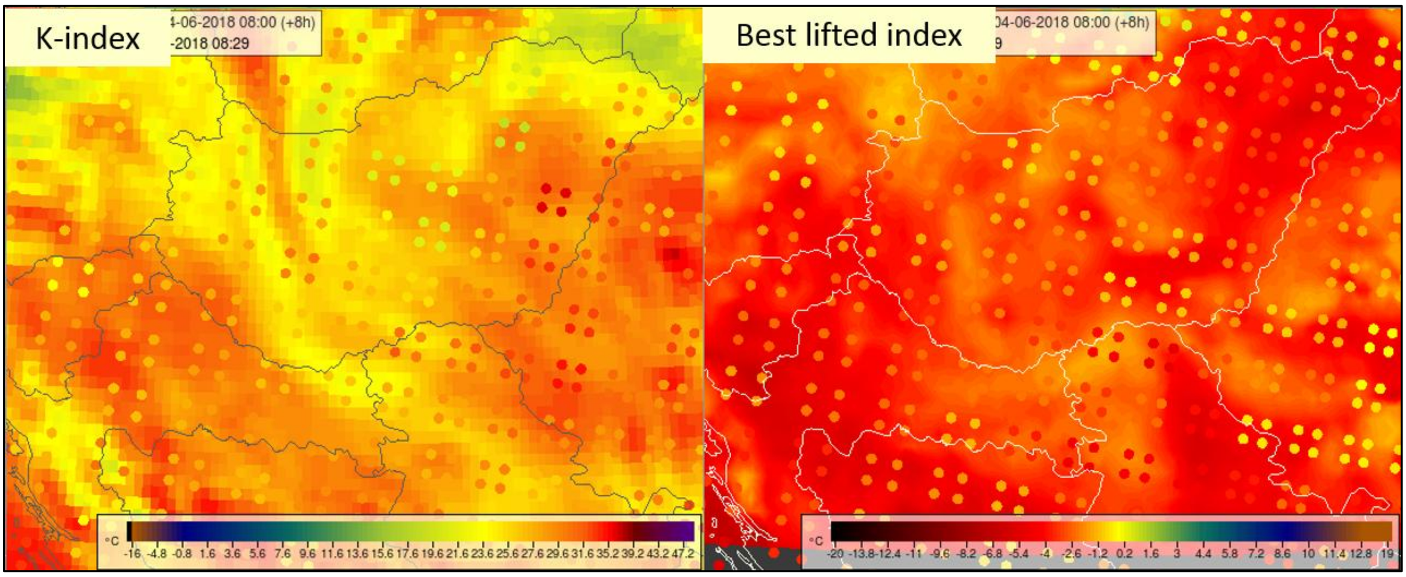

Fig. 3.36: ECMWF forecasted K-index valid for 08 UTC overlaid by IASI derived K-index measured at 08:29 UTC (left) and ECMWF forecasted Best lifted index valid for 08 UTC overlaid by IASI derived Best lifted index measured at 08:29 UTC (left).

To analyse the IASI and ECMWF data in more detail, we visualised the profiles in several locations. Fig. 3.37 shows ECMWF and IASI profiles in the studied Croatian region, where the IASI profiles indicate much less TPW than the forecast. The black circle in the left panel indicates the location of the forecasted and IASI derived profiles presented on the right panel.

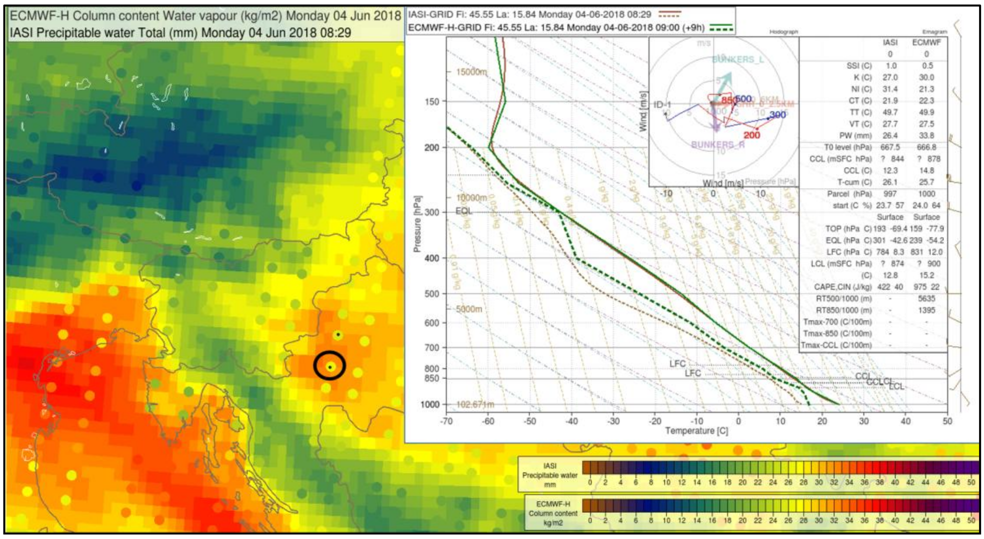

Fig. 3.37: ECMWF forecasted Total Precipitable Water overlaid by IASI Total Precipitable Water (left), ECMWF forecasted and the IASI derived Temperature and Dew point profiles (right). IASI data measured on at 08:29 UTC, while ECMWF forecast valid for 09 UTC. The circle in the left panel shows the location of the profiles presented on the right panel.

In Fig. 3.37 the IASI and ECMWF temperature profiles are almost the same in the troposphere. However, the whole IASI profile is drier than the forecast. The ECMWF dew point profile is close to its temperature profile at the top of the boundary layer. In such cases often small cumulus clouds appear. However, in the 08:25 UTC SEVIRI HRV Cloud RGB image there are no cumulus clouds in this region, (see the bottom left panel of Fig. 3.34). This hints that the IASI dew point profile might be more realistic (at least in the low layer).

The 04 June 2018 case was studied with IASI L2 (IRON) data as well. The main question was whether the added value found with IASI L2 (MWIR) data is present with IR-only data as well. As Fig.3.38 shows the 'added value' (that IASI has not confirmed the ECMWF forecasted TPW maximum over northwest Croatia) is present not only with IASI MWIR data but also with IASI IRON data.

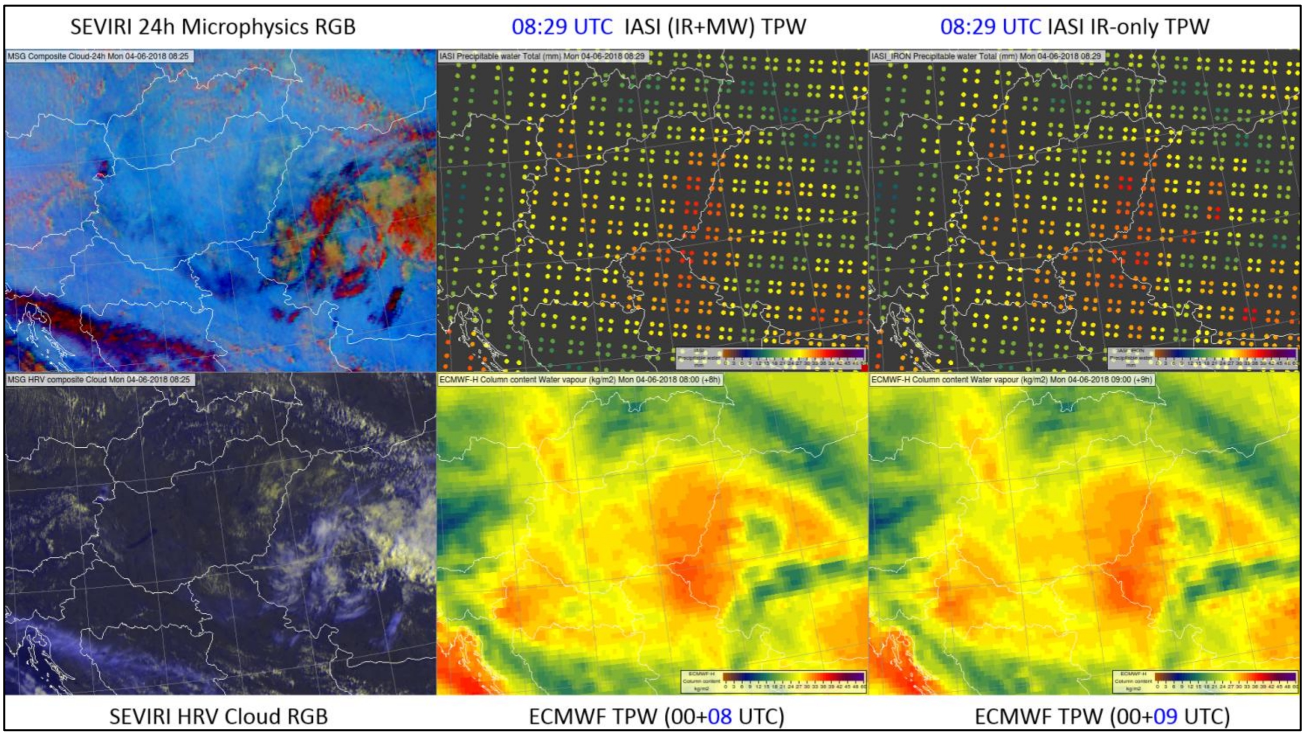

Fig.3.38: SEVIRI 24-hour Microphysics RGB (upper left), IASI L2 (MWIR) derived Total Precipitable Water (upper middle panel), IASI L2 (IR-only) derived Total Precipitable Water (upper right), SEVIRI

HRV Cloud RGB (bottom left), ECMWF forecasted Total Precipitable Water valid for 08 and 09 UTC (bottom middle and right panels). SEVIRI images taken at 08:25 UTC, IASI data measured at 08:29 UTC.

More detailed analyses of this case can be found in the presentations of first and second progress meetings.

3.3.2. Case 18 July 2019

Hungary was situated between two large-scale lows and influenced by an intermediary anti-cyclone (Fig. 3.39) without any frontal structures. The two lows were accompanied by long-wave troughs aloft (Fig. 3.40), and, embedded in the eastern one, a smaller scale disturbance was approaching the country from northwest, which led to the destabilization of atmosphere above the investigated area. The forecasters were expecting convection in the western part of the country (above the Transdanubian region) in the morning hours.

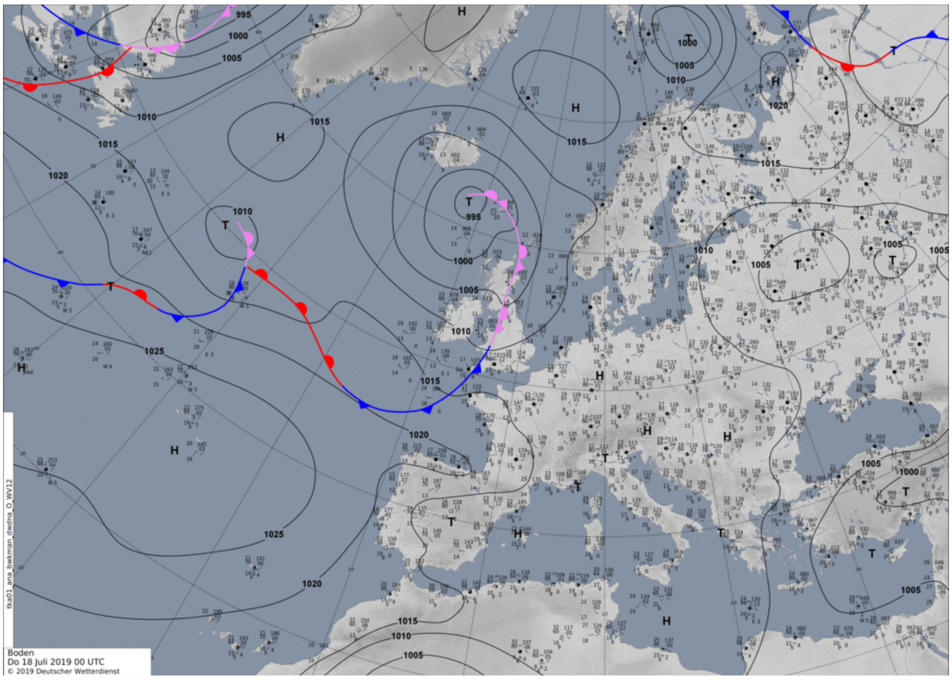

Fig. 3.39: Synoptic situation over Europe on 18 July 2019, at 00 UTC.

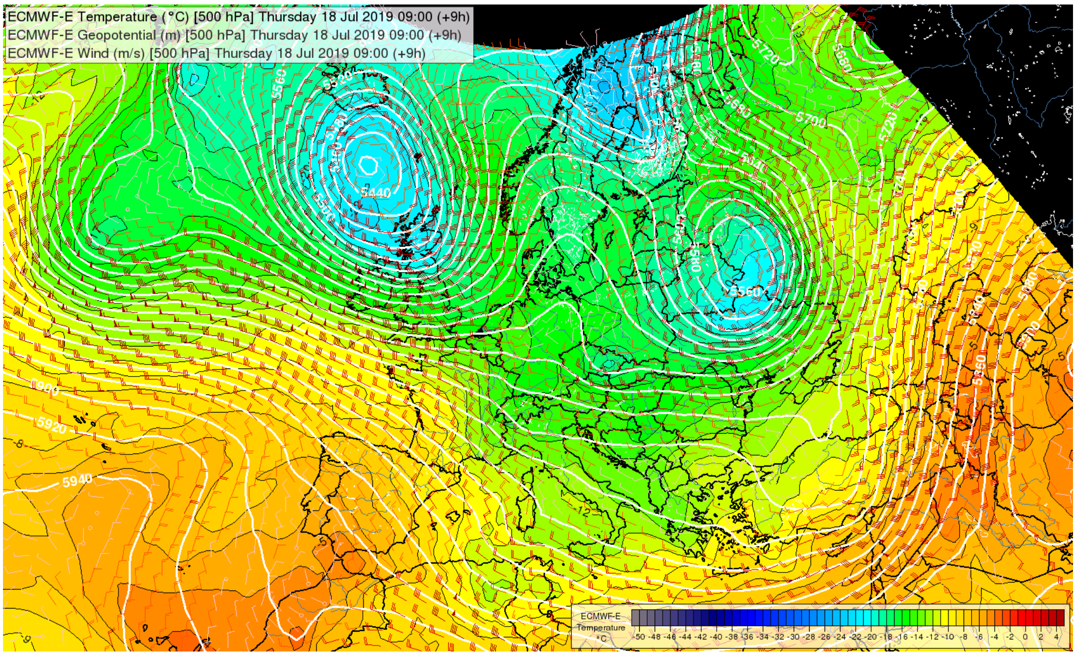

Fig. 3.40: 500 hPa temperature, wind and geopotential field over Europe at +09 hour forecasted by the 00 UTC 18.07.2019 ECMWF run.

However, the IASI measurements at the 09:05 UTC pass indicated less favourable conditions for thunderstorm development above that region (Fig. 3.41 – see the area around by the small, black-contoured hollow circle!). The IASI MLCAPE was considerably smaller than the ECMWF forecast (which is a common phenomenon), and the IASI Best Lifted Index was somewhat higher (still indicating unstable conditions though), as well. The TPW values were quite similar, while the average relative humidity was somewhat lower.

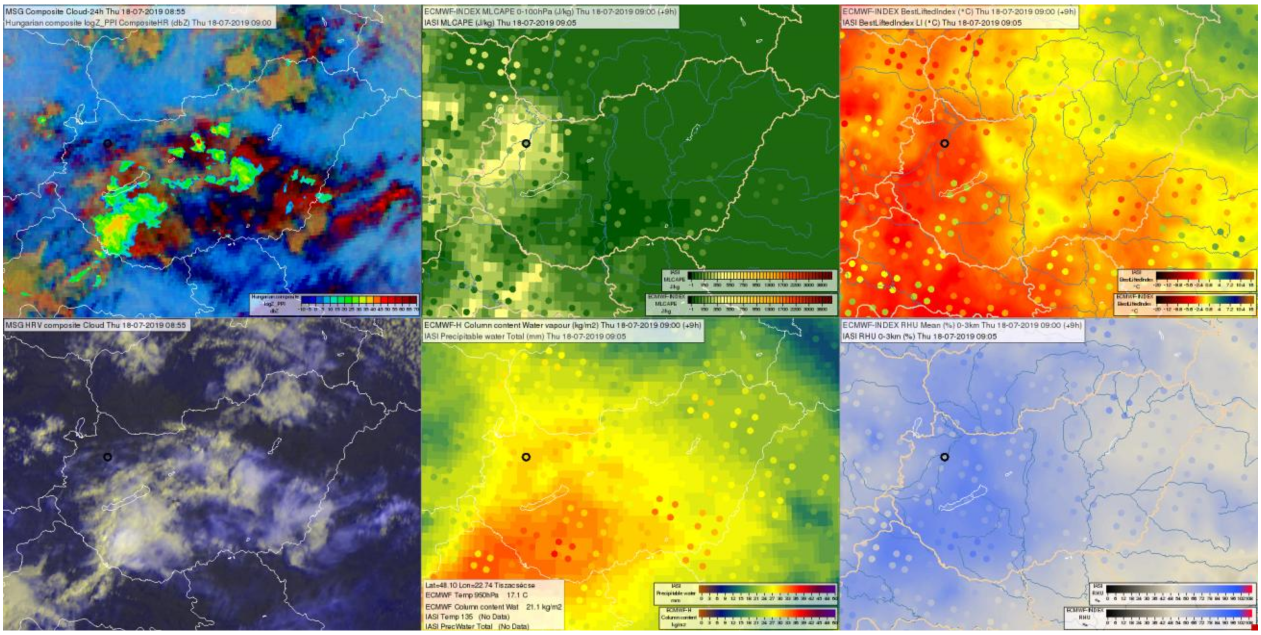

Fig. 3.41: Upper row: Left – column maximum radar reflectivity at 09:00 UTC overlaid on SEVIRI 24-hour Microphysics RGB at 08:55 UTC, Middle – IASI MWIR MLCAPE overlaid on ECWMF forecasted MLCAPE at 09:05 UTC, Right – IASI MWIR BLI overlaid on ECMWF BLI at 09:05 UTC. Bottom row: Left - SEVIRI HRV RGB at 08:55 UTC, Middle – IASI MWIR TPW overlaid on ECWMF TPW at 09:05 UTC, IASI MWIR, Right – relative humidity in 0-3 km layer overlaid on ECWMF relative humidity in 0-3 km layer at 09:05 UTC. ECMWF data valid for 09 UTC on 18 July 2019 (00 UTC run from the same day). The hollow black-contoured circle indicates the location of vertical profiles in Fig. 3.42.

If we look at the vertical profile of IASI temperature and moisture above the selected point (Fig. 3.42– denoted by a black-contoured hollow circle in Fig. 3.41), moderate-to-low instability can be seen (561 J/kg Surface Based CAPE) and some Convective Inhibition (12 J/kg). (See the CAPE, CIN parameters in the parameter list located on the left site of the profile plots.) The area of the Convective Inhibition was elongated in the vertical, so a deeper lifting would have needed to overcome this inhibition, which might have decreases the chance of deep convection initiation. The result of SYNOP merging indicated even smaller available convective energy (Fig. 3.42– see the middle picture), which caused by the fact that the surface dew point was appreciably lower in the SYNOP measurement than in the IASI. (The dew point difference was around 2.6 degrees. The CAPE is especially sensitive to the dew point temperature of initiation level). In summary, according IASI data the conditions were not favourable for the formation of deep convection at that time and over that region, while ECMWF forecasted low inhibition and around 750 J/kg surface based CAPE. However, when we merged the ECMWF field with SYNOP data at the surface we obtained lower SBCAPE, as well (not shown).

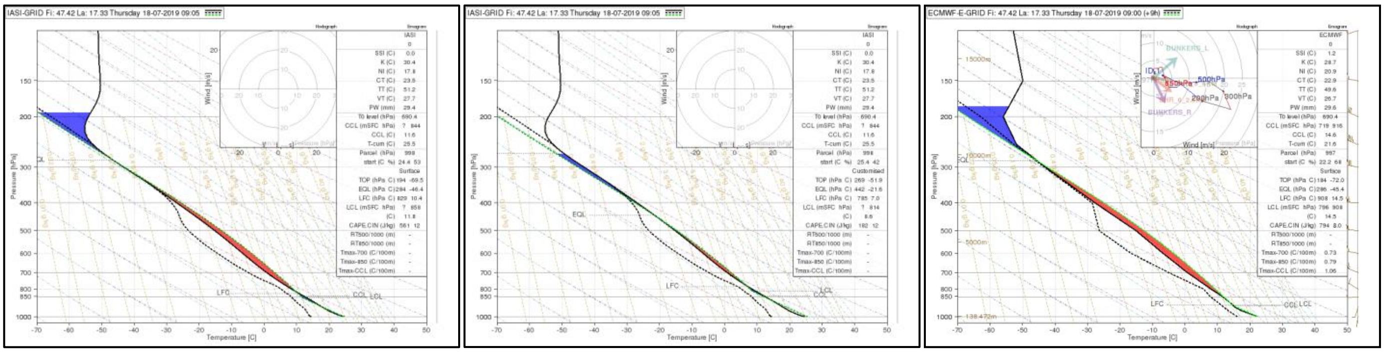

Fig. 3.42: Temperature and Humidity profiles on 18 July 2019. Left – IASI L2 MWIR at 09:05 UTC, Middle – IASI L2 merged with Synop at 09:05 UTC, Right – ECMWF forecast valid for 09 UTC.

And in reality, thunderstorm indeed did not develop over this area before 12 UTC (Fig. 3.43), only stratiform-like precipitation clouds were present to the south of the investigated area. It is needed to note that around 10-11 UTC smaller thunderstorms were approaching from the west and entered in the country, and later on, around 12 UTC, when the CIN might have eliminated, strong thunderstorms formed over the previously inhibited area.

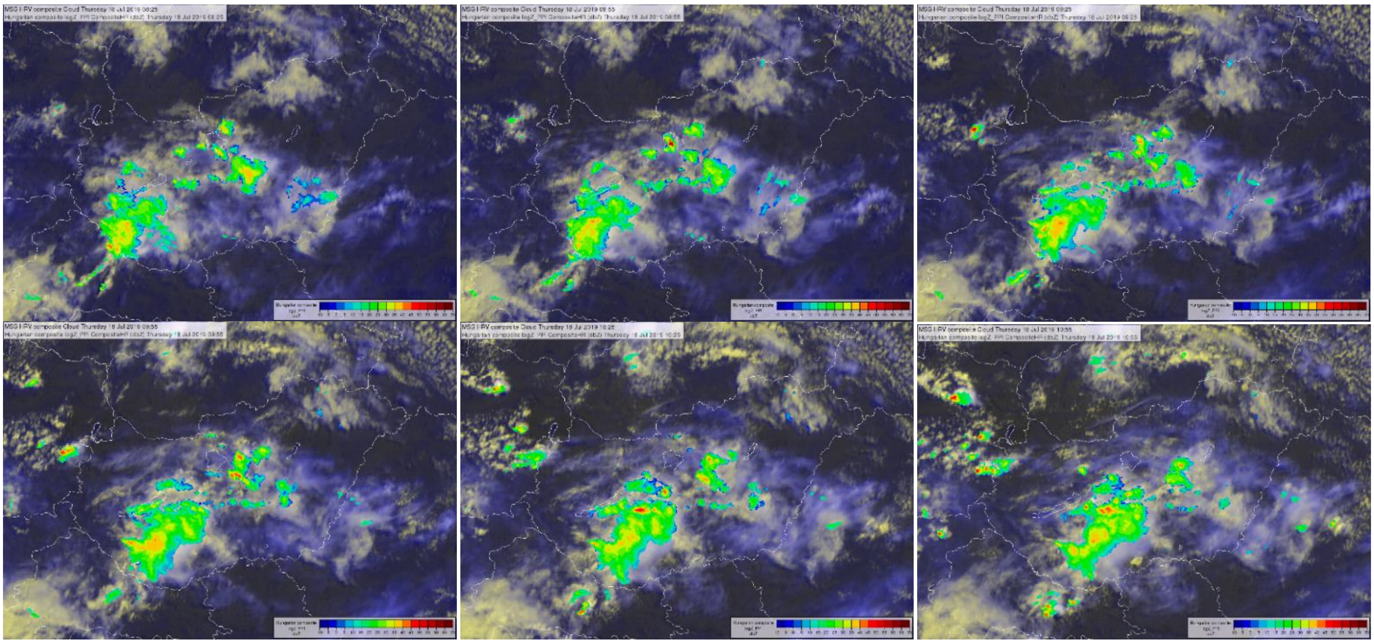

Fig. 3.43: Hungarian Radar Composite image overlaid on SEVIRI HRV Cloud RBG image at 08:25 UTC, 08:55 UTC, 09:25 UTC (upper row), 09:55 UTC, 10:25 UTC, 10:55 UTC (lower row) on 18 July 2019.

Meanwhile, in the middle part of the country, near Budapest, deep convection was initiated around 08-09 UTC (already seen in the upper left panel of Fig. 3.44, southeast of the black circle), where the ECMWF expected less instability. The IASI products indicated similarly low stability values, so at first glance, they corroborated the ECMWF prognosis. However, if we inspect the vertical profile temperature and moisture produced by IASI (Fig. 3.45) around the development time and location of the studied storm (see the black circle in Fig. 3.44), considerable surface based CAPE (445 J/kg) can be seen without any CIN. After the merging with the SYNOP data at the surface, low-to-moderate instability (324 J/kg) with no inhibition still remained in the column above the point. This instability might be partly due to the strong lapse rate around 800 hPa, which was absent in the ECMWF model vertical profile (see Fig. 3.45 right-hand side), and therefore the latter produced little CAPE (115 J/kg) and non-zero CIN (27 J/kg). So, the IASI seemingly caught the actual state of the convective environment as opposed to the ECMWF. However, this condition was only visible when we looked at the surface based stability parameters and examined the vertical profiles. This reinforces that conclusion, that the use surface based parameters such as SBCAPE can be more beneficial than the mixed layer versions when we are dealing with IASI products.

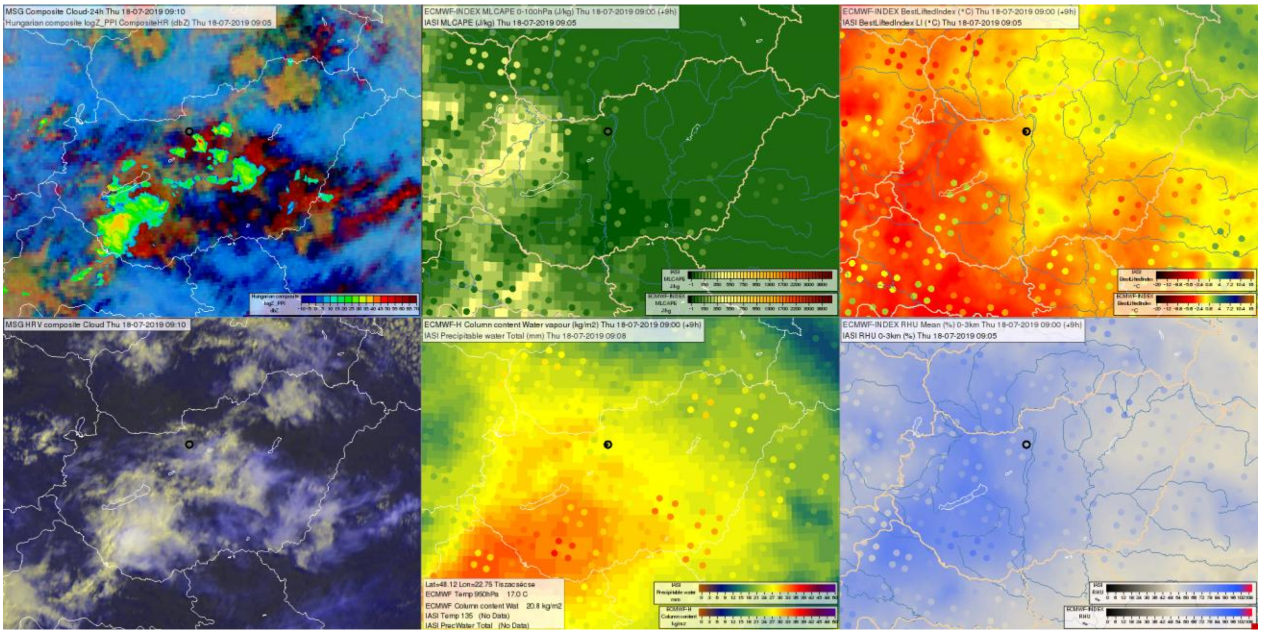

Fig. 3.44: Upper row: Left – column maximum radar reflectivity at 09:00 UTC overlaid on SEVIRI 24-hour Microphysics RGB, Middle – IASI MWIR MLCAPE overlaid on ECWMF forecasted MLCAPE, Right – IASI MWIR BLI overlaid on ECWMF BLI. Bottom row: Left - SEVIRI HRV Cloud RGB, Middle – IASI MWIR TPW overlaid on ECWMF TPW, Right – IASI MWIR relative humidity in 0-3 km layer overlaid on ECWMF relative humidity in 0-3 km layer. SEVIRI images were taken at 08:55 UTC. IASI measurements are from 09:05 UTC. ECMWF data valid for 09 UTC on 18 July 2019 (00 UTC run from the same day). The hollow, black-contoured circle indicates the location of vertical profiles in Fig. 3.45.

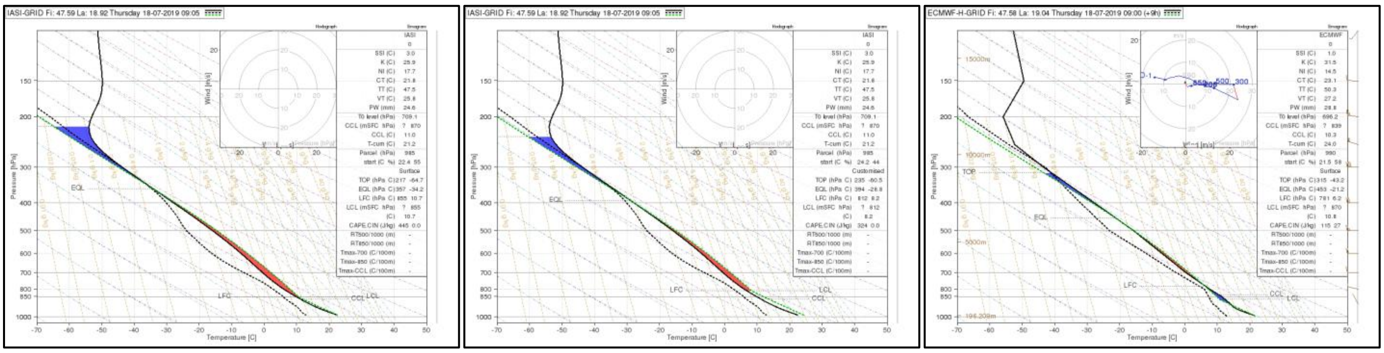

Fig. 3.45: Temperature and Humidity profiles on 18 July 2019. Left – IASI L2 MWIR at 09:05 UTC, Middle – IASI L2 MWIR merged with Synop at 09:05 UTC, Right – ECMWF forecast valid for 09 UTC.

Summarising this case:

The IASI showed less favourable conditions for storms in the Transdanubian region comparing with the ECMWF, and the convection was indeed absent in the next 2-3 hours.

Near Budapest, the IASI caught the steep lapse rate and the absence of CIN (in contrast to ECMWF) which led to a storm formation. However, this was only detectable if the surface based instability parameters and the vertical profile above the point was investigated. In this region, the IASI provided added value to the ECMWF forecast, though the actual formation of storms preceded its passing time, so the actual benefit from forecasting point of view was not realized.

3.3.3. Case 20 June 2019

On the **20 June 2019** thunderstorms developed throughout the day, starting around 08:00 UTC in the north- and southeast part of Hungary (Fig. 3.47). A low pressure gradient situation was present therefore local features influenced the convection (Fig. 3.46). ECMWF forecasted considerable instability in the eastern and western part of the country (CAPE > 2000 J/kg). Largest moisture was predicted in the northern and eastern areas, and convection was expected over the whole day.

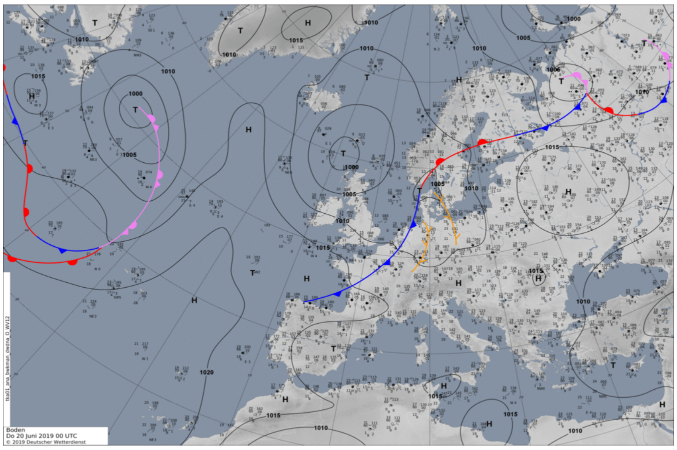

Fig. 3.46: Synoptic situation over Europe on 20 June 2019 at 00 UTC. (Source: DWD)

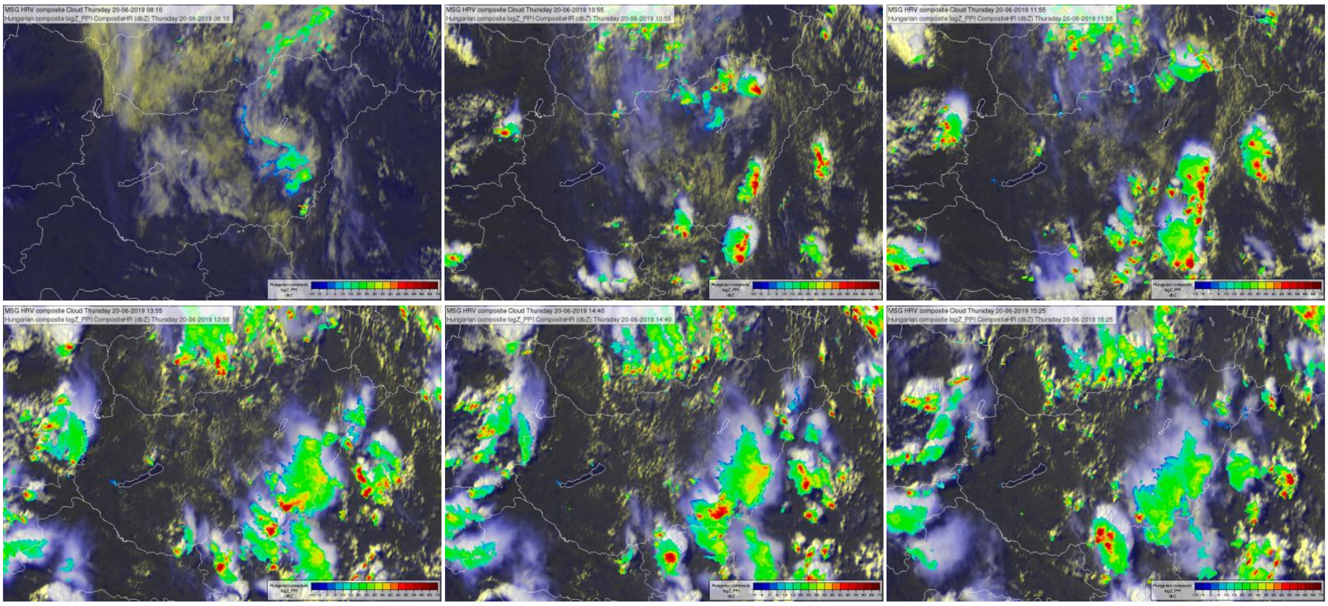

Fig. 3.47: Hungarian Radar Composite image overlaid on SEVIRI HRV Cloud RBG image at 08:10 UTC, 10:55 UTC, 11:55 UTC (upper row), 13:55 UTC, 14:40 UTC, 15:25 UTC (lower row) on 20 June 2019.

IASI L2 data showed less instability than ECMWF almost everywhere except south Hungary and around Budapest (Fig. 3.48). IASI derived TPW was also higher in these regions.

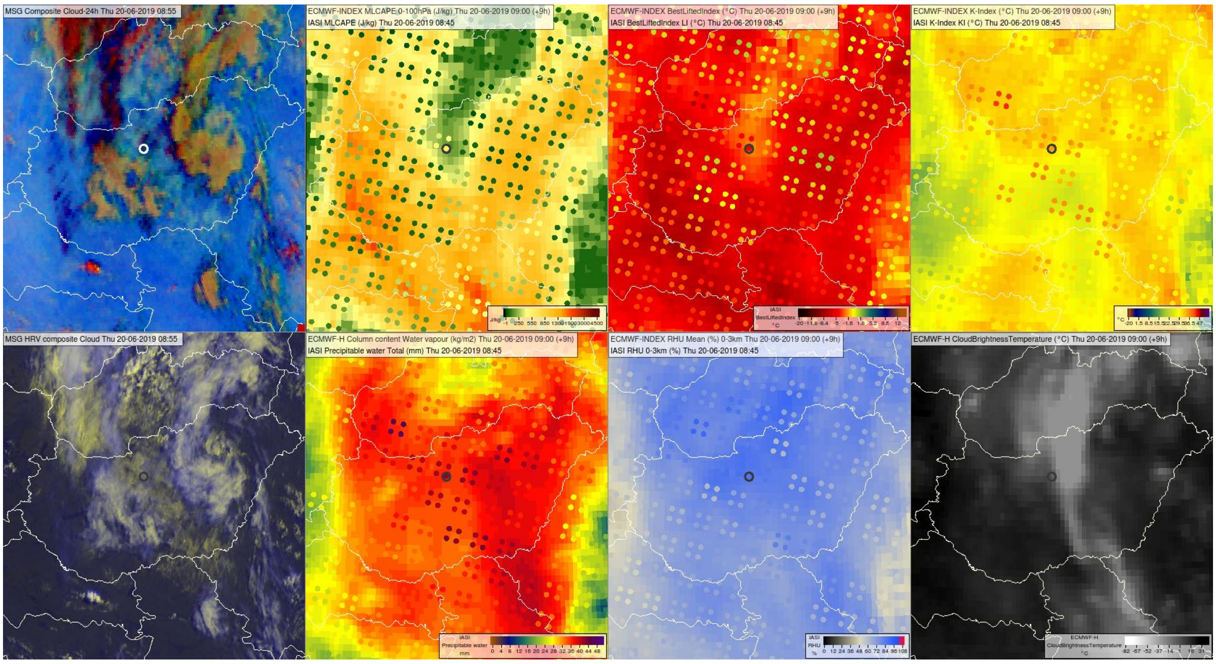

Fig. 3.48: Upper row: SEVIRI 24-hour Microphysics RGB at 08:55 UTC, IASI MWIR MLCAPE overlaid on ECWMF-forecasted MLCAPE, IASI MWIR Best lifted index overlaid on ECMWF Best lifted index, IASI MWIR K-index overlaid on ECWMF K-index; bottom row: SEVIRI HRV Cloud RGB at 08:55 UTC, IASI MWIR TPW overlaid on ECWMF TPW, IASI MWIR relative humidity in 0-3 km layer overlaid on ECWMF relative humidity in 0-3 km layer, ECMWF simulated 10.8 μm brightness temperature. IASI data measured at 08:45 UTC, ECMWF data valid for 09 UTC on 2 June 2019.

In South Hungary the ECMWF forecasted considerable instability which was also supported by IASI. IASI L2 data showed more moisture in this region (42.8 mm against 37.9 mm, see the PW values in the parameter lists in the right side of the panels of **Fig. 3.49**). Merging IASI data with Synop measurements corroborated the forecast even more as the SBCAPE values rose even higher (see the CAPE values in the parameter lists of Fig. 3.49). Comparing the profiles for Szeged city, ECMWF forecasted profile was a lot dryer in the layer between 900 and 600 hPa (Fig. 3.49).

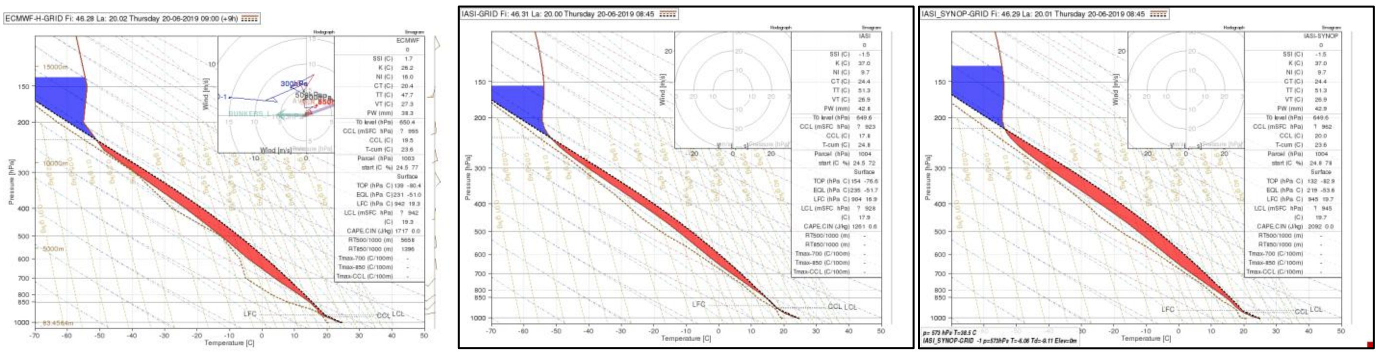

Fig. 3.49: Temperature and humidity profiles for Szeged city on 20 June 2019. Left: ECMWF forecasted valid for 09 UTC. Middle: IASI L2 MWIR at 08:45 UTC. Right: Merged IASI L2 with Synop at 08:45 UTC.

Fig. 3.48 showed higher instability in the IASI parameters compared to ECMWF around Budapest. The cloudiness forecasted by the model was different from the actual cloudiness (Fig. 3.50) which can be a possible reason for the large differences in the IASI and ECMWF instability indices in this location. In the lowest layer ECMWF temperature profile was a lot colder (Fig. 3.51) than the IASI temperature profile; the latter might be closer to reality as the measured surface temperature was closer to the IASI-retrieved temperature (Table 3.2). In addition ECMWF forecasted humidity profile was also drier than the IASI-retrieved one.

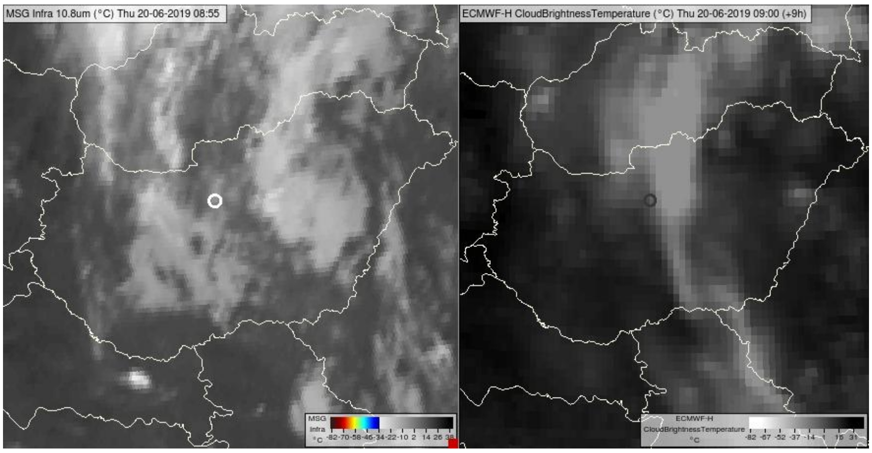

Fig. 3.50: SEVIRI IR10.8 image at 08:55 UTC (left) and ECMWF simulated BT10.8 image valid at 09 UTC on 20 June 2019.

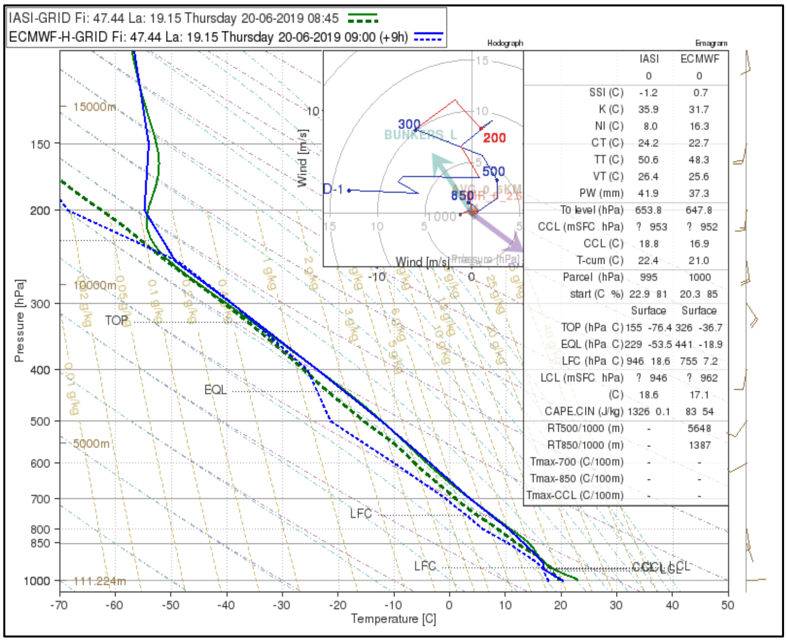

Fig. 3.51: ECMWF (blue) valid for 09 UTC and IASI MWIR (green) at 08:45 UTC temperature (solid line) and humidity (broken line) profiles on 20 June 2019.

	Synop 08:50 UTC	ECMWF 09 UTC	IASI 08:45 UTC
2 m temperature (°C)	22.9	20.3	22.9
2 m dew point (°C)	18.2	18.6	19.5

Table 3.2: 2 meter temperature and dew point values.

3.4. Example cases when IASI confirm the forecast

There were several cases when the IASI data confirmed the ECMWF forecast. Two cases are presented here as examples.

3.4.1. Case 3 August 2018

The IASI derived parameters and profiles presented in this case study were derived from **IASI L2 (MWIR)** product.

On 3 August 2018, a front was situated north-west from Hungary; see the surface chart of 6 UTC in Fig. 3.52.

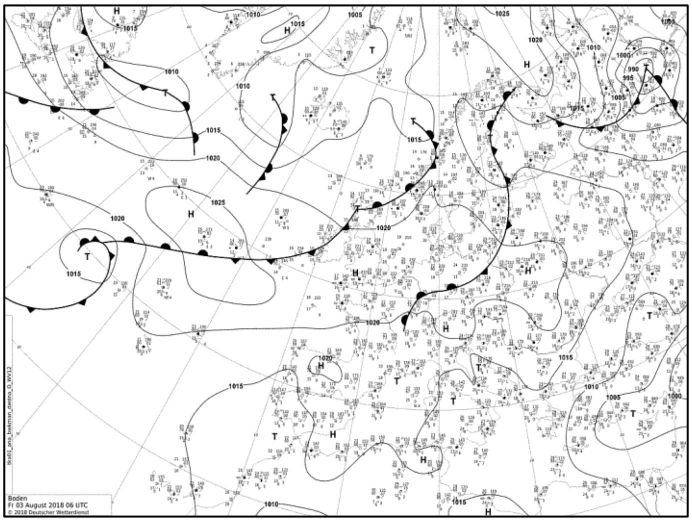

Fig. 3.52: Surface chart for 03 August 2018, 06 UTC.

At the time of the METOP overpass, SEVIRI 24-hour Microphysics RGB (left panel of Fig. 3.53) showed large cloud-free regions, and the low-level moisture distribution was also visible (more blue shades indicating more moisture at low levels). Over the Baltic countries, Poland, East Germany and northwest Czech Republic, a mainly cloud-free frontal region was elongated where the moisture content was higher. In Hungary, that day thunderstorms formed mainly over west and southeast of the country (right panel of Fig. 3.53). No thunderstorms formed over the northeast corner of the country.

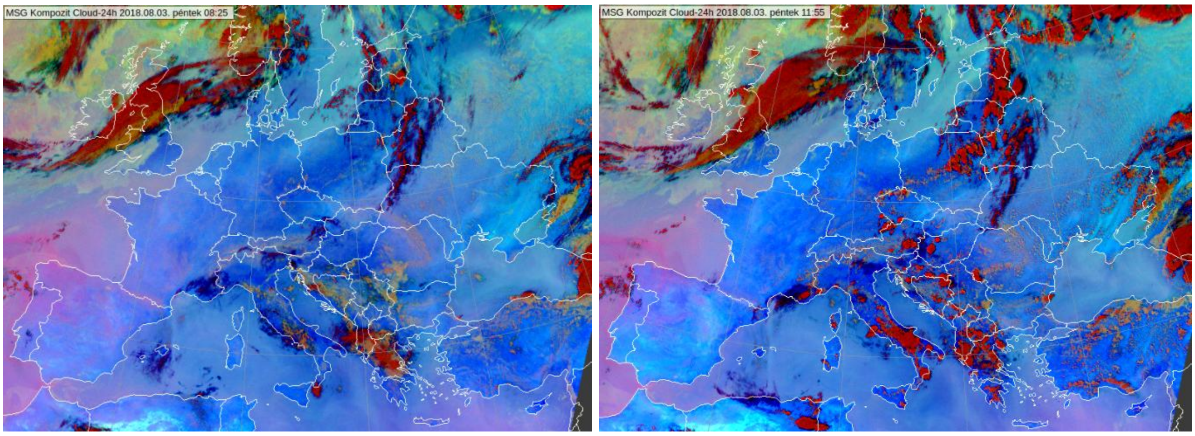

Fig. 3.53: SEVIRI 24-hour Microphysics RGB taken at 08:25 UTC (left) and 11:55 UTC (right).

At the time of the Metop overpass, the country was mainly cloud-free, except some small cumulus clouds and very thin cirrus clouds (Fig. 3.54). The IASI and the ECMWF TPWs are shown in Fig. 3.54, while the instability parameters are displayed in Fig. 3.55. Both the IASI and ECMWF yielded high TPW values over the country except in the northeast region. Here, large differences were found between IASI and ECMWF moisture and instability parameters, first of all in the TPW. IASI yielded even less TPW than the ECMWF forecast. ECMWF predicted rather stable environment in the studied region (see the CAPE distribution in the bottom panel of Fig. 3.55). IASI produced even lower instability in that region than the forecast (see the upper panels of Fig. 3.55). Note that the averaged uncertainty of IASI-retrieved T and Td profiles were less than 1.2 and 2 K, respectively; indicating that the uncertainty of the IASI-retrieved environmental parameters might be low.

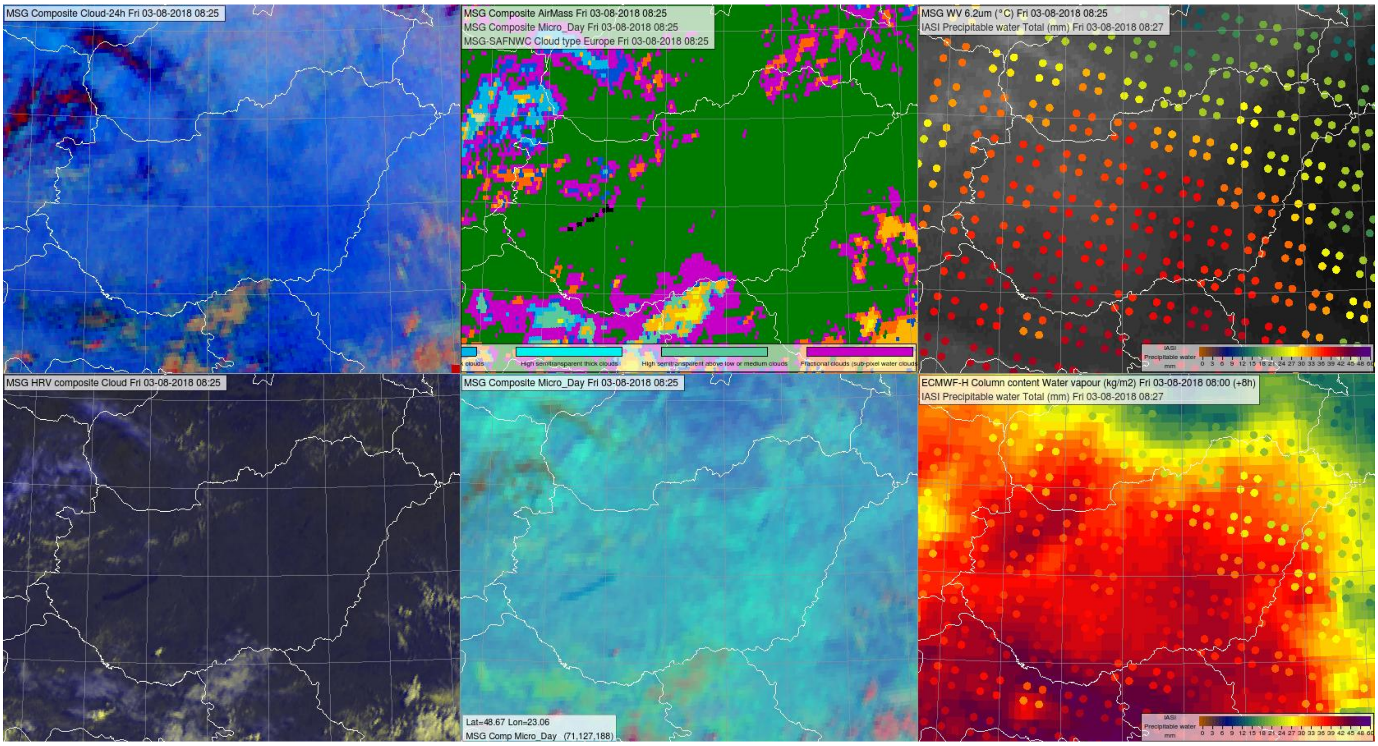

Fig. 3.54: SEVIRI 24-hour Microphysics RGB (upper left), NWCSAF Cloud Type product (upper middle panel), IASI-derived Total Precipitable Water (upper right), SEVIRI HRV Cloud RGB (bottom left), SEVIRI Day Microphysics RGB (bottom, middle panel), ECMWF-forecasted Total Precipitable Water overlaid by IASI Total Precipitable Water (bottom right). SEVIRI images taken on 03 August 2018 at 08:55 UTC, IASI data measured at 08:27 UTC, while ECMWF forecast valid for 08 UTC.

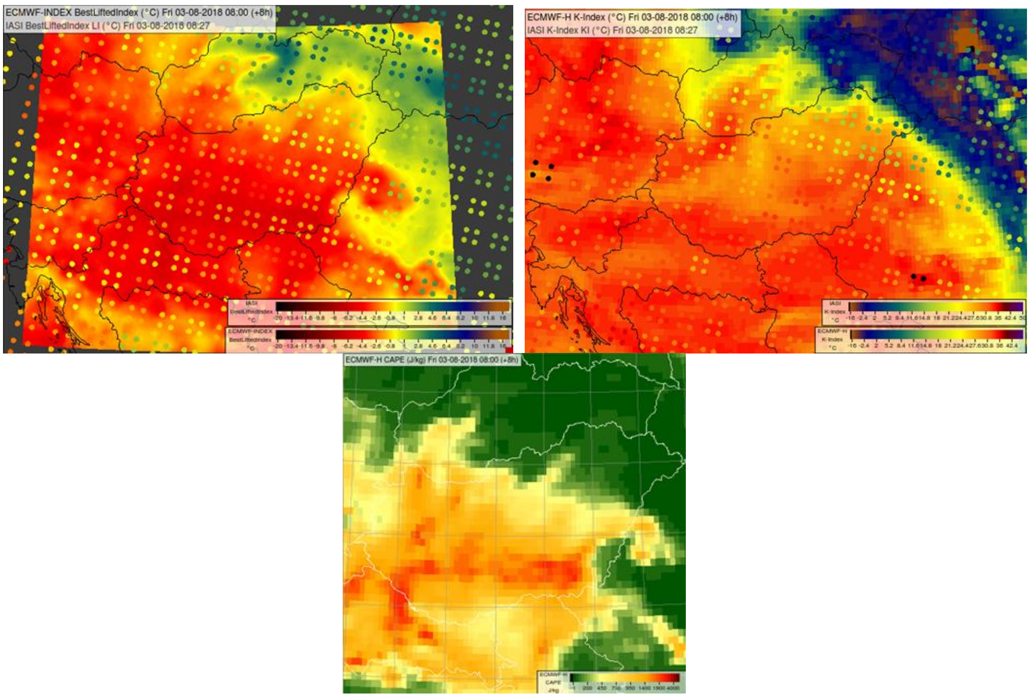

Fig. 3.55: ECMWF forecasted Best Lifted Index overlaid by IASI derived Best Lifted Index (upper left), ECMWF forecasted K-index overlaid by IASI derived K-index (upper right), ECMWF forecasted CAPE (bottom). ECMWF forecast valid for 08 UTC, IASI measured at 08:27 UTC.

To analyse the IASI and ECMWF data in more detail, we visualised the profiles in several locations. In Fig.3.56 and Fig. 3.57, we present a profile-pair in the studied northeast region and another one in an unstable region within the capital. The circle in the right panel of Fig.3.56 indicates the location of the forecasted and IASI-derived profiles presented on the left panel.

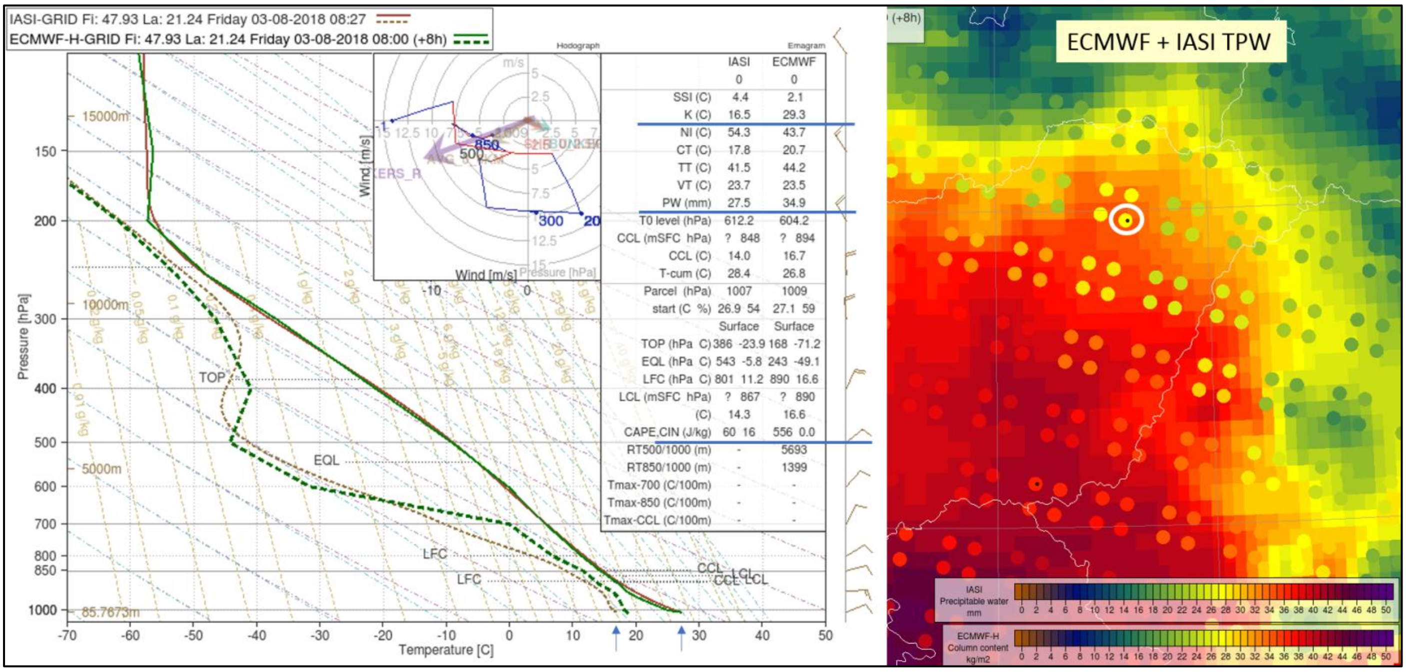

Fig.3.56: ECMWF-forecasted and IASI-derived Temperature and Dew point profiles in green and brown colours (left), ECMWF-forecasted Total Precipitable Water overlaid by IASI Total Precipitable Water (right). IASI data measured on at 08:27 UTC, while the ECMWF forecast valid for 08 UTC. The circle in the right panel shows the location of the profiles presented on the left panels.

Both IASI and ECMWF profiles showed a very dry layer between 300 and 700 hPa. Note that, at 12 UTC, the nearest radiosonde measurement (shown in Fig. 3.58) confirmed this very dry layer. The low layer is drier according the IASI data than forecasted. The blue arrows in the left panel show the surface T, Td measurements. Surface Td measurement was closer to the IASI surface Td value.

We analysed IASI and ECMWF profiles in several locations in the unstable region, as well. One profile pair is shown in Fig. 3.57. The circle on the right panel indicates the location of the forecasted and IASI derived profiles presented on the left panel.

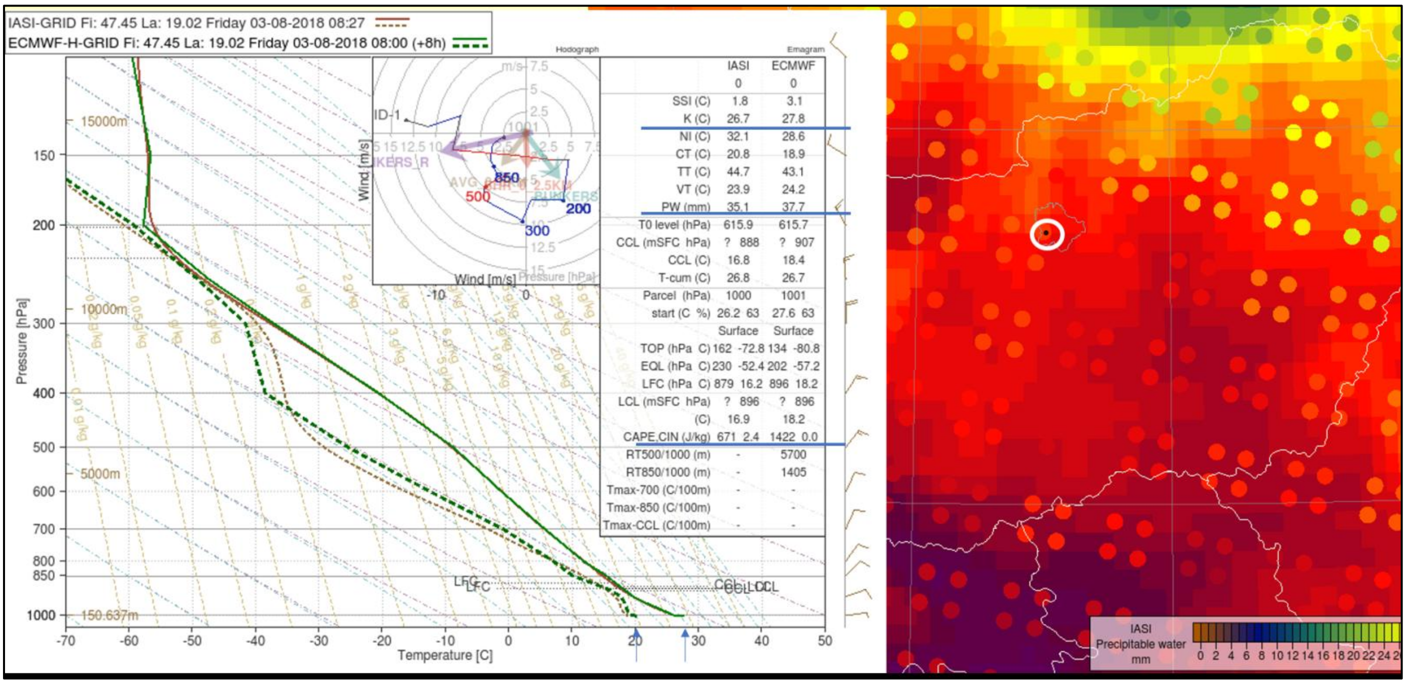

Fig. 3.57: ECMWF forecasted and the IASI derived Temperature and Dew point profiles in green and brown colours (left), ECMWF forecasted Total Precipitable Water overlaid by IASI Total Precipitable Water

(right). IASI data measured on 03 August 2018 at 08:27 UTC, while ECMWF forecast valid for 08 UTC. The circle in the right panel shows the location of the profiles presented on the left panels.

At this location, the ECMWF and IASI derived TPW and K-index were similar. The SBCAPE (surface based CAPE) showed large difference (1422 J/kg against 671 J/kg, see the CAPE values in the parameter list in the right side of the profile panel in **Fig. 3.57**). The reason is the following: in the lower layers, IASI was somewhat drier, but the difference between IASI and ECMWF Td was not so high except on the surface. In the ECMWF profile, the feature called "foot" can be seen (described in section 3.2.5). ECMWF 2-meter T and Td were much higher than at the level just above it. (The same can be seen in the radiosonde measurements, see Fig. 3.58). This „jump" was missing from the IASI profiles. In case of the SBCAPE, the virtual air parcel is lifted from the surface and the CAPE is extreme sensitive to the starting dew point value (also sensitive to the starting T value). This caused the large difference between IASI and ECMWF SBCAPE values.

The blue arrows in the left panel of Fig. 3.58 show the surface T, Td measurements. In that location, the surface measurements were closer to the forecasted values.

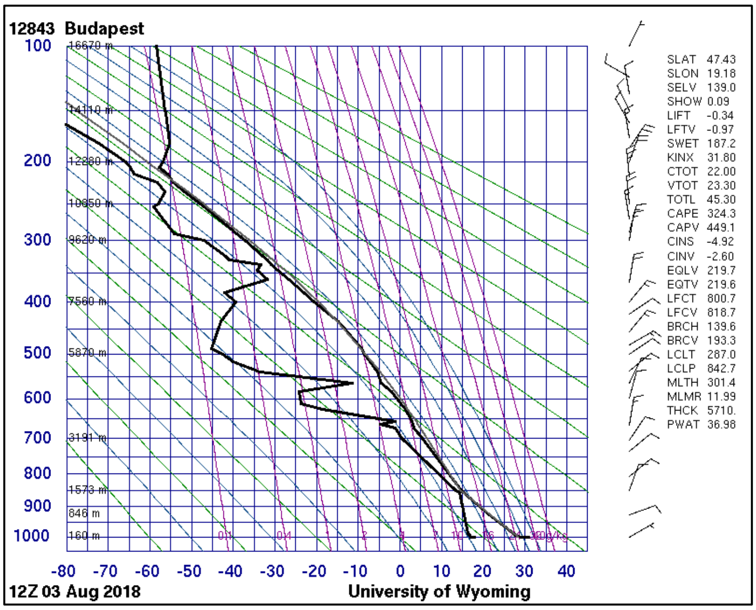

Fig. 3.58: 12 UTC radiosonde measurement for Budapest.

The radiosonde profile showed very dry mid-layer. 2m T and Td were much higher than at the level just above it. (This „jump" can be seen in the ECMWF profile as well, see Fig. 3.57).

More detailed analyses of this case can be found in the presentations of the mid-term meetings.

Summarising this case:

- Large differences were found between the ECMWF forecasted and the IASI derived environmental parameters in the northeast corner of the country.
    - Both ECMWF and IASI TPW's were lower in this region than over the remaining parts of the country. The drier environment was confirmed by the SEVIRI 24-hour Microphysics RGB, as well (less blue shades).
    - IASI yielded even lower low-level moisture content than the ECMWF. 10-minute surface dew point measurements were closer to the IASI-derived value than to ECMWF-forecasted one in this area, confirming the IASI profile on the surface level.
    - The ECMWF forecasted CAPE was low in this region. Based on this, the forecasters did not expected thunderstorms in the northeast region. As IASI showed even less moisture and instability as forecasted in this area, it confirmed the "no thunderstorms are expected in the

northeast region" forecast. According to the IASI-derived parameters, the probability of thunderstorm formation was even less.

- The other regions of the country were unstable both by ECMWF and IASI data. At the studied location the T, Td "jump" between the surface and the first level above it was present in ECMWF and radiosonde profiles, but not in IASI.

3.4.2. Case 11 July 2018

Pre-frontal thunderstorms were expected in the middle part of Hungary. Fig. 3.59 shows the convergence line presences at 9 UTC. Storms started to develop in the morning in the middle and eastern part of the country (Fig. 3.60).

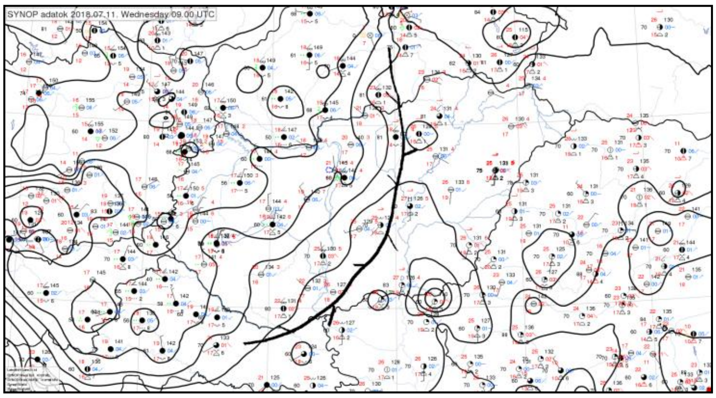

Fig. 3.59: Synop measurements at 09 UTC 11 July 2018.

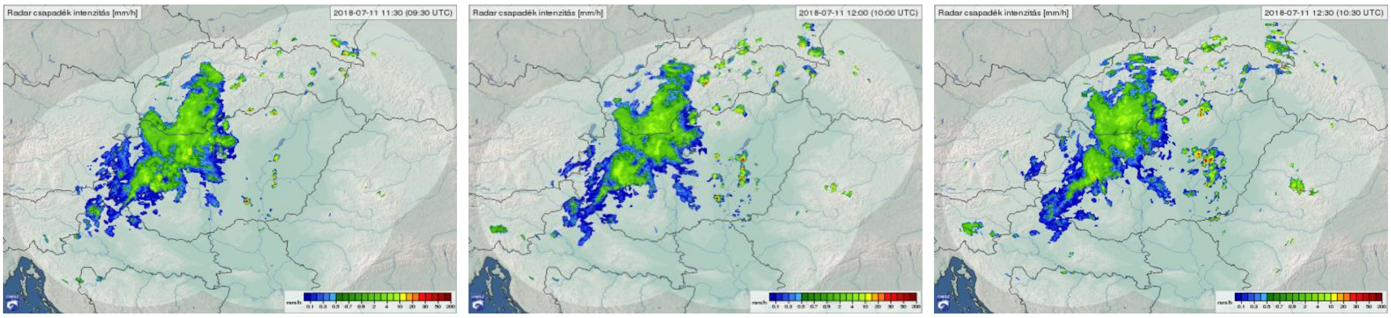

Fig. 3.60: Radar measurements at 9:30 (left), 10:00 (middle) and 10:30 (right) on 11 July 2018.

IASI data confirmed the forecast; the retrieved TPW and K-index were higher in the middle and eastern part of the country, indicating even higher probability of thunderstorm forming (Fig. 3.61).

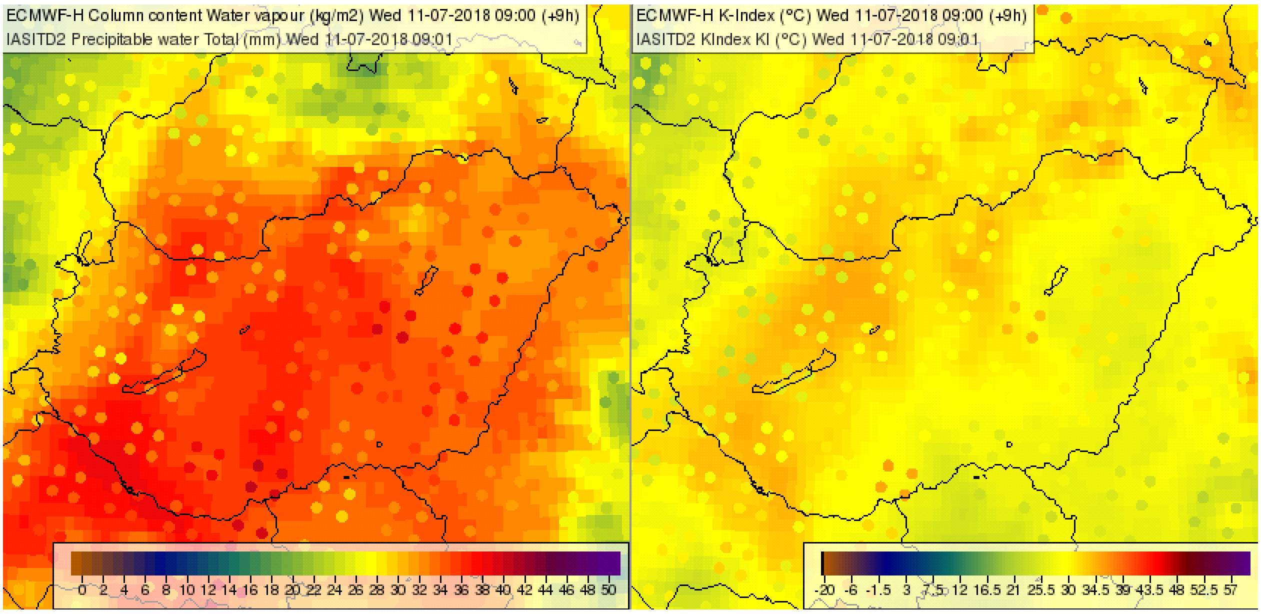

Fig. 3.61: IASI TWP (left) and K-Index (right) at 09:01 UTC overlaid on ECMWF-forecasted fields valid at 9 UTC 11 July 2018.

SEVIRI 24-hour Microphysics RGB images also showed increased low level moister in the area (Fig. 3.62) which confirms the IASI TPW. Fig. 3.63 shows the IASI and ECMWF temperature and humidity profiles close to the area where the thunderstorms formed. It is clearly seen that the ECMWF-forecasted humidity was less than the IASI-retrieved one.

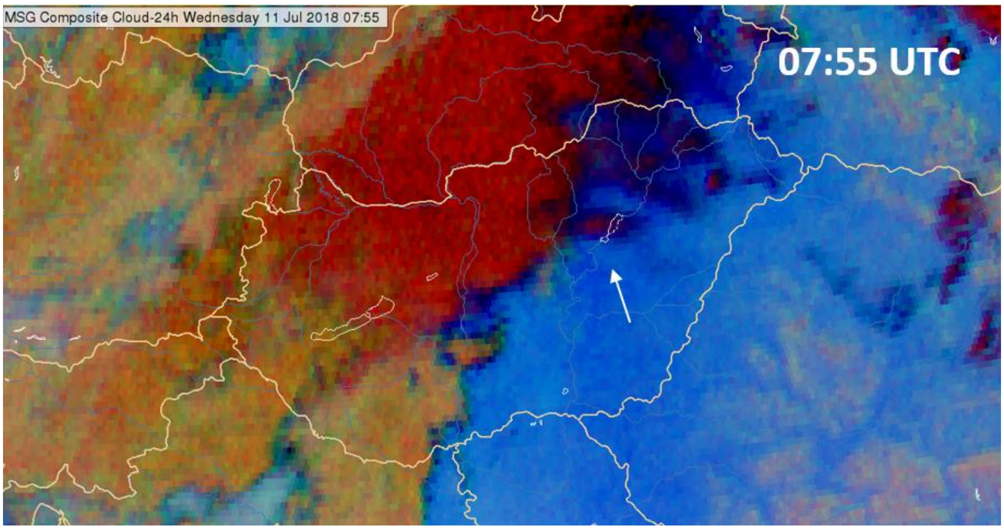

Fig. 3.62: SEVIRI 24-hour Microphysics RGB image at 07:55 UTC 11 July 2018. The arrow indicates the location of the profiles shown in Fig. 3.63.

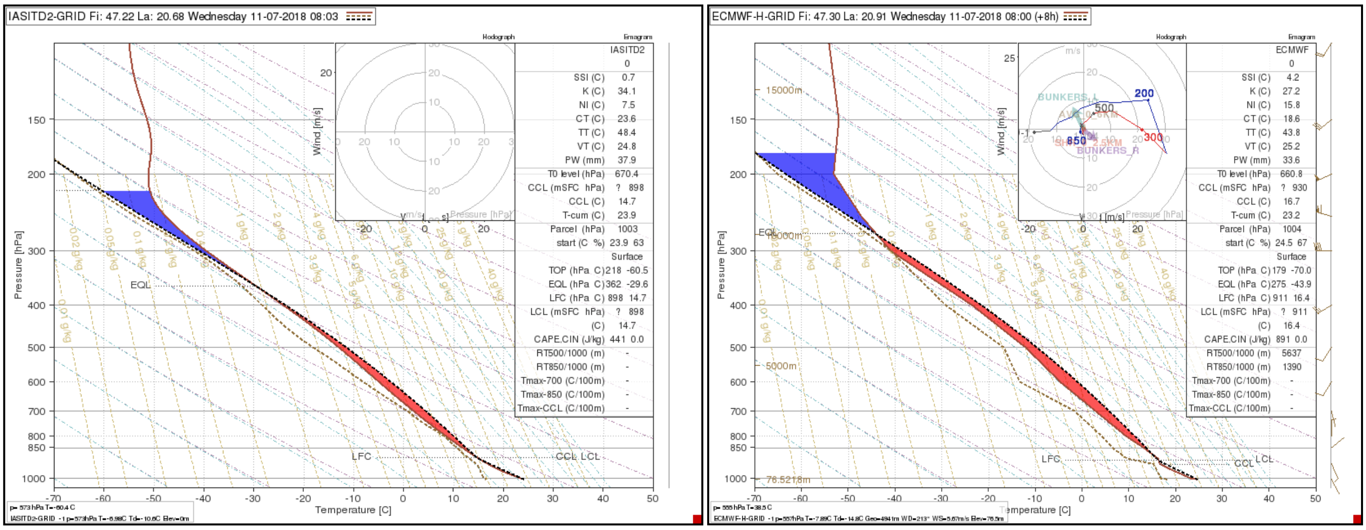

Fig. 3.63: IASI (left) and ECMWF (right) temperature and humidity profiles at 08 UTC 11 July 2018 at the location shown in Fig. 3.62.

The case was also presented at the 2018 EUMETSAT Conference (Kocsis et al., 2018).

4. Quantitative comparison of the instability indices

IASI L2 IRON derived parameters were compared to 15-minute EUMETSAT processed GII parameters. The GII parameters (K-Index, Lifted Index, KO Index, Maximum Buoyancy, Total Precipitable Water and Layer Precipitable Water) were calculated from the IASI L2 IRON profiles in the same way as in the GII algorithm.

In order to do the comparison IASI pixels needed to be collocated with GII pixels. GII is calculated on 3x3 MSG pixel bases which resolution is too coarse so it was scaled down to MSG pixel resolution (Fig. 4.1).

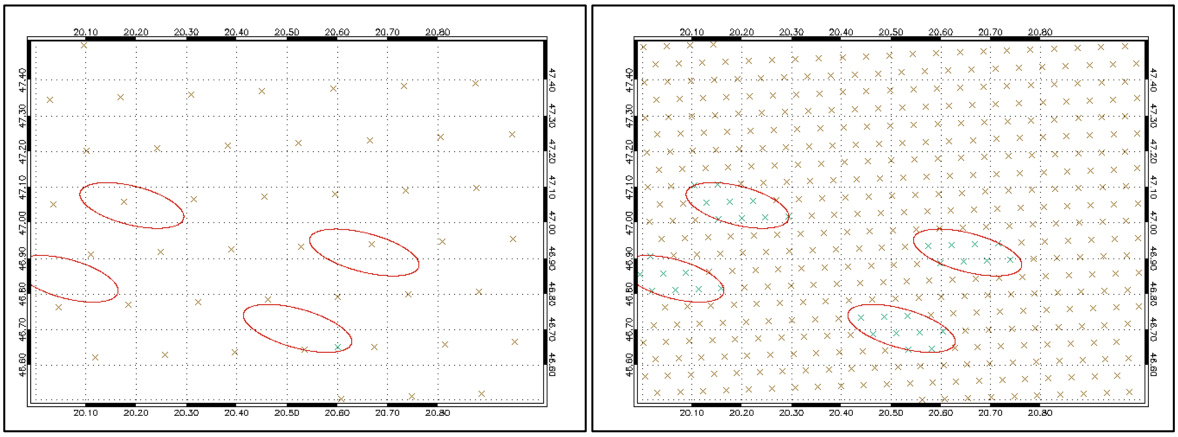

Fig. 4.1: GII (left) and MSG pixel (right) overlaps with IASI ellipses.

The values in MSG pixels within the IASI ellipse were averaged, and then statistics (Mean Difference, RMSE, STD, and correlation) were calculated for both land and sea for the following geographical areas:

- North pole: Lat ≥ 60°
- North: 30° < Lat < 60°
- Tropic: -30° < Lat ≤ 30°
- South: -60° < Lat ≤ -30°
- South pole: Lat ≤ -60°

The comparison was carried out for the time period of April – October 2016, for both Metop B and A.

The results were compared with the results of the previous study when SEVIRI/GII was compared with the same parameters retrieved from **IASI L2 product (based on MW and IR measurements).**

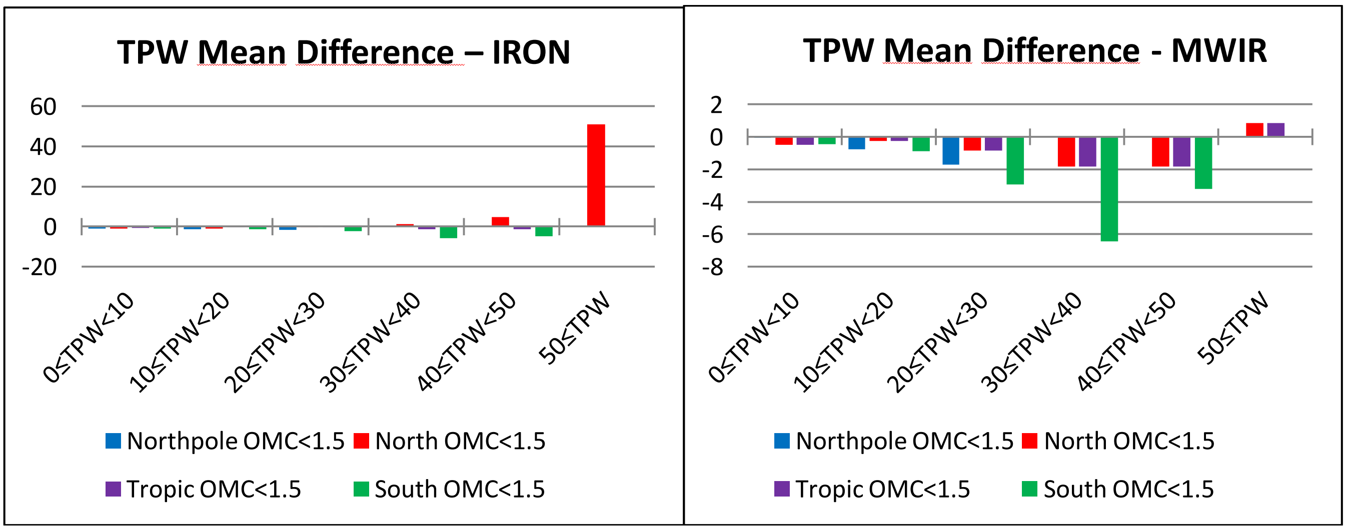

Fig. 4.2: Mean difference for TPW over land for Metop-B using IR-only (left) and MWIR (right) L2 data. (OMC<1.5 means low cloud contamination within the IASI ellipse.)

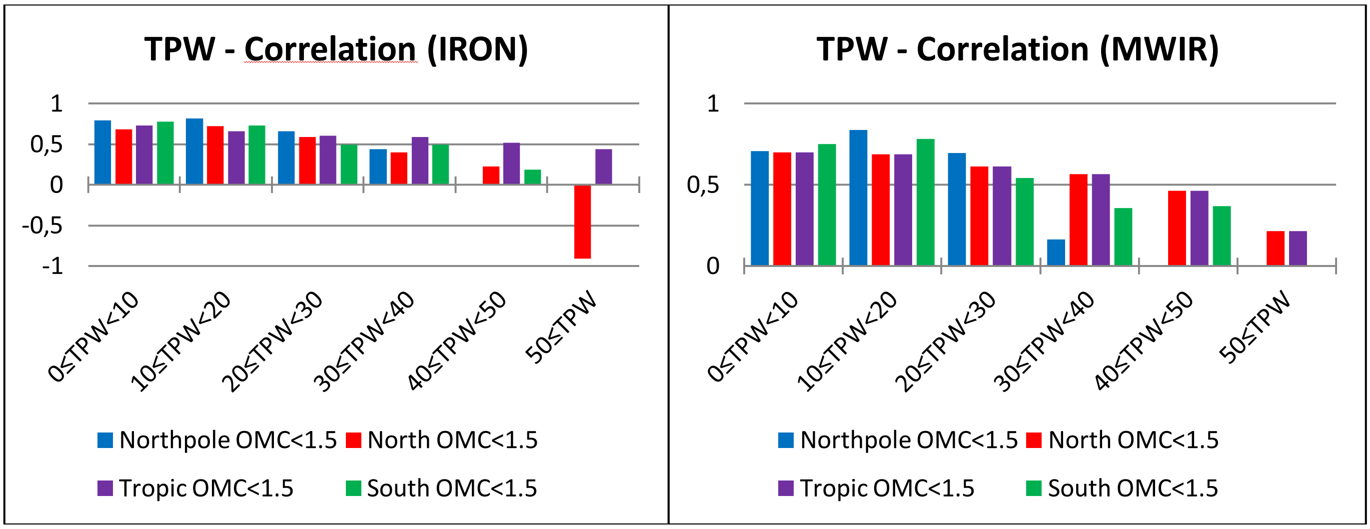

Fig. 4.3: Correlation for TPW over land for Metop-B using IR-only (left) and MWIR (right) L2 data. (OMC<1.5 means low cloud contamination within the IASI ellipse.)

The statistical comparison between the IASI L2 IRON and GII data gave similar result to the one performed with the MWIR L2 data. Fig. 4.2 and Fig. 4.3 show the mean difference and correlation between the IASI and the GII total precipitable water (TPW) over land. For very high TPW cases IASI IRON overestimates the moisture compared to GII in the northern mid-latitudes – this was not present in IASI MWIR. The correlation values are similar to the MWIR values with exception of cases when TPW is larger than 50 mm in the northern mid-latitudes. This category shows negative correlation between IASI IRON and GII TPW.

For the instability indices fewer differences were present in the statistical parameters between IASI IRON and GII data. Fig. 4.4 and Fig. 4.5 show the mean difference and correlation for the Lifted-index (LI). The correlation for unstable areas is a little bit smaller but comparable for the IRON data than for the MWIR (Fig. 4.5).

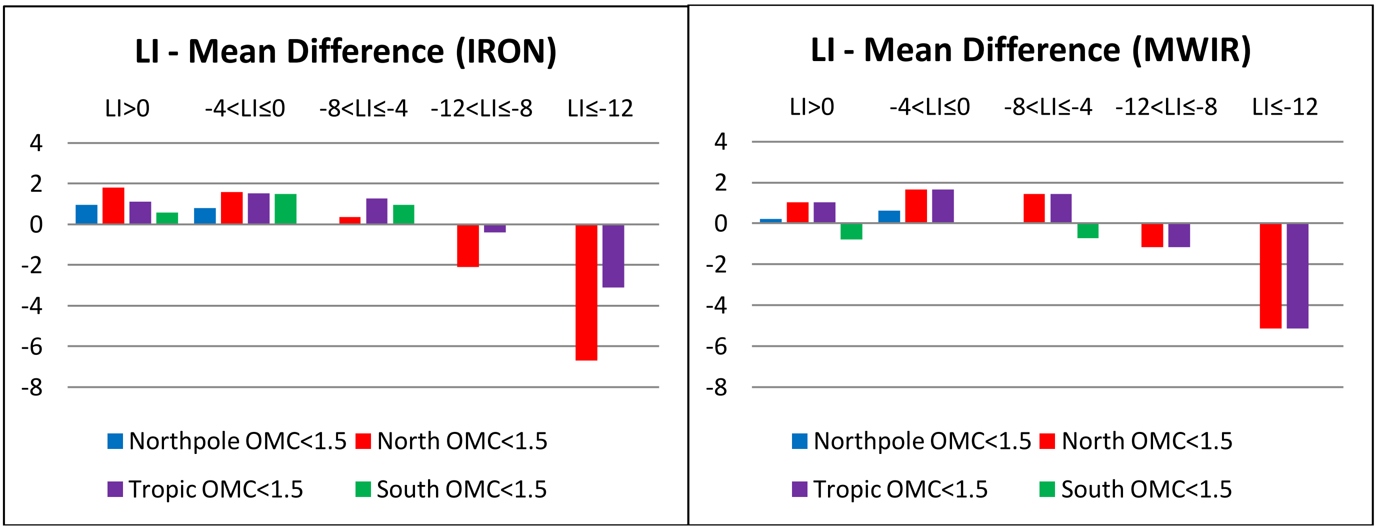

Fig. 4.4: Mean difference for LI over land for Metop-B using IR-only (left) and MWIR (right) L2 data. (OMC<1.5 means low cloud contamination within the IASI ellipse.)

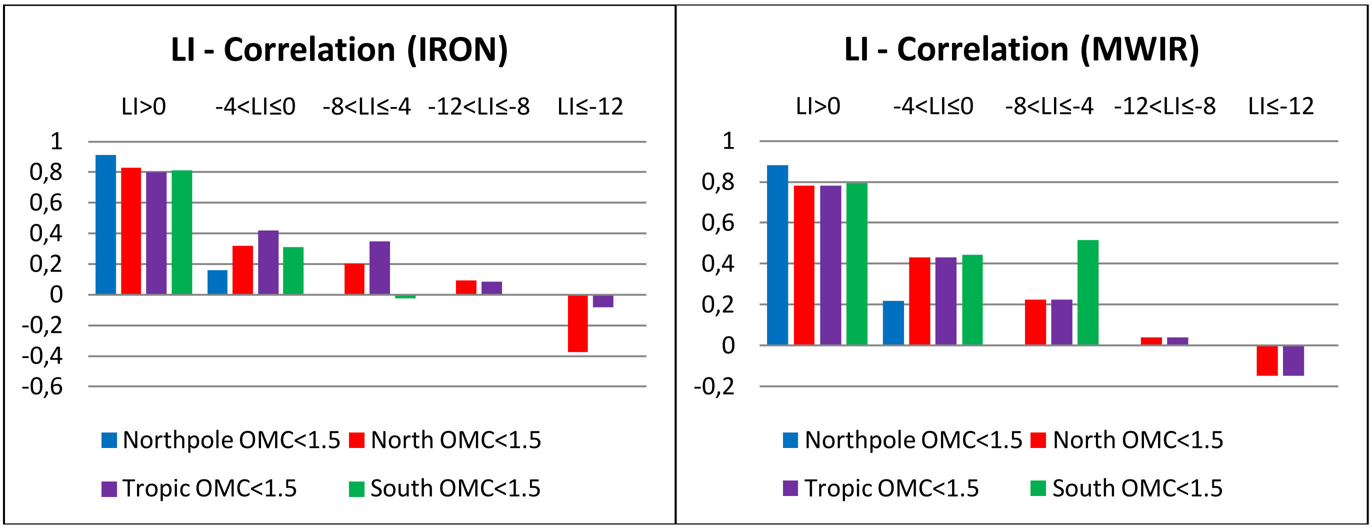

Fig. 4.5: Correlation for LI over land for Metop-B using IR-only (left) and MWIR (right) L2 data. (OMC<1.5 means low cloud contamination within the IASI ellipse.)

Similar pattern can be seen over see as well. The figures for the sea and for the other indices can be found in the appendix.

5. Forecast and L2 differences dataset

A database has been built with convective cases where the ECMWF forecasted and the IASI L2 MWIR and IRON derived convective environment parameters **differ significantly.** The cases are classified according the **nature of the differences.** The database contains the following parameters:

- a code indicating why the profile is included in the database (described in

Code	**Description**
1	IASI TPW is considerably lower than forecasted
2	IASI TPW is considerably higher than forecasted
3	Higher forecasted humidity in the boundary layer than in the IASI profile ECMWF humidity profile shows a well-mixed boundary layer, which is not the case in IASI
4	Lower forecasted humidity in the boundary layer than in the IASI profile
5	Sudden increase between the forecasted surface temperature (humidity) and the first level above it which is not present in the IASI profile – ‚foot' in ECMWF
6	‚foot' in ECMWF and IASI TPW is higher
7	‚foot' in ECMWF and IASI TPW is lower
8	IASI TPW is considerably lower than the forecasted and ECMWF humidity profile shows a well-mixed boundary layer, which is not the case in IASI
9	IASI profile indicates less instability than ECMWF profile
21	The IASI profile does not show the frontal characteristics, which is present in ECMWF (the low layer is drier in ECMWF)
22	The IASI profile does not show the frontal characteristics, which is present in ECMWF (the low layer is moister in ECMWF)
41	Fog/stratus
42	Sunglint

- Table **5.1**),
- geolocation,
- date/time,
- satellite angles,
- quality indicators,
- information on the cloudiness,
- NWP analysed or forecasted temperature and relative humidity profiles on isobaric levels,
- IASI L2 MWIR pressure, temperature and specific humidity profiles,
- IASI L2 IRON pressure, temperature and specific humidity profiles,
- environmental parameters derived from the above profiles,
- 2m temperature and relative humidity measurements,
- references to the original IASI file names.

The following ECMWF environmental parameters included in the database: 0-3 km averaged relative humidity, Best Lifted Index, MLCAPE, K-index. The following parameters calculated from the IASI profiles included in the database: TPW, 0-3 km averaged relative humidity, Best Lifted Index, MLCAPE, K-index, Maximum Buoyancy, 400/700 and 600/925 hPa lapse rates.
The files are in hdf5 format, one files contains pixels from one IASI overpass.

Code	**Description**
1	IASI TPW is considerably lower than forecasted
2	IASI TPW is considerably higher than forecasted
3	Higher forecasted humidity in the boundary layer than in the IASI profile

	ECMWF humidity profile shows a well-mixed boundary layer, which is not the case in IASI
4	Lower forecasted humidity in the boundary layer than in the IASI profile
5	Sudden increase between the forecasted surface temperature (humidity) and the first level above it which is not present in the IASI profile – ‚foot' in ECMWF
6	‚foot' in ECMWF and IASI TPW is higher
7	‚foot' in ECMWF and IASI TPW is lower
8	IASI TPW is considerably lower than the forecasted and ECMWF humidity profile shows a well-mixed boundary layer, which is not the case in IASI
9	IASI profile indicates less instability than ECMWF profile
21	The IASI profile does not show the frontal characteristics, which is present in ECMWF (the low layer is drier in ECMWF)
22	The IASI profile does not show the frontal characteristics, which is present in ECMWF (the low layer is moister in ECMWF)
41	Fog/stratus
42	Sunglint

Table 5.1: Description of the codes indicating why the profile is included in the database.

6. Merging IASI L2 product with surface measurements

Satellite derived environmental parameters **may be not accurate enough for nowcasting purposes** because many environmental parameters depend strongly on the (near) surface temperature and dew point values. These are the levels where the uncertainty of the satellite derived profiles is the largest. To overcome these problems, we have the following options:

- either to focus on less surface dependent environmental parameters, and/or
- **combine the satellite derived profiles with in situ surface temperature and dew point measurements.**

The IASI measurements represent a larger area (pixel) while the in situ measurements are point measurements. The surface measurements were used to modify only the lowest level temperature and dew point values. (The lowest level represents the 2 meter values). In some of the cases we performed interactive merging using the in-built tools of the HAWK visualisation system.

For the automatic merging, we chose the following procedure which is illustrated in Fig. 6.1:

1. Interpolating the ground-based measurement to a grid (0.02°) using inverse distance weighting (IDW) and taking topography into account. – For each grid, the stations within 50 km were used. This step was done with the help of the HAWK3 software.
2. Making an average temperature and dew point using the grid point values within the IASI ellipse.
3. Using this new T, Td as the surface value in the IASI profile.

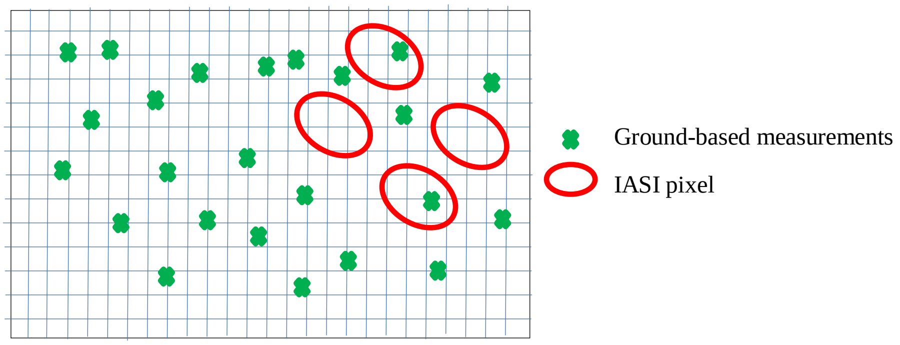

Fig. 6.1: Illustration of the automatic merging technique.

Fig. 6.2 shows an example of the IASI 2 meter temperature and dew point values together with the interpolated values from the Synop measurements. Differences between the surface measurements and retrieved IASI 2m Td are up to 3 °C.

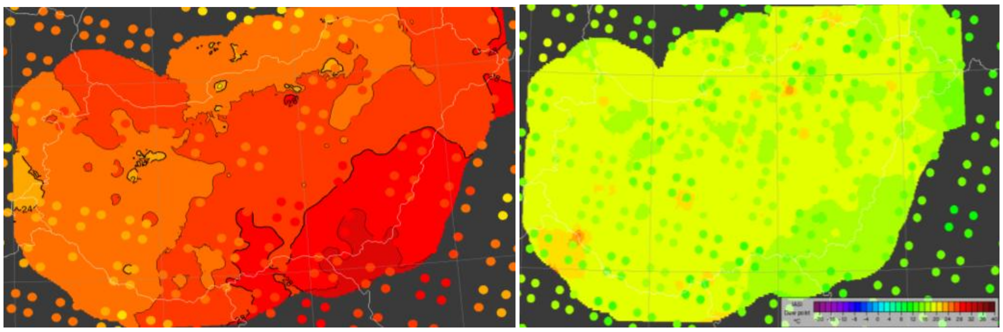

Fig. 6.2: IASI 2 meter temperature (left) and dew point (right) overlaid on the interpolated surface measured 2 meter temperature (left) and dew point (right) on 24 August 2019 at 08:28 UTC. The surface measurements are based on 10-minute surface measurements at 08:30 UTC performed by the Hungarian automatic station network.

6.1. Which parameters are affected by the merging?

The K-index and the 400/700 and 600/925 hPa lapse rates and are not affected by the merging. TPW and 0-3km mean RH are only slightly affected by the merging, as the merging modifies only the surface temperature and humidity. The MLCAPE parameter is affected by merging as it is slightly sensitive to the surface temperature and dew point values. (It is extreme sensitive to the mean Td of the lowest 100 hPa layer.) The Best Lifted index is either the most sensitive to the surface temperature and dew point values, or not effected by them at all. (The Best lifted index is calculated by lifting the virtual air parcel from several levels inside the lowest 100 hPa layer and the highest value is taken. If the highest value belongs to a lifting from an elevated level, then BLI is not affected by the surface temperature and humidity.)

The IASI profiles have larger uncertainties at low levels, they are often drier (and colder) than indicated by the model profiles or surface measurements. Combining the IASI profiles with Synop measurements can improve indices which are more dependent on the 2m values (Fig. 6.3). As mentioned above MLCAPE is dependent in the lowest 100 hPa layer which is still often dryer in the IASI retrieval than the models. When using merged indices MUCAPE (Most Unstable CAPE) might be a better choice (Fig. 6.3).

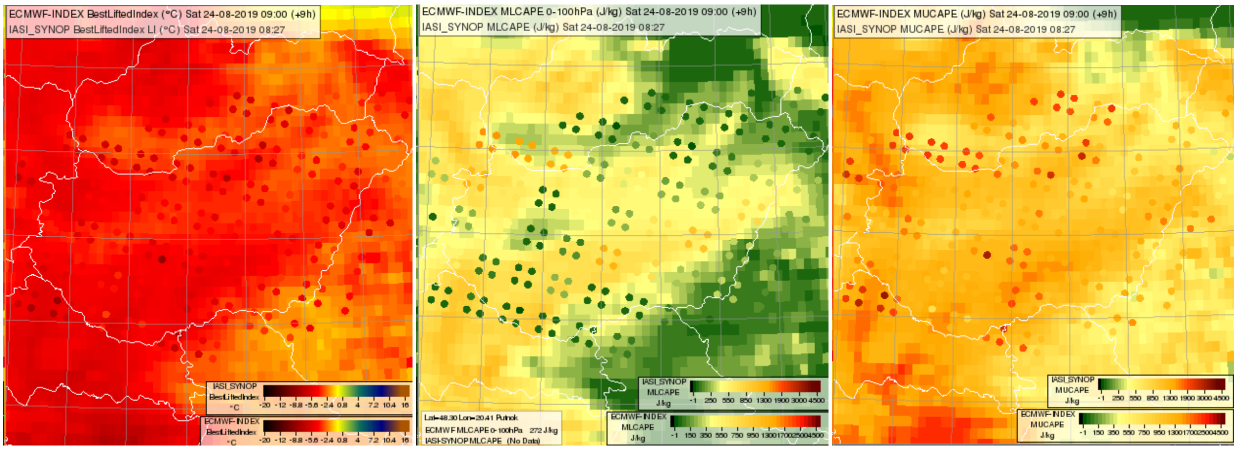

Fig. 6.3: Merged Best Lifted Index (left), merged IASI MLCAPE (middle), Merged IASI MUCAPE (right) at 08:27 UTC overlaid on the forecasted ECMWF Best Lifted Index (left), MLCAPE (middle) and MUCAPE (right) valid for 09 UTC on 24 August 2019.

Fig. 6.4 shows the indices for the case 4 June 2018. Merging increased the humidity for most of the Hungarian pixels. The MLCAPE and the Best Lifted index parameters has been increased as well. They became closer to the forecast and their structure became more similar to the forecast.

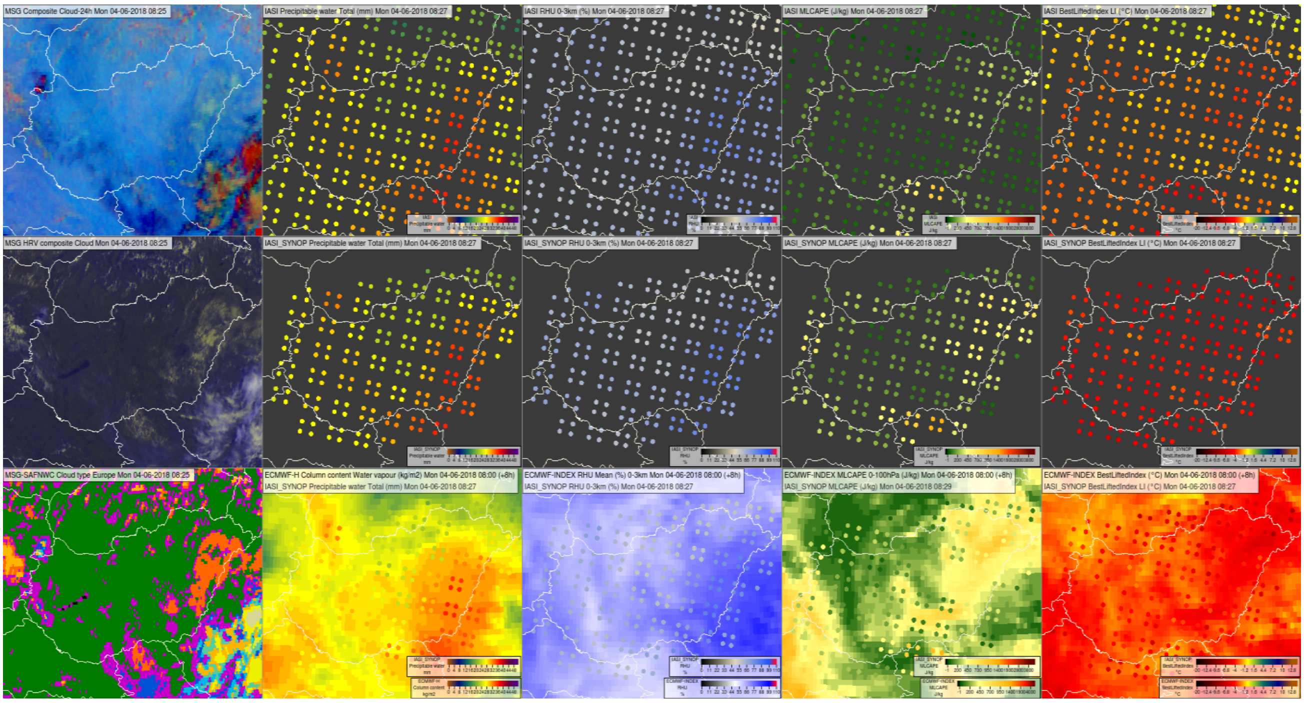

Fig. 6.4: Upper row: SEVIRI 24-hour Microphysics RGB at 08:25 UTC, IASI MWIR TPW, IASI MWIR Relative Humidity at the lowest 3 km layer, IASI MWIR MLCAPE, IASI MWIR Best Lifted Index at 08:27 UTC. Middle row: SEVIRI HRV RGB at 08:25 UTC, Merged IASI TPW, Merged IASI Relative Humidity at the lowest 3 km layer, Merged IASI MLCAPE, Merged IASI Best Lifted Index at 08:27 UTC. Bottom row: SEVIRI NWCSAF CT at 08:25 UTC, Merged IASI TPW overlaid on ECMWF forecasted TPW, Merged IASI Relative Humidity at the lowest 3 km layer overlaid on ECMWF forecasted Relative Humidity at the lowest 3 km layer, Merged IASI MLCAPE overlaid on the ECMWF forecasted MLCAPE, Merged IASI Best Lifted index overlaid on ECMWF forecasted Best Lifted Index. ECMWF forecast is valid for 08 UTC on 04 June 2018.

Why do we consider being beneficial if the merged IASI data become often closer to the forecast?
In most of the cases the forecast is rather good. If an IASI parameter very often differs strongly from the forecast – the forecaster will not trust it.
The IASI derived parameter may differ from forecast because

- the forecast is not enough accurate or
- the IASI retrieval is not enough accurate.

We are interested in cases when the forecast is not enough accurate. To find them, we try to exclude cases when the IASI retrieval is not enough accurate. Merging IASI profiles with surface measurements improves the quality of the IASI retrieval, thus it will be more useable for nowcasting purposes.

6.2. Effect of the network density (both in space and time)

Tests were performed on a couple of cases to assess the impact of the station number used in the interpolation of the surface measurements. We also looked at the impact of temporal frequency. Fig. 6.5 shows the impact the number of station and time frequency. With less stations we can relatively cover the overall pattern of the distribution of the temperature; however some of structure is missing. Using only hourly data we can have larger differences as the parameters can change a lot in 20-30 minutes.

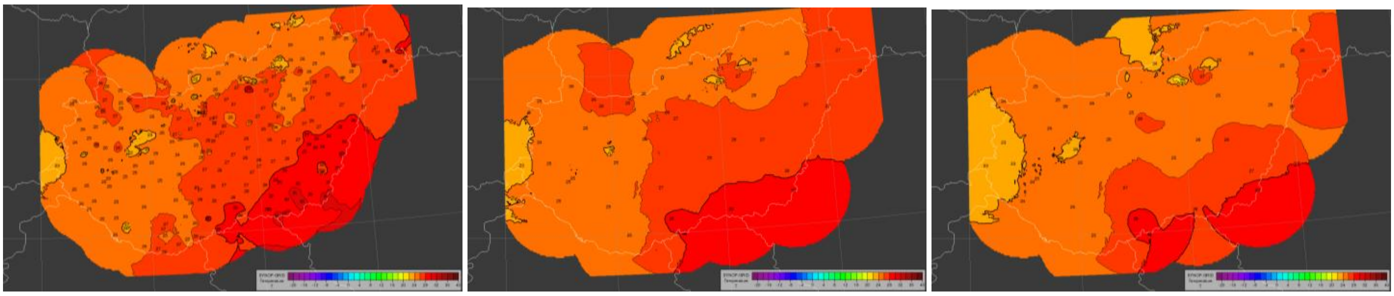

Fig. 6.5: Interpolated 2m temperature using all stations at 2019.08.24. 8:20 UTC (left), using only WMO stations at 2019.08.24. 8:20 UTC (middle), using WMO stations at 2019.08.24. 8:00 UTC (right).

An example of station number's and measurement time effect on the indices is shown in Fig. 6.6. Using the closest surface measurements in time to the IASI overpass is more important than a very high number of stations.

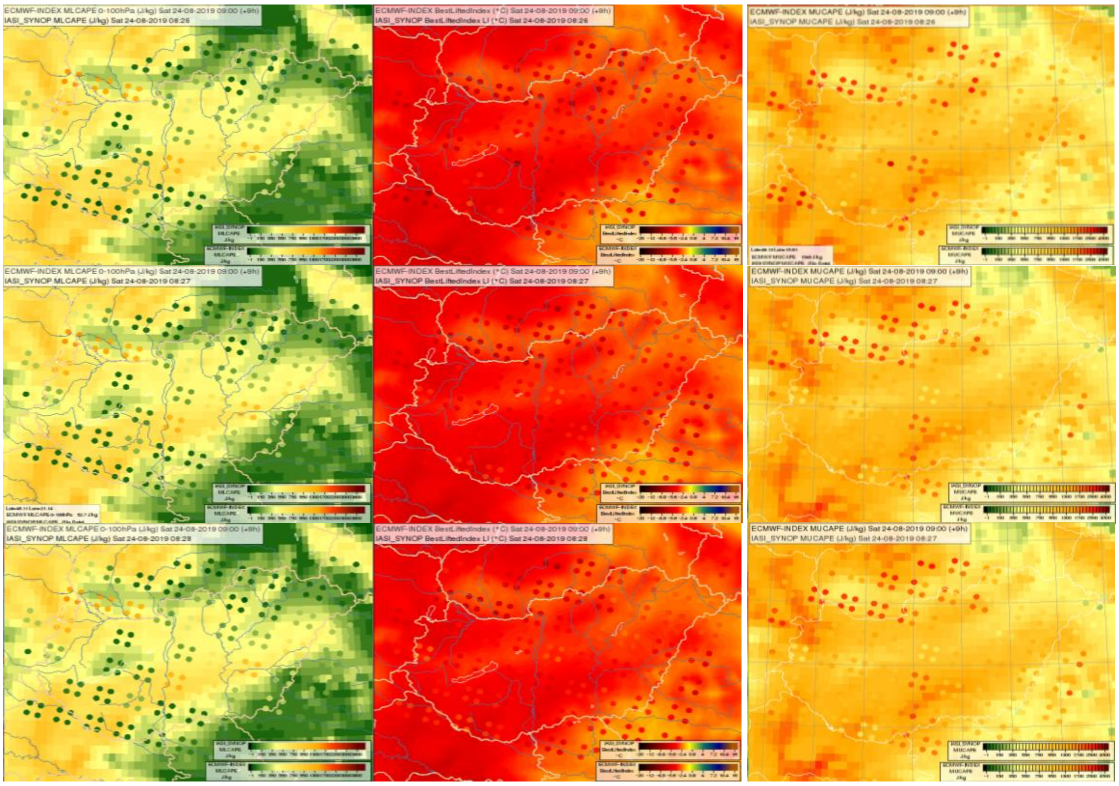

Fig. 6.6: Upper row: Merged MLCAPE (left), Best Lifted Index (middle), MUCAPE (right) using all stations at 2019.08.24. 8:20 UTC. Middle row: Merged MLCAPE (left), Best Lifted Index (middle), MUCAPE (right) using only WMO stations at 2019.08.24. 8:20 UTC. Bottom row: Merged MLCAPE (left), Best Lifted Index (middle), MUCAPE (right) using WMO stations at 2019.08.24. 8:00 UTC. All merged IASI parameters are overlaid on the ECMWF forecast valid for 09 UTC:

7. Suggestions

Suggestions for IASI L2 users:

- Use a **pre-sorting program** to find the potentially interesting cases with considerable differences between IASI derived and forecasted environmental parameter fields.
- Draw attention to the **typical features of IASI derived profiles**, like smoothness, higher uncertainty close to the surface.
- Draw attention to the **limitations**, like
    - **frontal characteristics** may be missing,
    - It might not be reasonable to calculate those parameters for which good vertical resolution and accurate values are needed. For example, calculating a reliable CIN (convective inhibition) value, information is only needed from the lowest layer but accurate temperature and humidity information is required with good vertical resolution.

- Draw attention to the importance of the **vertically averaged errors.**
- Draw attention that IASI retrieval reflects the **actual cloudiness**, while the forecasted cloudiness may differ from the real one (which impacts the forecasted profile shape).
- It is worth to perform **synergy of IASI profile with surface measurement**. In that case using merging surface-based instability parameters are recommended, like SBCAPE, MUCAPE, Best lifted index.
- It is worth to use IASI retrieval together with numerical forecasts and radiosonde measurements, as supplementary data.

In case of **visual applications:**

- Consider to **remove over-saturation.**
- It might be useful to **visualize the uncertainty of the profiles**. (It would be even better if we had vertical distribution of the error not only the vertically averaged value.)
- We suggest masking **the non-reliable pixels**. For MWIR data, pixels with large vertically averaged error should be removed. In case of IRON data, we suggest to mask:
    - pixels with large vertically averaged error,
    - large absolute value of OMC,
    - pixels covered by mid- or high-level opaque clouds (taking into account the Cloud Type classes).

Remark:
For an **automatic application** it might not be so important to **mask** the less reliable IASI pixels, if quality flags (error values), Cloud Type and Cloud Top Pressure products are available along with a description/recommendation how to take them into account.
In case of **visual application masking** is more important because forecasters have limited time, and they had to process visually a lot of different kinds of information.

8. Summary

The quantitative comparison showed good correspondence between IASI L2 IRON, MWIR and GII data. Performance degradation was observed for IASI L2 IRON data in cloudy cases, as expected.

IASI L2 IRON retrievals were studied together with MWIR data in cloud-free and different cloudy situations. **On cloud-free areas, and areas covered by thin cirrus or small cumulus** the structure of the retrieved parameters and the profiles are usually similar, the differences are not high in general. The IRON profiles and parameters calculated from them are considerably different from the MWIR and forecasted ones for **opaque mid/high level clouds**. In accordance with this, the uncertainties in the IRON retrieval for these cloud types are much higher than in the MWIR data. In these cases the profiles are not reliable below the cloud top. In general the vertically averaged errors are usually higher for IRON data than for MWIR data. It can reach even 5-6 °C. It is worth considering **masking** (or cutting the profiles below the cloud top) the areas covered by mid/high level opaque clouds and/or non-reliable IASI pixels (the ones with very high uncertainty). This could be done based on uncertainty, OMC, and cloud type and cloud top pressure products.

During the summer of 2019, IASI L2 EARS data have been evaluated by forecasters. One of the aims of the evaluation was to look for value added cases. Unfortunately, only a couple of cases with added value was found which is due to the facts that Hungary is a small country and the morning Metop overpasses are usually happening a longer time before the convection starts (most of the convection is in the afternoon, early evening). With half hour IRS data even for a smaller area we expect to have more interesting and value added cases. In addition, with IRS data one will able to see the temporal tendencies of humidity content and instability.

The following features were observed in the IASI L2 data (regardless on the retrieval type):

- the clouds are usually indicated in the profiles. IASI data reflect the effect of the real cloudiness on the profiles, while cloudiness in the model may be different.
- Moisture boundaries can be seen in the moisture field of the IASI data, while they are sometimes misplaced in the forecast data. The correct position of the moisture boundaries can improve to forecast.
- A dry bias in the L2 products in the bottom layer is suspected in mild to strong pre-convective situations, yielding to low CAPE values.
- IASI MLCAPE is very often underestimated compared to the forecast which can be misleading.
- Sunglint has a degrading effect on the IASI retrieval. QI is correctly reflecting poorer quality.
- Thermal inversion often can be observed which would be interesting in other high impact weather forecasting such as fog.

The quality indicators were found mostly significant to the quality of the retrieved profiles and were proved to be very useful. However, uncertainty profiles would be needed to locate levels of highest confidence. The scalar quality indicator is very limiting.

Blending IASI profiles with ground based measurements shows potential to better characterise instabilities especially when very near-surface based. It may make possible to retrieve more accurate surface based instability indices. In future plans, we intend to study the blended environmental parameters in more detail.

Database has been built from convective cases where the ECMWF forecasted and the IASI L2 MWIR and IRON derived convective environment parameters differ significantly**.**

Wind shear information is very important for monitoring convective environment and to forecast severe convection. IRS data will include 3D wind information which brings a very important question - Will it be enough accurate to derive wind shear?

9. Comparison of IASI and ECMWF fields - Respective benefits and limitations

IASI L2	ECMWF	Radiosonde
Based on radiation measurement	Based on numerical forecast	Based on in-situ measurement
Based on statistical retrieval	Based on physical, dynamical processes	Based on in-situ measurement
Reflects the real situation, real cloud cover	The cloud cover in the model might be different than the real cloud cover	Reflects the real situation, real cloud cover
Lower horizontal resolution, not a continuous field	Higher horizontal resolution Continuous field	Low horizontal resolution, unequal distribution of the stations
IRS will have half hour temporal resolution	Hourly forecast	Low temporal resolution (most often ones/twice a day)
IASI has low temporal resolution Only a few Metop overpass a day	Hourly forecast	Low temporal resolution (most often ones/twice a day)
More smooth profiles	Less smooth profiles	Detailed profile, good vertical resolution
Sudden changes like frontal characteristics may not present in the profile	Forecasted profiles reflect the frontal characteristics	Measured profiles reflect the frontal characteristics
IASI L2 (IR-only) does not provides reliable data for mid/high level opaque clouds	ECMWF provides data both for cloudy and cloud-free areas	Measurements both in cloudy or cloud-free situation
IASI L2 (IR+MW) provides data both for cloudy and cloud-free areas	ECMWF provides data both for cloudy and cloud-free areas	Measurements both in cloudy or cloud-free situation

Table 9.1: Benefits (green) and limitations (blue) of the IASI L2 and ECMWF profile data while radiosonde is shown as reference.

10. Acknowledgements

We are grateful to **Thomas August** and **Tim Hultberg** (EUMETSAT) for the valuable advises and IASI data. We also thank Peter Baar, Roland Goth, Tibor Kelemen and Andras Vaszko forecasters of the Hungarian Meteorological Service for the daily evaluation of the IASI L2 data during the summer 2019.

11. References

Kertész S., 2000: The HAWK system: Recent developments at HMS. Proceedings of the 11th EGOWS meeting held in Helsinki, 5-8 June, 2000. pp: 13-14.

Kocsis, Zs., Simon, A., Csirmaz, K., Putsay, M. and T. August, 2019: 10th European Conference on Severe Storms (ECSS2019), Krakkow, Poland, November 2019.

Kocsis, Zs., Simon, A., Putsay, M. and T. August, 2018: Possible Usage of IASI L2 data in Nowcasting. 2018 EUMETSAT Meteorological Satellite Conference, Tallin, Estonia, September 2018.

König, M., Tjemkes, S. A., Kerkmann, J., 2001: Atmospheric Instability Parameters Derived from MSG SEVIRI Observations. 11th Conference on Satellite Meteorology and Oceanography.

Putsay M., Simon A., Kocsis Zs., Csirmaz K. and Szenyán I., 2017: 'Investigation of MSG SEVIRI and EPS IASI derived atmospheric instability in relation of other observations'. Final report, EUMETSAT study, Contract number EUM/CO16/4600001802/KJG.

Rajnai M., Kertész, S., Szabó, L., Vörös, M., 2005: Recent developments at HMS, 16th EGOWS conference, Exeter, United Kingdom, 2005. Available:
http://www.metoffice.gov.uk/egows2005/presentations/Rajnai.pdf

Appendix 1: Further statistics for the GII IASI comparison

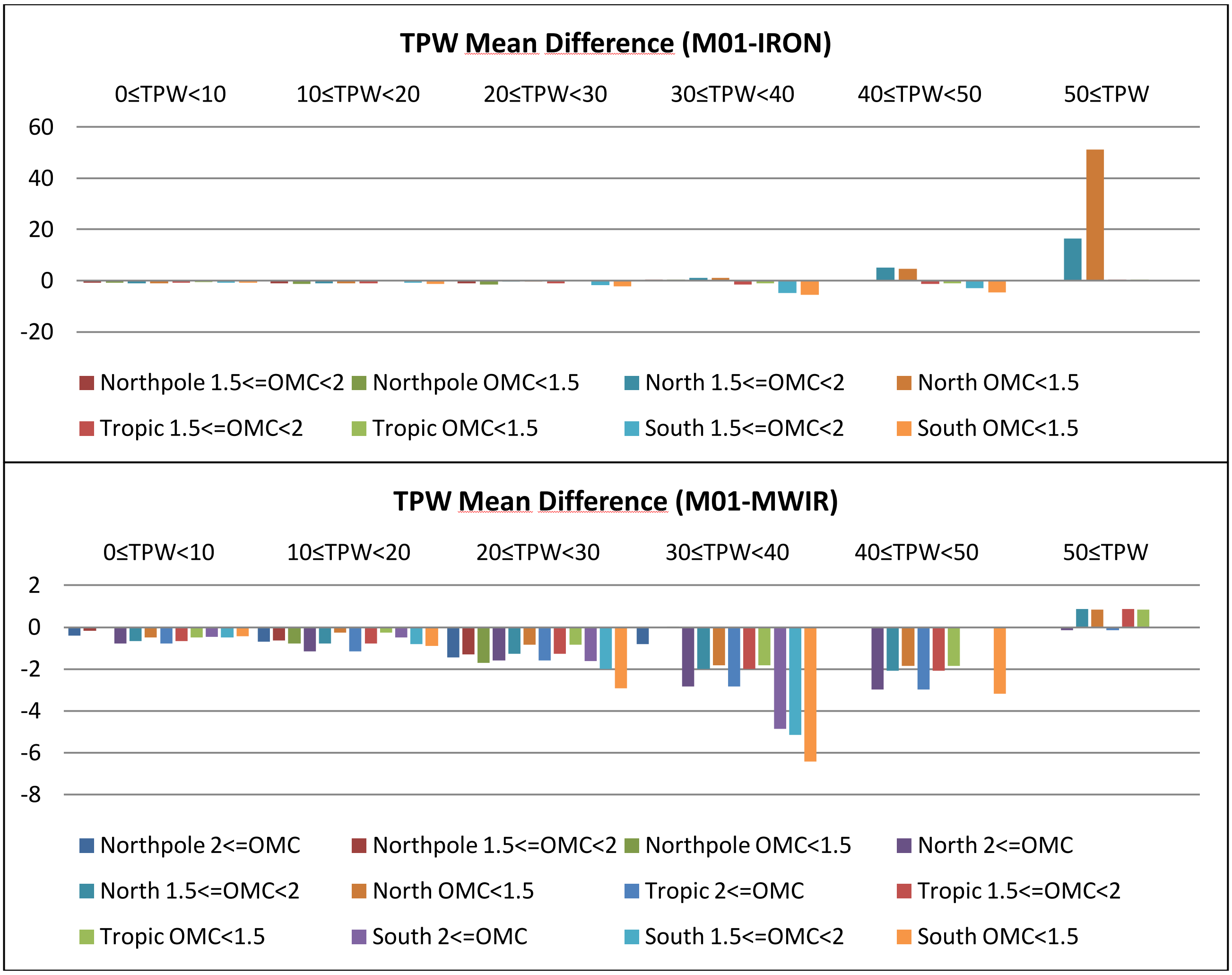

Fig. A1.1: Mean difference for TPW for different IASI pixel clarity categories over land for Metop-B for IRON (upper) and MWIR (lower) retrievals.

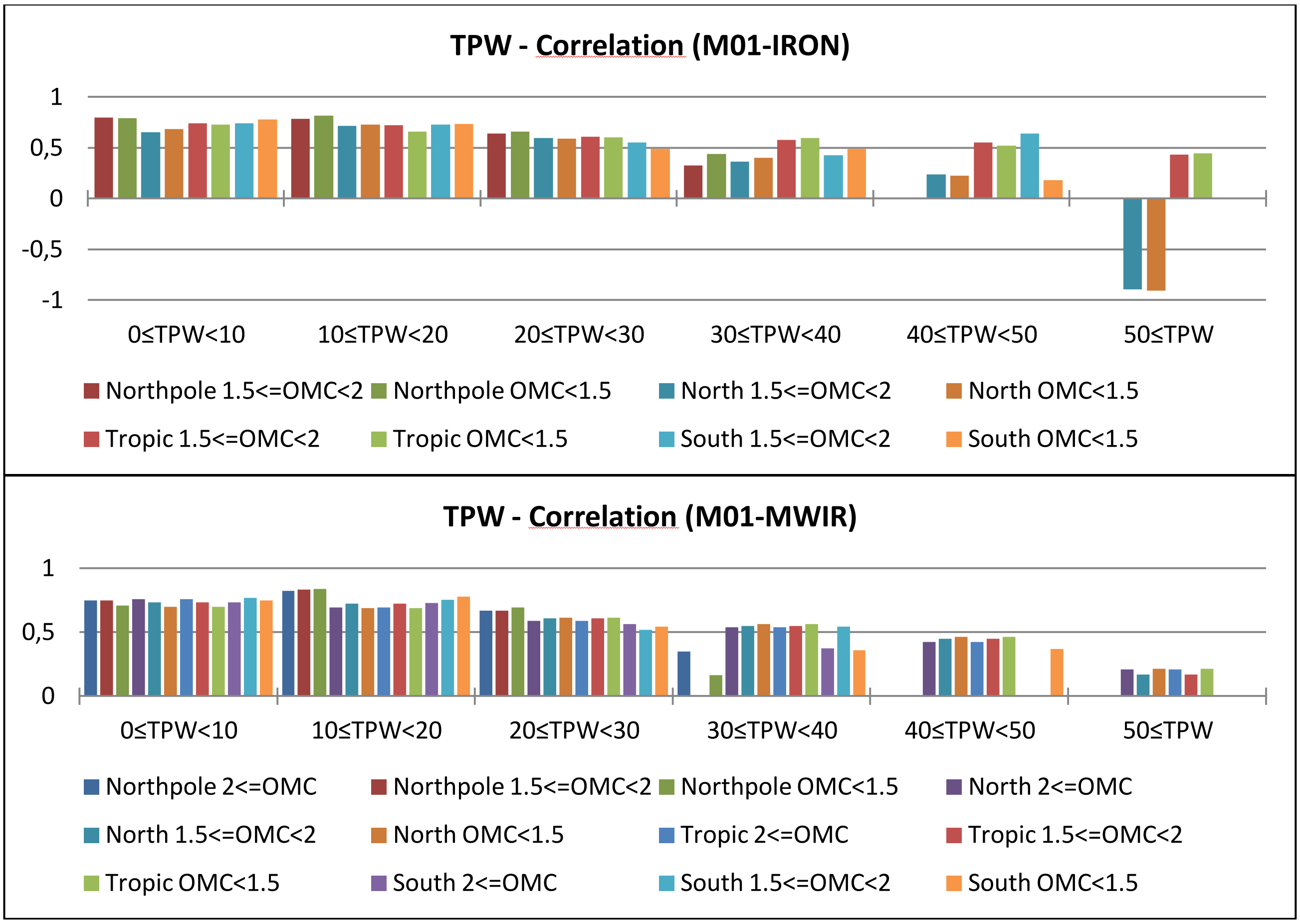

Fig. A1.2: Correlation for TPW for different IASI pixel clarity categories over land for Metop-B for IRON (upper) and MWIR (lower) retrievals.

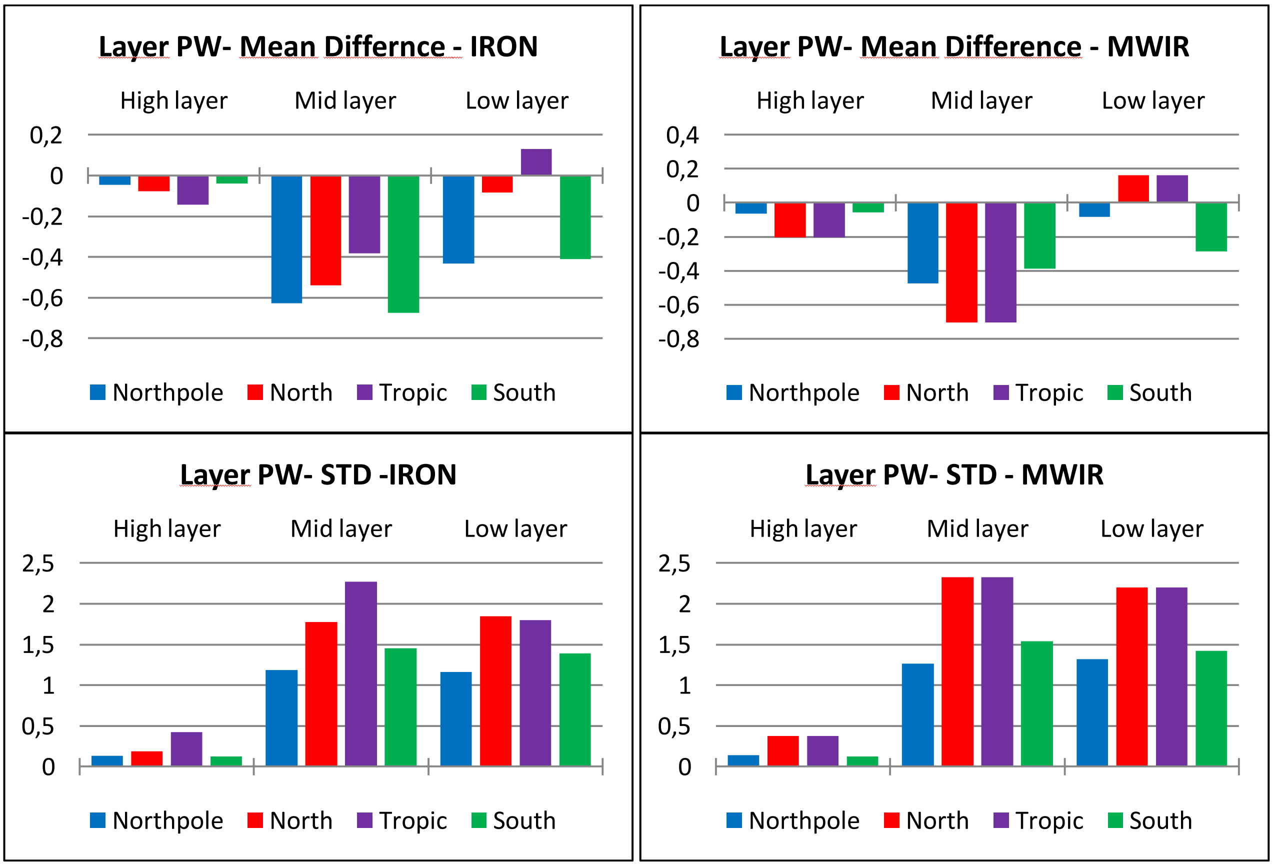

Fig. A1.3: Mean difference and STD for layer precipitable water over land for Metop-B for IRON (left) and MWIR (right) retrievals.

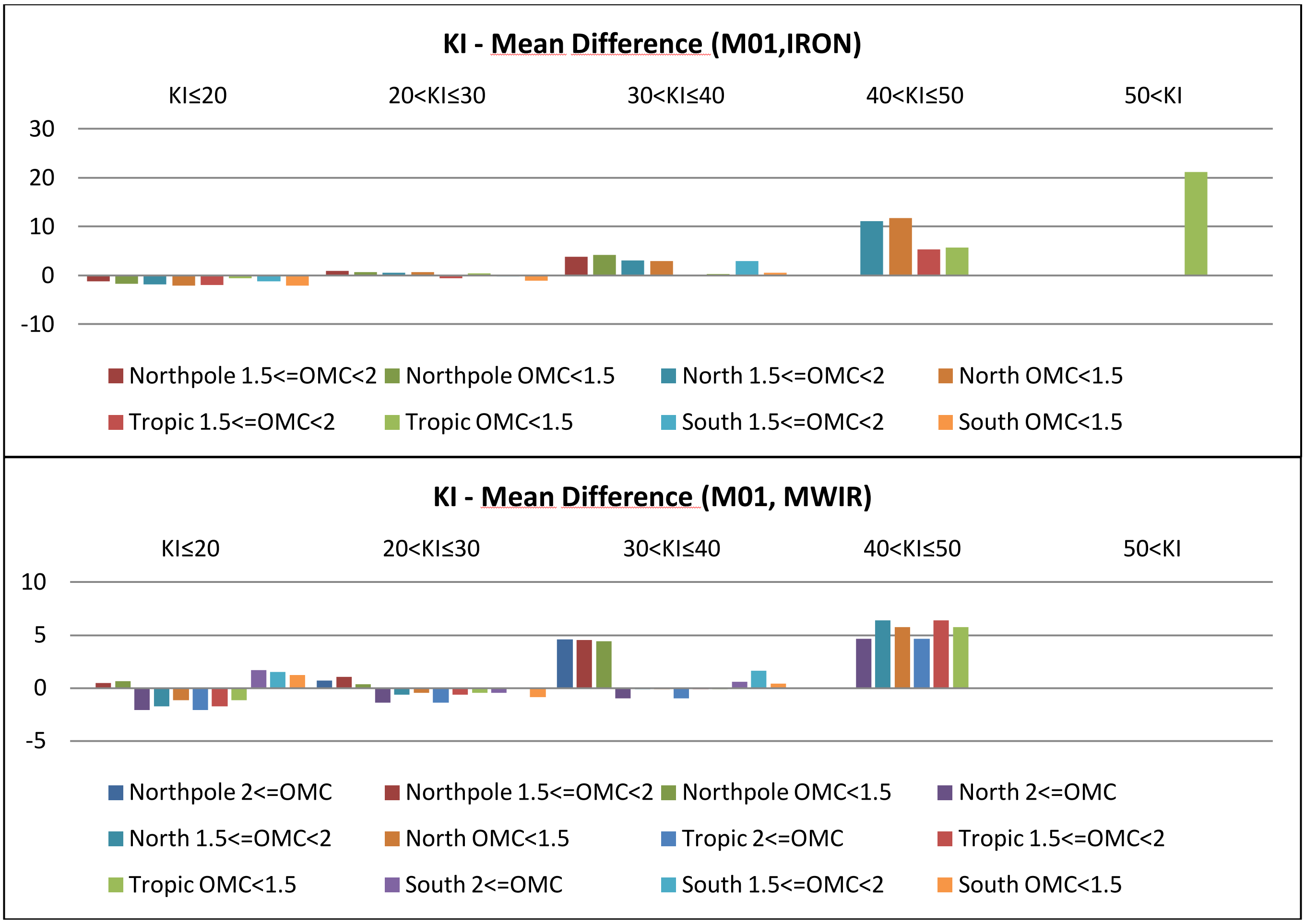

Fig. A1.4: Mean difference for KI for different IASI pixel clarity categories over land for Metop-B for IRON (upper) and MWIR (lower) retrievals.

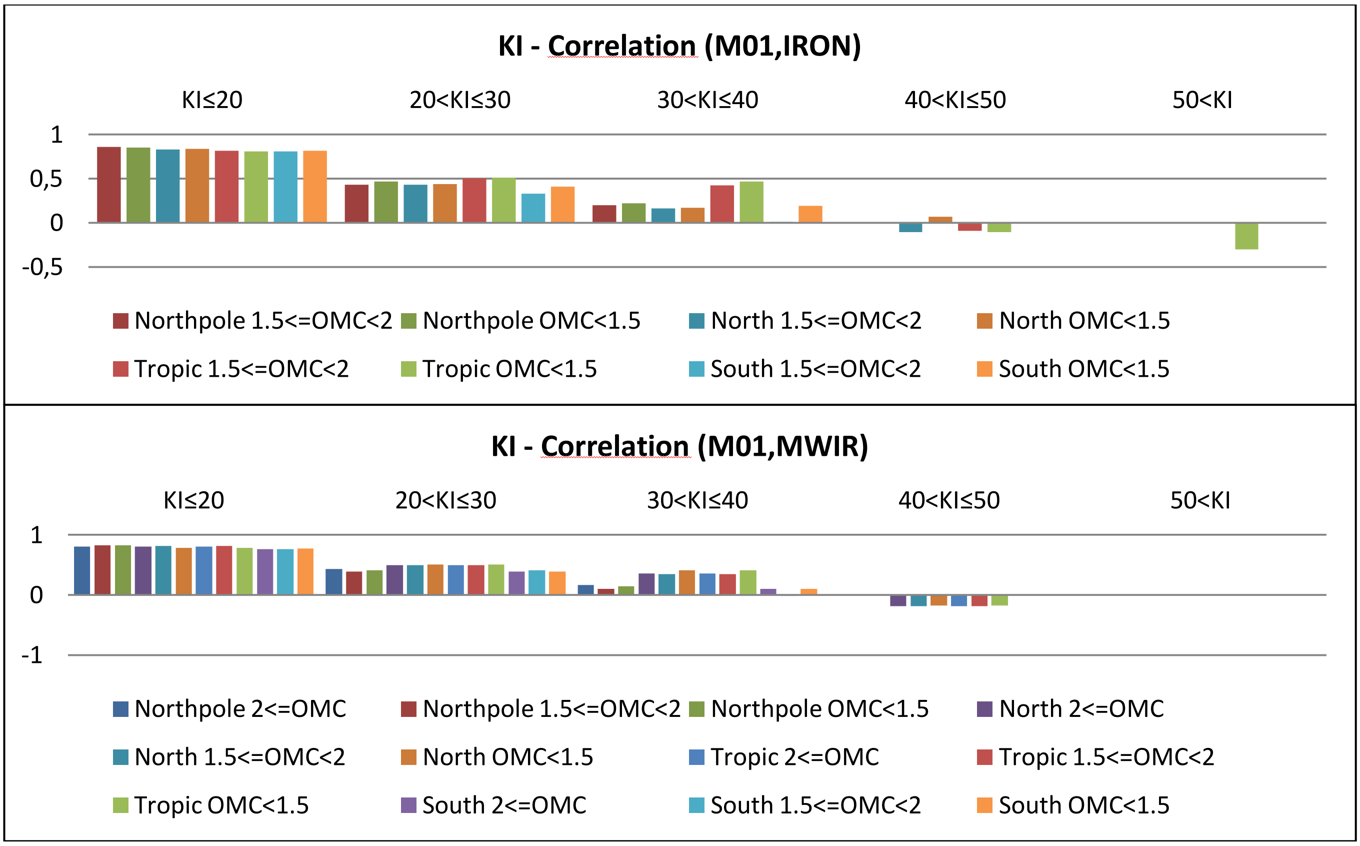

Fig. A1.5: Correlation for KI for different IASI pixel clarity categories over land for Metop-B for IRON (upper) and MWIR (lower) retrievals.

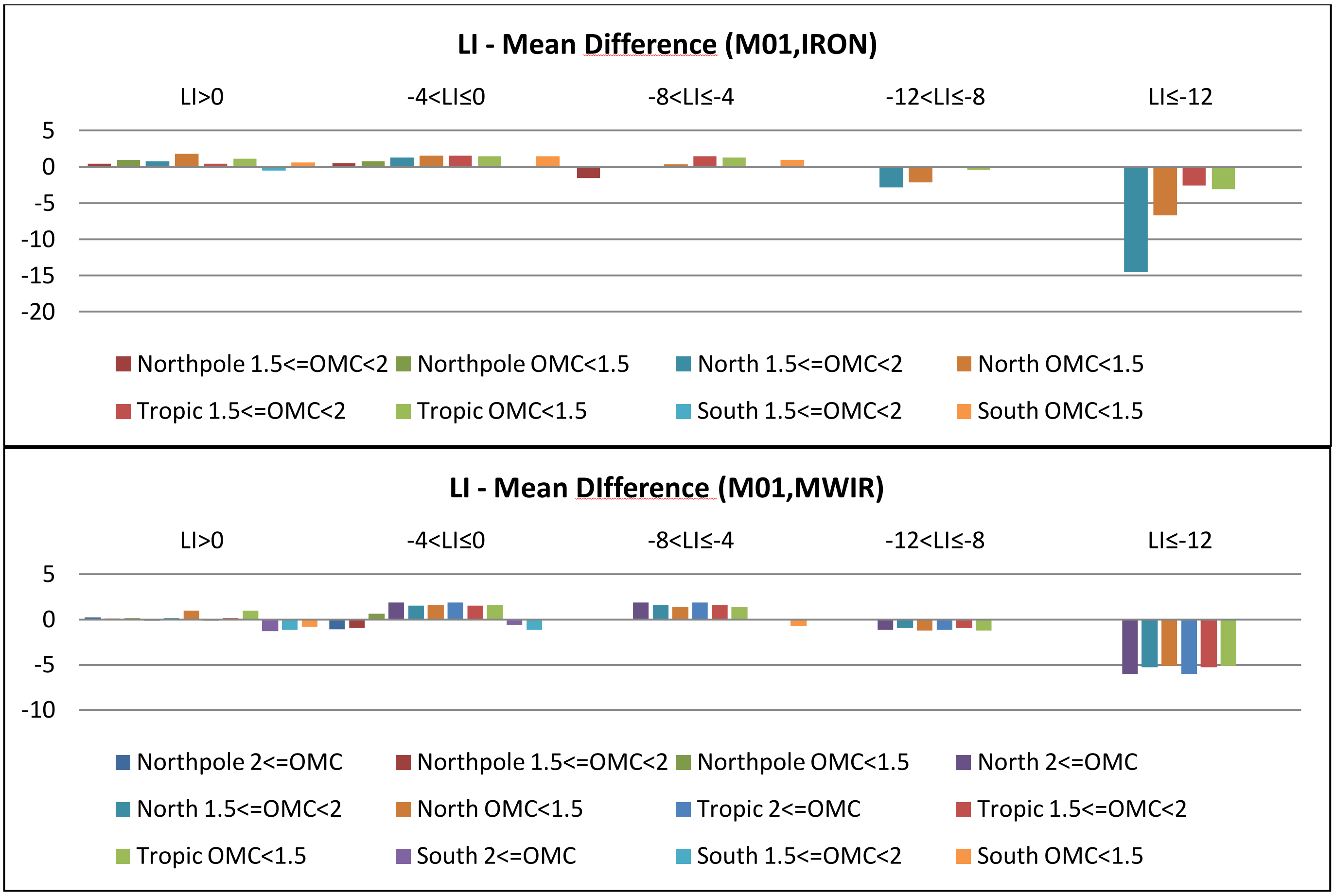

Fig. A1.6: Mean difference for LI for different IASI pixel clarity categories over land for Metop-B for IRON (upper) and MWIR (lower) retrievals.

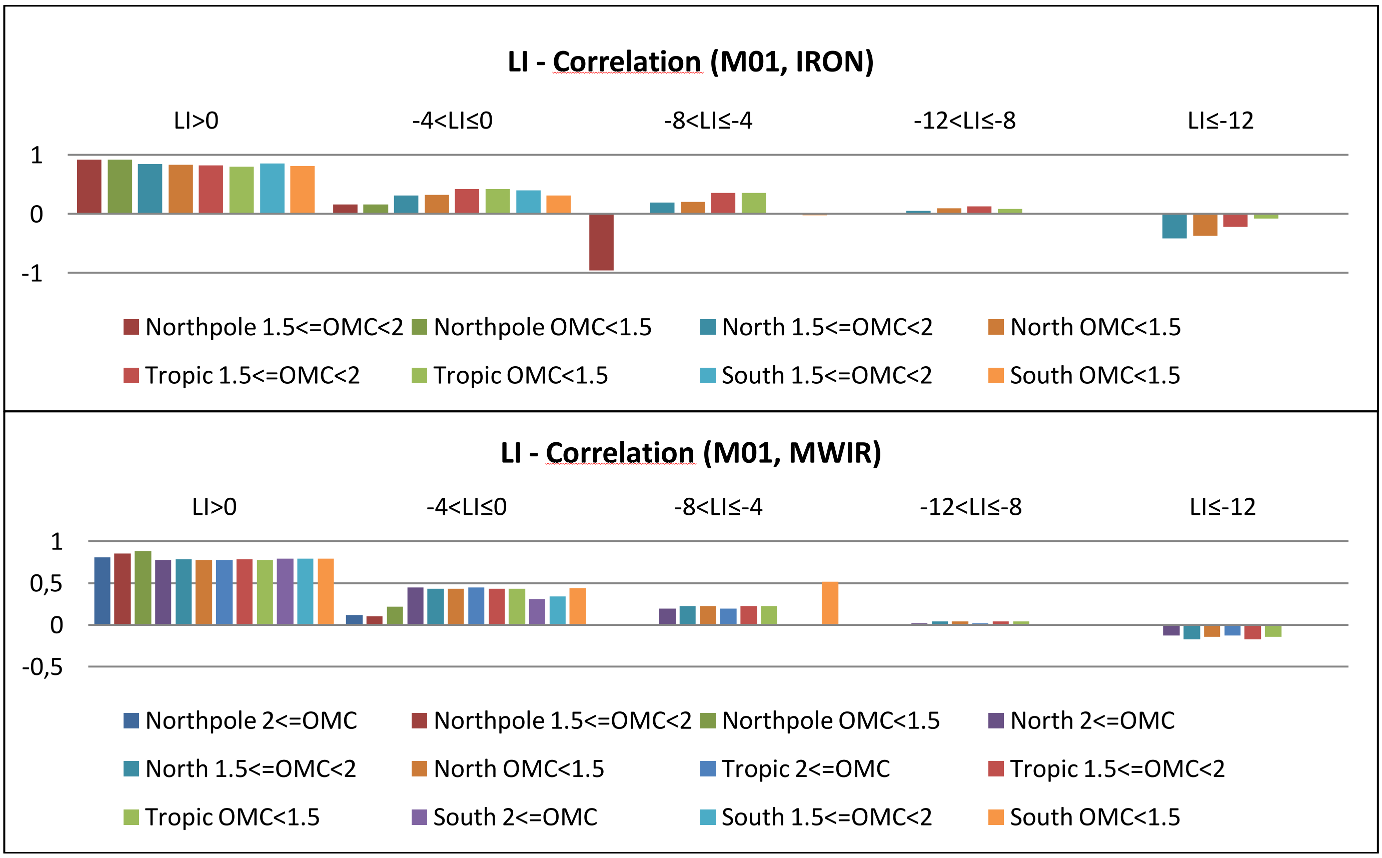

Fig. A1.7: Correlation for LI for different IASI pixel clarity categories over land for Metop-B for IRON (upper) and MWIR (lower) retrievals.

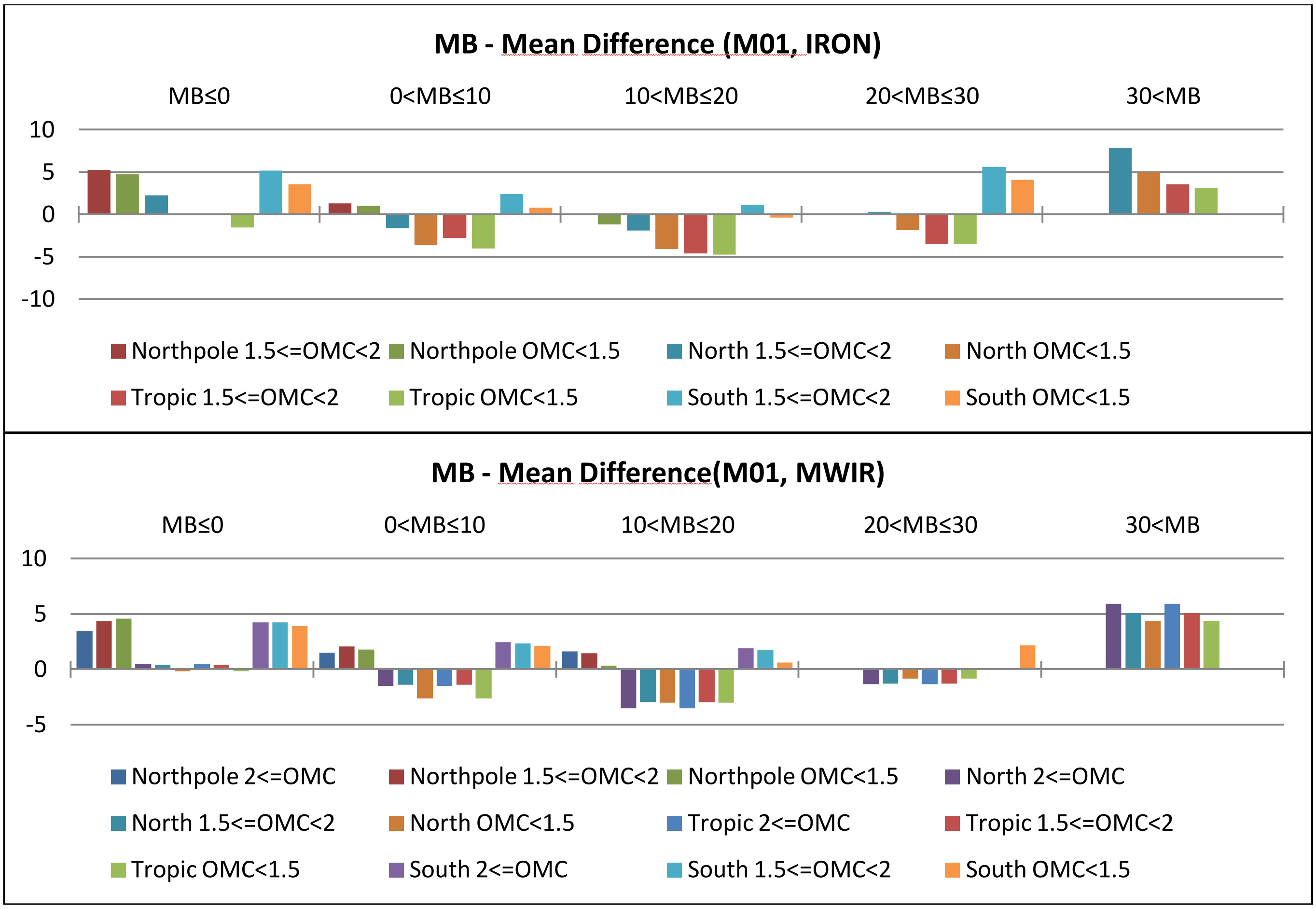

Fig. A1.8: Mean difference for Maximum Buoyancy for different IASI pixel clarity categories over land for Metop-B for IRON (upper) and MWIR (lower) retrievals.

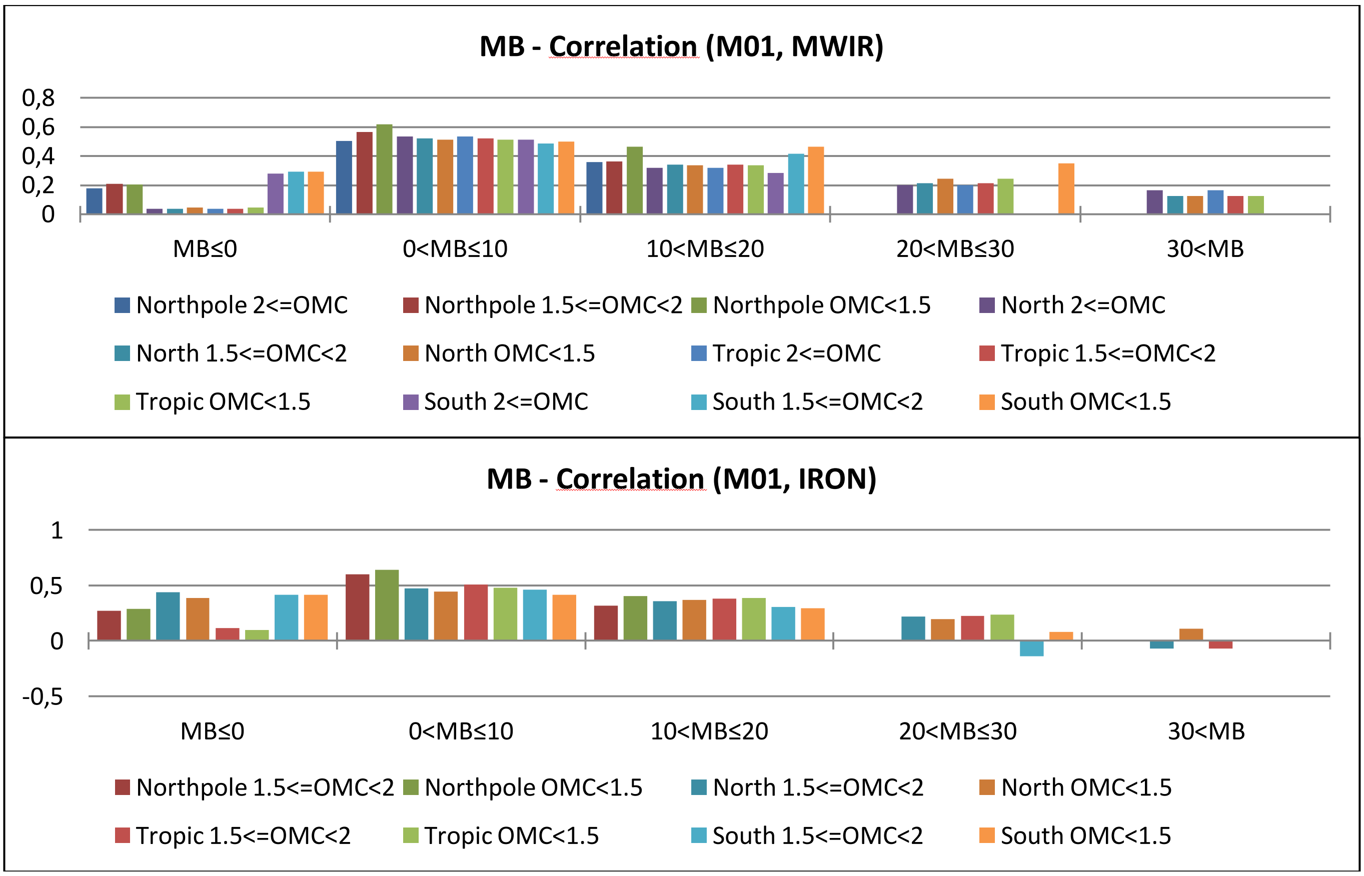

Fig. A1.9: Correlation for Maximum Buoyancy for different IASI pixel clarity categories over land for Metop-B for IRON (upper) and MWIR (lower) retrievals.

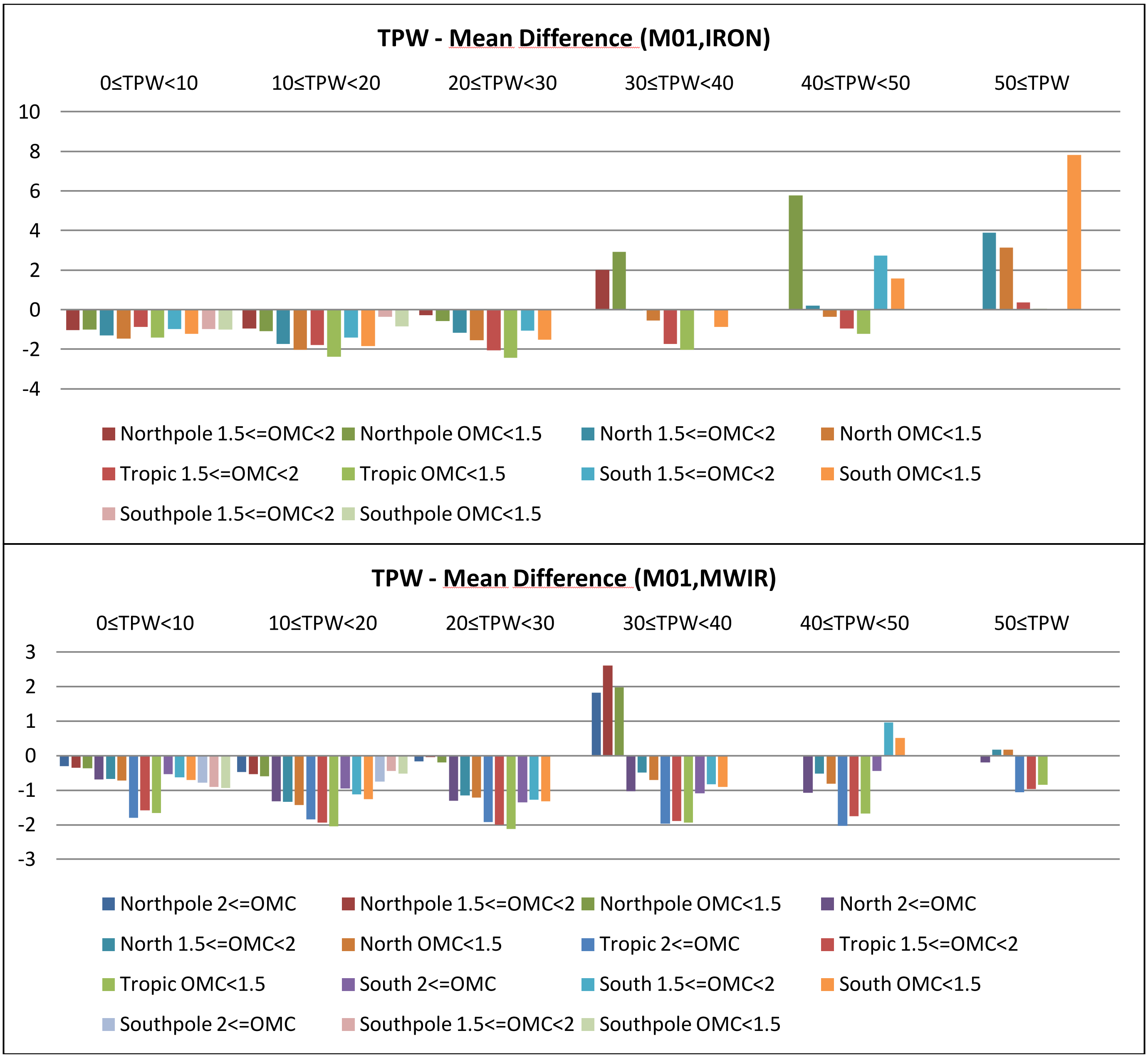

Fig. A1.10: Mean difference for TPW for different IASI pixel clarity categories over sea for Metop-B for IRON (upper) and MWIR (lower) retrievals.

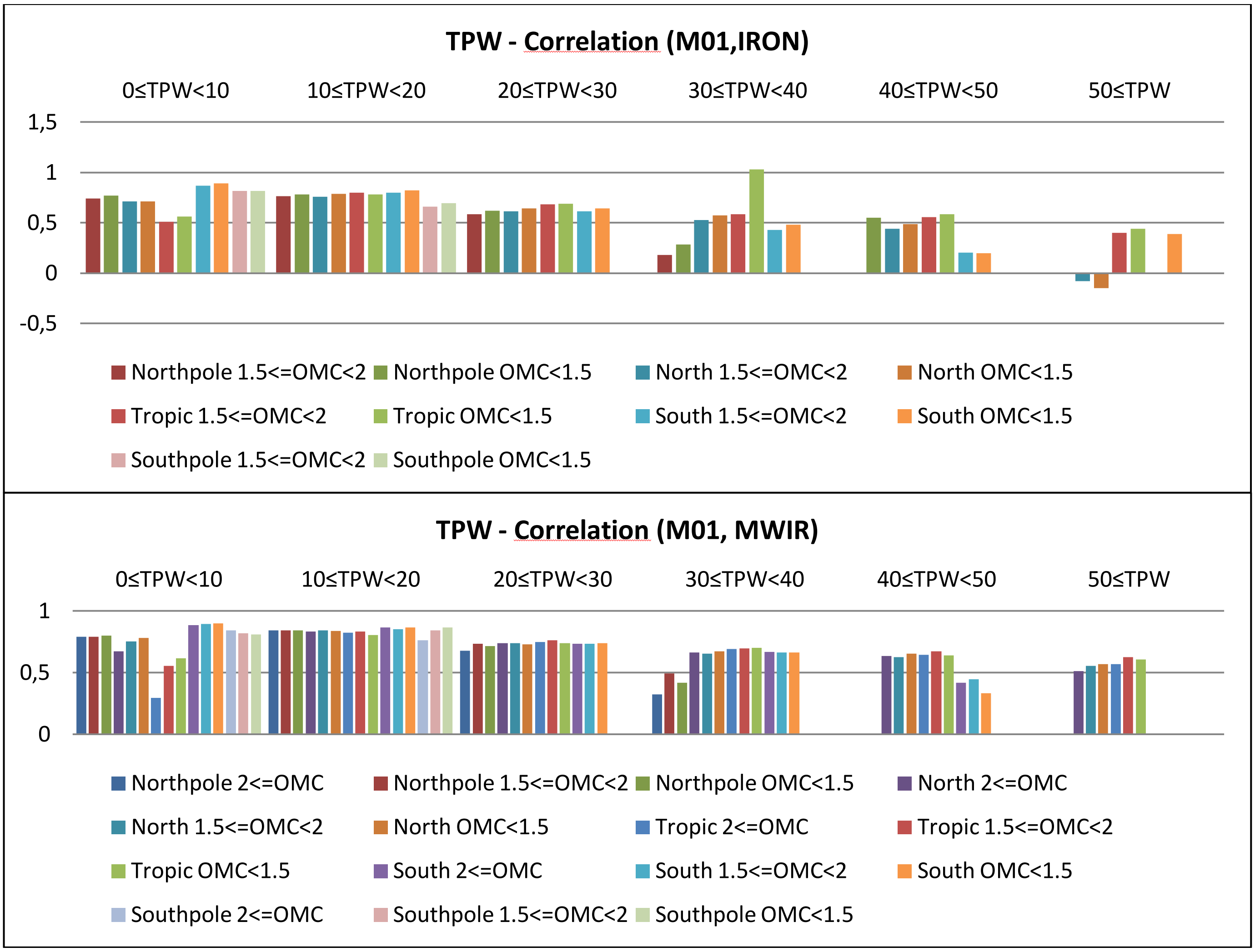

Fig. A1.11: Correlation for TPW for different IASI pixel clarity categories over sea for Metop-B for IRON (upper) and MWIR (lower) retrievals.

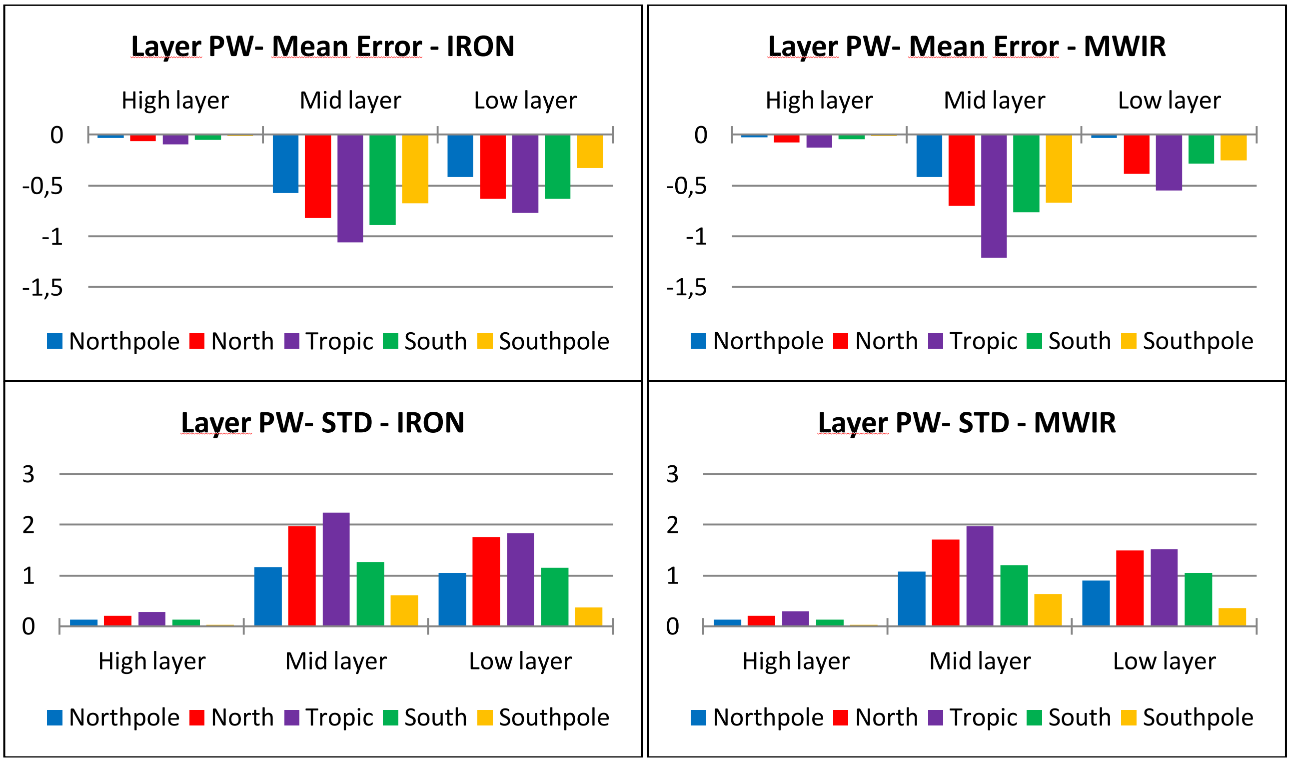

Fig. A1.13: Mean difference and STD for layer precipitable water over sea for Metop-B for IRON (left) and MWIR (right) retrievals.

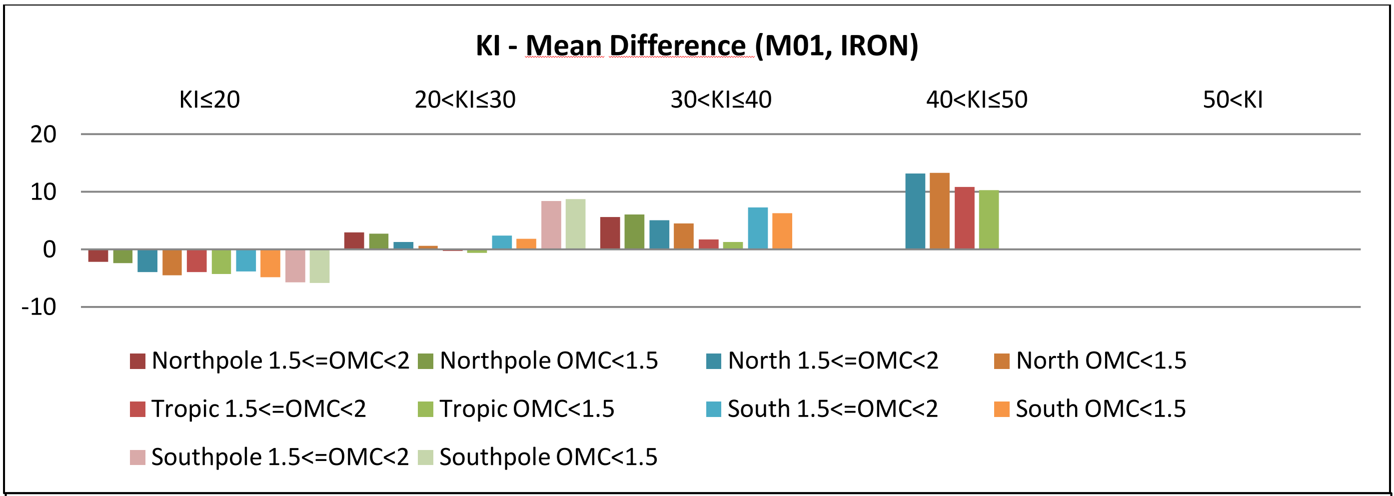

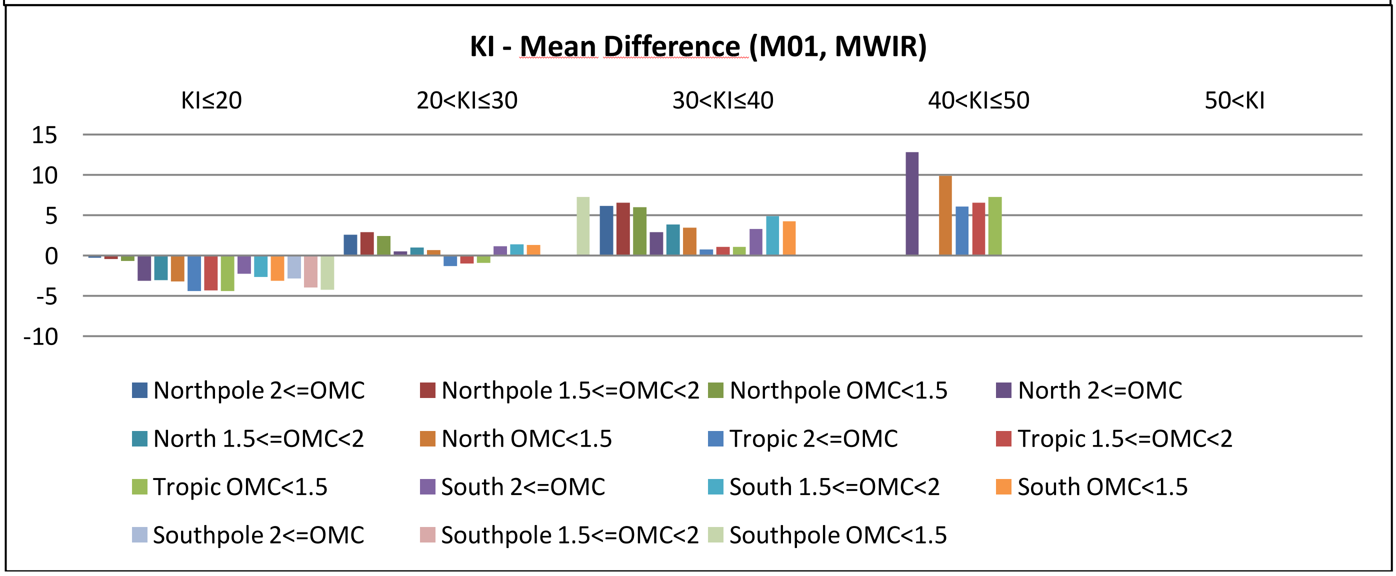

Fig. A1.14: Mean difference for KI for different IASI pixel clarity categories over sea for Metop-B for IRON (upper) and MWIR (lower) retrievals.

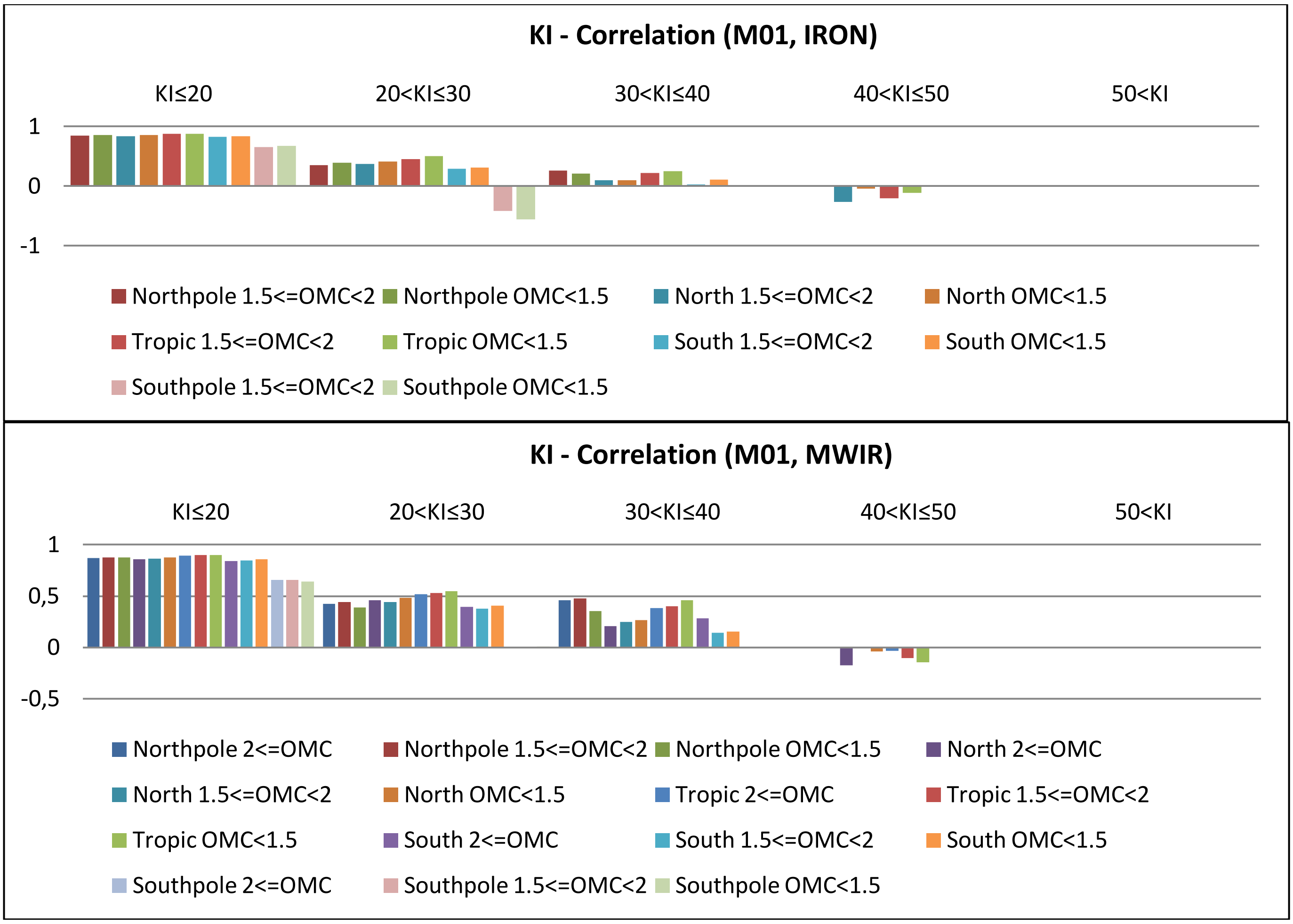

Fig. A1.15: Correlation for KI for different IASI pixel clarity categories over sea for Metop-B for IRON (upper) and MWIR (lower) retrievals.

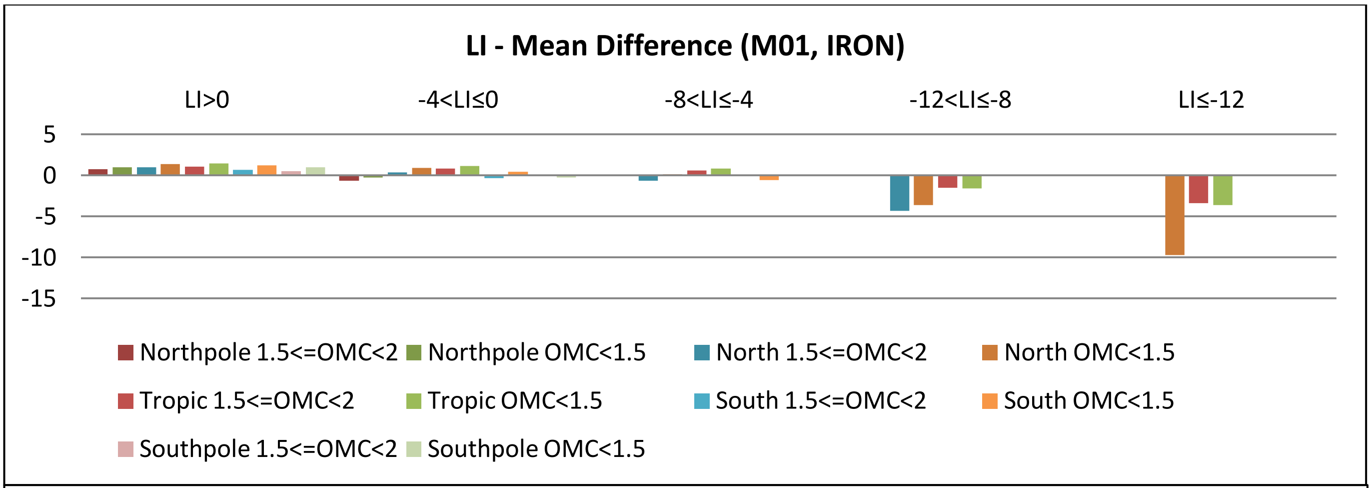

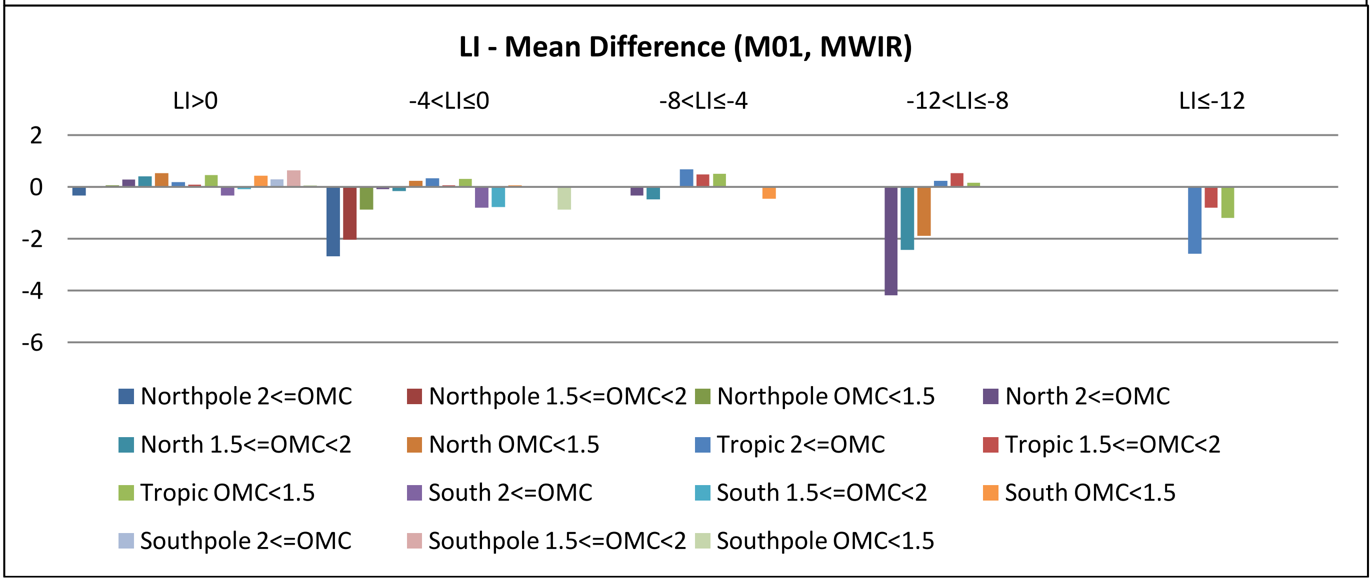

Fig. A1.16: Mean difference for LI for different IASI pixel clarity categories over sea for Metop-B for IRON (upper) and MWIR (lower) retrievals.

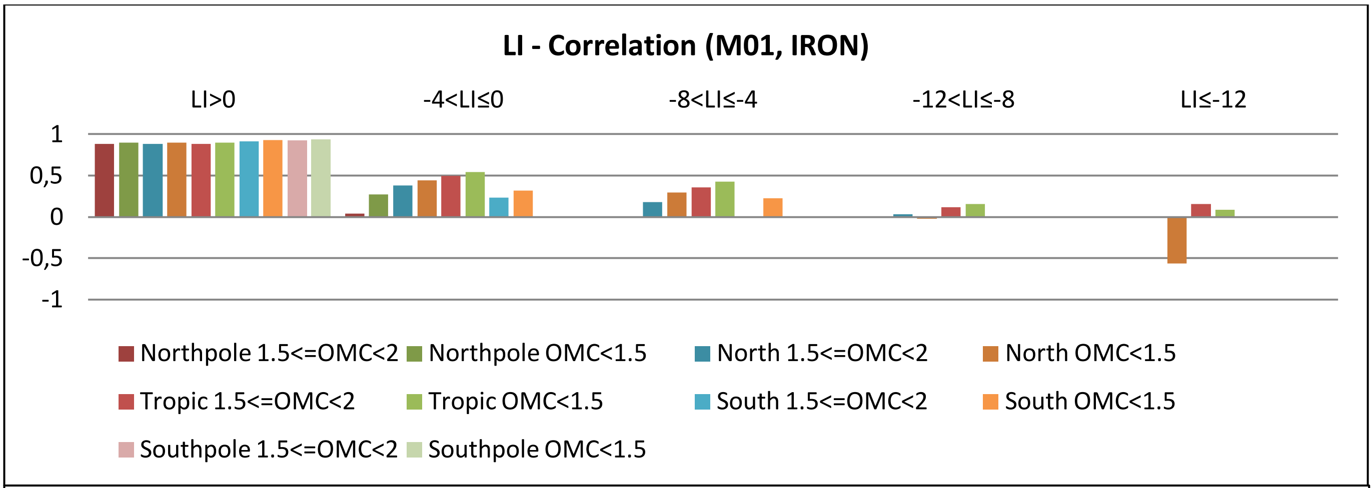

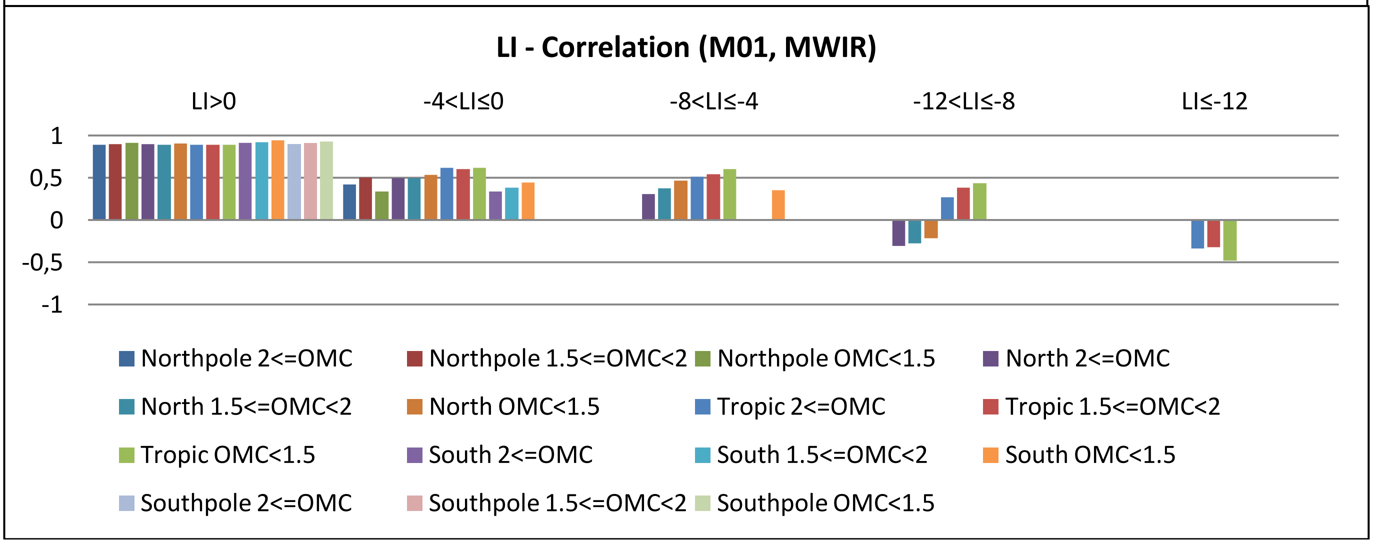

Fig. A1.17: Correlation for LI for different IASI pixel clarity categories over sea for Metop-B for IRON (upper) and MWIR (lower) retrievals.

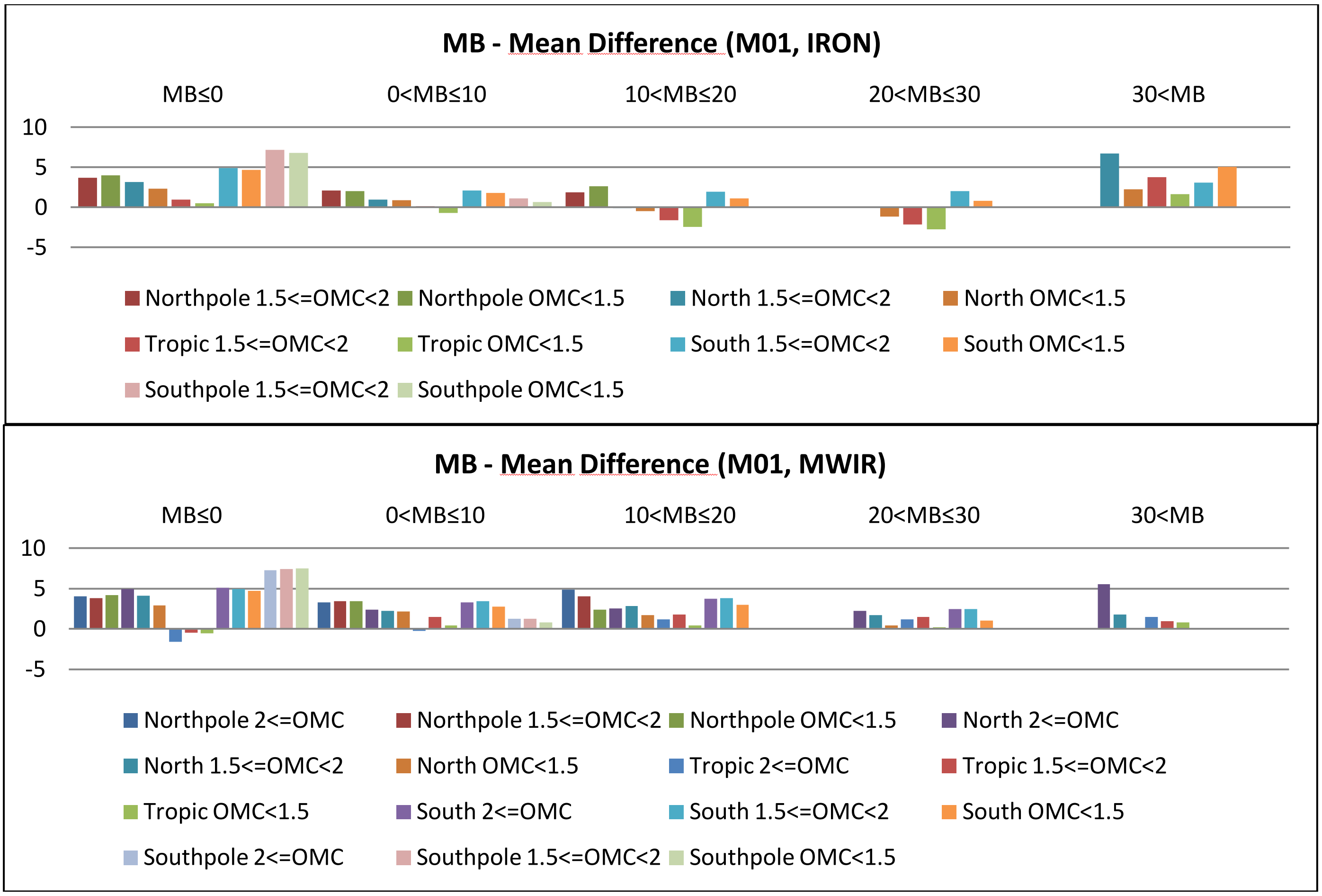

Fig. A1.18: Mean difference for Maximum Buoyancy for different IASI pixel clarity categories over sea for Metop-B for IRON (upper) and MWIR (lower) retrievals.

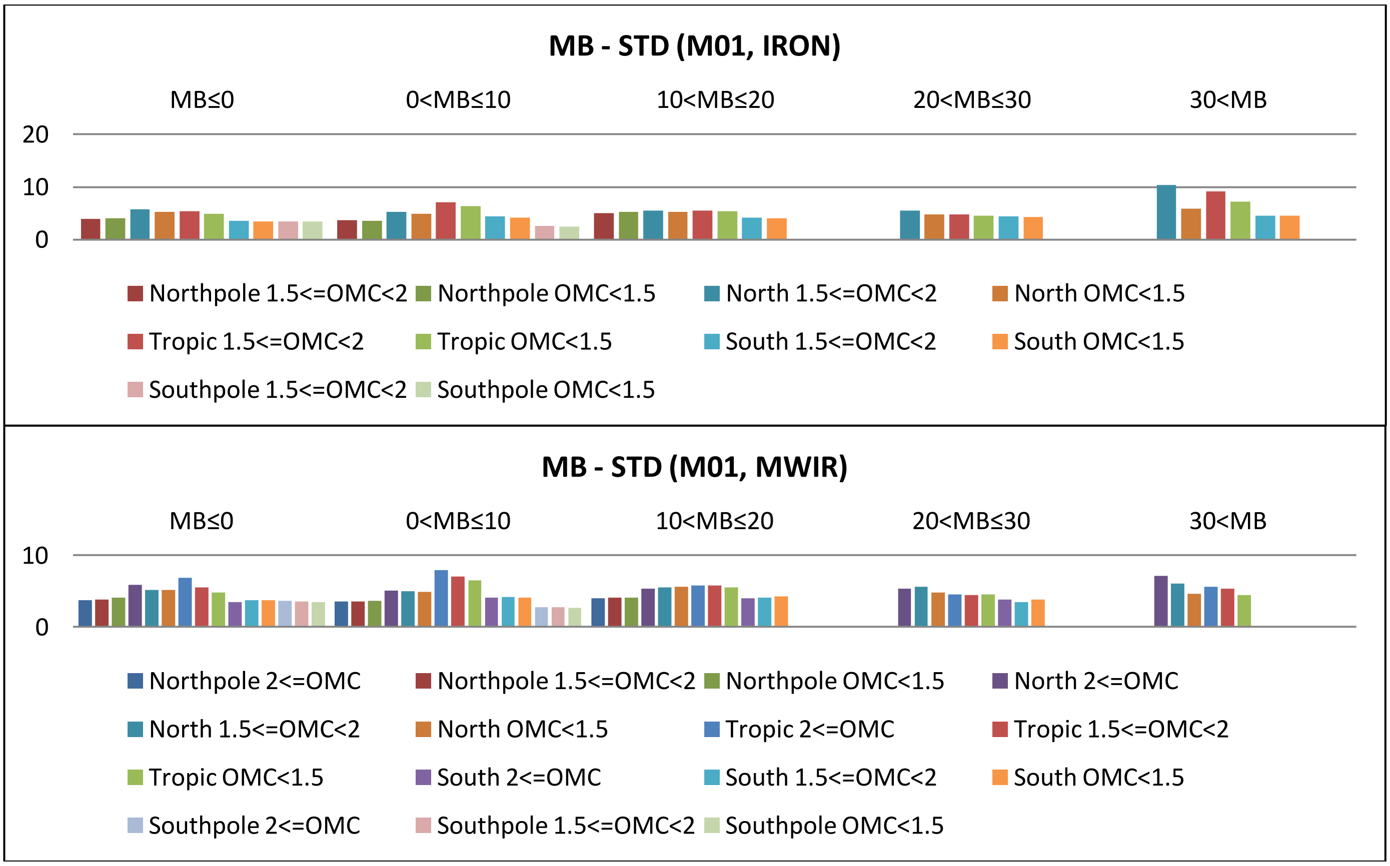

Fig. A1.19: Standard Deviation for Maximum Buoyancy for different IASI pixel clarity categories over sea for Metop-B for IRON (upper) and MWIR (lower) retrievals.

Appendix 2: Colour scale of the NWCSAF Cloud type product

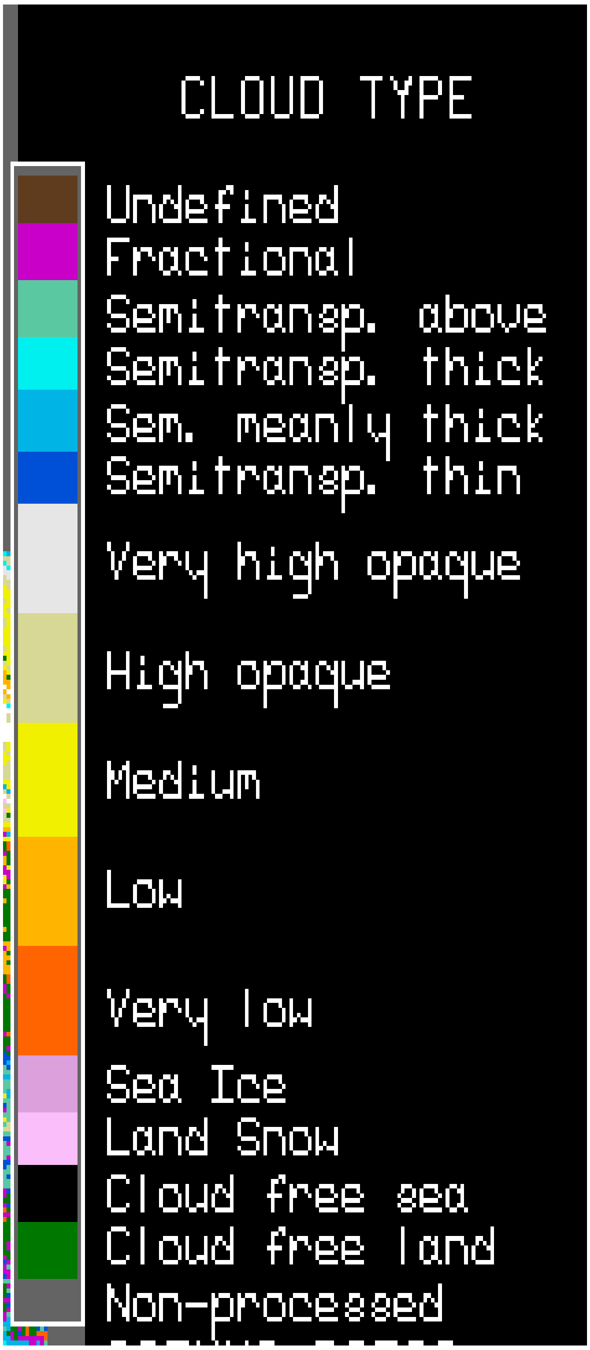

Appendix 3: Definitions of the environmental parameters

Over the last decades, several parameters were developed in order to diagnose the conditions for deep convection. These parameters are related to the environment of the expected thunderstorms, which is in hydrostatic equilibrium.

Definitions

Convective Available Potential Energy, CAPE [J/kg]

Maximum amount of potential energy which the air parcel has available for convection.
CAPE is calculated by integrating over pressure the virtual temperature difference of the adiabatically lifted air parcel and the environment.

$$\boxed{\begin{gathered} CAPE = -R_d \int_{p1}^{p2} (T_{v,parcel} - T_{v,env})\, d \ln p, \\ \text{if } T_{v,parcel} > T_{v,env} \end{gathered}}$$

where

p_1 is the pressure level the air parcel is lifted from (or the pressure of the Level of the Free Convection, LFC)
p_2 is the pressure of the equilibrium level (EL, neutral buoyancy),
$T_{v,parcel}$ is the virtual temperature of the adiabatically lifted parcel,
$T_{v,env}$ is the virtual temperature of the environment,
R_d is the specific gas constant for dry air

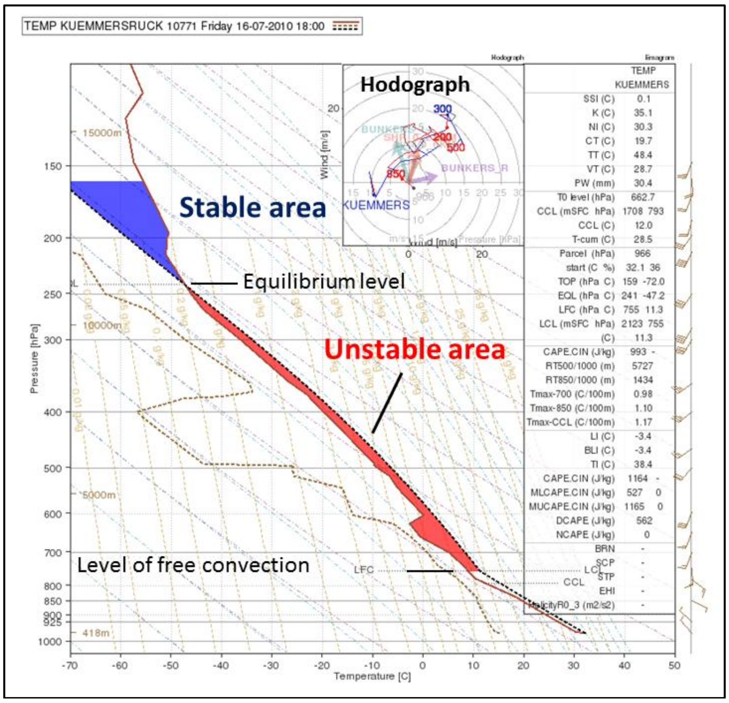

Fig. A3.1: Example of sounding with depicted stable and unstable layers and special levels important for the CAPE calculation.

If an air parcel is lifted adiabatically upward, it first moves dry-adiabatically from the starting pressure level to the **Lifted Condensation Level** (LCL, where it becomes saturated) and then moist-adiabatically. On a thermodynamic diagram CAPE is represented by the area enclosed between the environmental temperature profile and the temperature of an adiabatically rising air parcel, over the layer(s) within which the air parcel temperature is warmer than the environmental temperature (positive area) – see Fig. A11.1. In some cases, there can be several stable and unstable areas in the troposphere.

From the **level of free convection** the parcel can move along the moist adiabat without additional forcing, until it would reach the **equilibrium level** (EL, level of neutral buoyancy).

Definitions of different CAPE values:
There are different kinds of CAPE indicators. The forecasters use them simultaneously.
The Hungarian forecasters use the following kinds of CAPE values:

Surface Based CAPE, SBCAPE [J/kg]
The virtual air parcel is lifted from the surface.

Mixed Layer CAPE, MLCAPE [J/kg]
It takes the daytime mixing of the boundary layer into account.
The lowest 100 hPa layer just above the surface is mixed and the virtual air parcel is lifted from the top of this mixed layer with the 'averaged' temperature and humidity values. (Average T is calculated from the mean potential temperature; average humidity is the mean mixing rate.)

Most Unstable CAPE, MUCAPE [J/kg]
The CAPE value belonging to the most unstable level under 500 hPa is the MUCAPE.
MUCAPE helps to estimate the probability of elevated convection in case of a stable near surface layer (e.g. at night or behind a cold front)

Convective Inhibition, CIN
Convective inhibition (J/kg) is a numerical measure that indicates the amount of energy that prevents an air parcel from rising from the surface to the level of free convection. By strong lift (e.g. related to convergence line or frontal circulation) the rising motions may overcome this barrier or can start above the surface layers with large CIN (elevated convection). Severe storms often develop along lines with strong lift, while in their surroundings, there is an area of CIN inhibiting other clouds to grow and share/decrease he potential energy sources. Convection can be also inhibited by elevated stable (inversion) levels (called also as capping inversion, cap, lid).

K-index (George, 1960)
It is a combined index to assess the potential for thunderstorm development concerning mid-level temperature lapse rate (between 500 and 850 hPa levels) and humidity (850 hPa dewpoint, dewpoint depression, DD at 700 hPa). There exist also other, slightly different versions of K-index. Note that the presence of dry air at mid-levels can have an opposite effect in K-index as for the Maximum Buoyancy. The K-index also does not concern stability conditions below 850 hPa level, thus, it is not sensitive to radiation and daily course of surface temperature and dewpoint.

$$K = T_{850} - T_{500} + T_{D850} - DD_{700}$$

Lapse-rate
Temperature lapse rate of the environment is often examined between the 700 and 400 hPa levels or 925 and 600 hPa levels as a measure of conditional instability (when its value lies between moist and dry adiabatic lapse rate). Steep lapse rates can sometimes indicate potential for rapidly developing or severe convection.

Li-index: Lifted Index (Galway, 1956)

It compares the temperature of the environment and a parcel rising from the surface (at first dry and subsequently, moist adiabatically) at 500 hPa. The **BLI (Best Lifted Index**) is a version of LI, which represents the lowest (most unstable) LI computed from a series of levels from the surface to about 850 mb.

$$LI = T_{500}^{environment} - T_{500}^{parcel}$$

Maximum Buoyancy (König et al., 2001)

It is supposed to diagnose areas with vertically decreasing equivalent potential temperature, which are considered to be conditionally unstable:

$$MB = \left(\max \theta_e\right)_{SFC}^{850hPa} - \left(\min \theta_e\right)_{700hPa}^{300hPa}$$

Total Precipitable Water, TPW (mm)

Total amount of atmospheric water vapour in the vertical column of the atmosphere. It is expressed in terms of precipitation, which would be generated if all the water vapour would be condensed. However, the actual convective precipitation can be bigger due to dynamical and microphysical processes in the cloud, which are not taken into account. We calculated also partial TPW related only to boundary layer (BL) or mid-layers (ML).

$$TPW = \left(\frac{1}{g}\right) \int_{p\,SFC}^{0} q(p)\,dp$$

Appendix 4: Abbreviations

BLI – Best Lifted index
CAPE - Convective Available Potential Energy
CIN - Convective Inhibition
EARS - EUMETSAT Advanced Retransmission Service
ECMWF – European Centre for Medium-Range Weather Forecasts
EUMETSAT - European Organisation for the Exploitation of Meteorological Satellites
EumetCast - EUMETSAT's broadcast system
HRV – High Resolution Visible
IASI – Infrared Atmospheric Sounding Interferometer
IASI L2 – IASI level 2 profile product
IASI L2 MWIR - IASI level 2 profile product based on infrared and microwave measurements
IASI L2 IRON - IASI level 2 profile product based only on infrared measurements
IR – infrared
IRS - Infra-Red Sounder
KI - K-index
LFC - Level of Free Convection
LI - Lifted Index
MLCAPE - Mixed-Layer Convective Available Potential Energy
MTG - Meteosat Third Generation
MUCAPE - Most Unstable Convective Available Potential Energy
MW – microwave
MWIR – microwave and infrared
NWP - Numerical Weather Prediction
RMSE – Root Mean Square Error
SBCAPE – Surface-based Convective Available Potential Energy
STD – standard deviation
T – temperature
Td – dew point temperature
TPW - Total Precipitable Water
WMO - World Meteorological Organisation